The Differential Effects of Nitrate and Ammonium on the Growth, Nodulation and Nitrogen Fixation of *Medicago truncatula* Gaertn. and the Analysis of Differential Gene Expression During the Initiation of Symbiosis with *Sinorhizobium meliloti*

BY

JIAN JUN GUO

A Thesis
Submitted to the Faculty of Graduate Studies
in Partial Fulfillment of the Requirements
for the Degree of

MASTER OF SCIENCE

Department of Plant Science
University of Manitoba
Winnipeg, Manitoba

THE UNIVERSITY OF MANITOBA

FACULTY OF GRADUATE STUDIES

*****

MASTER'S THESIS/PRACTICUM FINAL REPORT

The undersigned certify that they have read the Master's Thesis/Practicum entitled:

The Differential Effects of Nitrate and Ammonium on the Growth, Nodulation and Nitrogen Fixation of *Medicago truncatula* Gaertn. and the Analysis of Differential Gene Expression During the Initiation of Symbiosis with *Sinorhizobium meliloti*

submitted by

JIAN JUN GUO

in partial fulfillment of the requirements for the degree of

MASTER OF SCIENCE

The Thesis/Practicum Examining Committee certifies that the thesis/practicum (and oral examination if required) is:

Approved
(Approved or Not Approved)

☑ Thesis

☐ Practicum

Advisor: J. K. Vessey, Plant Science

Advisory Committee:

C. Stasolla, Plant Science

J. Markham, Botany

Date: August 15, 2005

THE UNIVERSITY OF MANITOBA

FACULTY OF GRADUATE STUDIES

*****

COPYRIGHT PERMISSION PAGE

The Differential Effects of Nitrate and Ammonium on the Growth, Nodulation and Nitrogen Fixation of *Medicago trunculata* Gaertn. and the Analysis of Differential Gene Expression During the Initiation of Symbiosis with *Sinorhizobium meliloti*

BY

Jian Jun Guo

A Thesis/Practicum submitted to the Faculty of Graduate Studies of The University of Manitoba in partial fulfillment of the requirements of the degree of

MASTER OF SCIENCE

TABLE OF CONTENTS

ABSTRACT

Ammonium and nitrate have differential effects on nodulation of legumes. Two experiments were conducted to investigate the effects of ammonium and nitrate on nodulation in the *Medicago truncatula* Gaertn. - *Sinorhizobium meliloti* symbiosis in sand culture. Inoculated plants were provided static concentrations (0.0, 0.1, 0.5 or 1.0 mM) of ^{15}N-labelled NH_4^+ or NO_3^- in a flow-through sand culture system. Plants were harvested at 10 and 20 days after inoculation and assessed for root, shoot and nodule dry weight, nodule counts, and total N and ^{15}N content. A third experiment was conducted in a growth pouch culture system in which the effects of two concentrations (0.1 and 0.5 mM) of NH_4^+ and NO_3^- on nodulation were compared together.

Both ammonium and nitrate enhanced plant growth at all three concentrations compared to the 0-N controls. Although all mineral N treatments increased whole plant nodulation (nodules plant^{-1}), at 0.1 mM level, NO_3^- resulted in decreases in specific nodulation (nodules g^{-1} root DW), while NH_4^+ had specific nodulation levels similar to the 0-N controls. As specific nodulation is a more accurate measure of the development the legume-rhizobia symbioses *per se* than whole plant nodulation, it can be concluded that nitrate has a more negative effect on the establishment of the symbiosis than ammonium. At 0.5 mM or above, NO_3^- also had more inhibitory effects on individual nodule DW compared to NH_4^+. These results are consistent with previous studies conducted in pea (*Pisum sativum* L.) and white clover (*Trifollium repens* L.).

A large-scale differential gene expression analysis during the initiation of symbiosis with and without the presence of mineral nitrogen sources was conducted by utilizing *Mt16kOLI1* DNA microarrays. Inoculated plants were grown in growth pouch culture system in the presence of 0.1 mM NO_3^-, 0.1 mM NH_4^+ or 0-N nutrient solutions and harvested at 6, 12 and 24 hours post inoculation. Non-inoculated plants with similar age were used as the reference levels of genes expression to which the genes expression levels in all other samples were compared to.

Considering only probes that were continuously up-/down-regulated throughout the first 24 hours post inoculation and significantly changed 1.5 fold or more at least at two of the three time points, 83, 246 and 79 probes were identified in related to the inoculation-only, inoculation plus NH_4^+ and inoculation plus NO_3^- treatments respectively. These probes represented genes involved in most aspects of cell function, of which, genes involved in secondary metabolism and hormone metabolism, defence and cell rescue, abiotic stimuli and development are discussed on their possible involvement in initiation of nodulation. Other probes that were possibly related to nodulation or nitrate/ ammonium metabolism are also discussed.

ACKNOWLEDGEMENT

I would like to first express my thanks to Dr. J. Kevin Vessey for supplying me this great opportunity to take part in such a fascinating project in his lab. I also greatly appreciate his incredible patience, generosity, trust and support on me throughout these three years; I couldn't have progressed so quickly and smoothly in my project without his guidance and numerous precious suggestions. I would like to express my great appreciation to Dr. John Markham and Dr. Claudio Stasolla for their agreeing to sit on my Committee and for their valuable suggestions and support on my project. I'm also grateful for Dr. Helge Küster (Bielefeld University, Germany) for supplying the microarray and accompanied protocols, as well as for his always prompt reply to my questions; the microarray work could not have been accomplished without his help. Many thanks to Dr. Sylvie Cloutier (Cereal Research Center, Agriculture Canada) for allowing me to use their microarray scanner and microarray bioinformatics software. I'm also appreciative of Dr. Brian W. Fristensky, Dr. Robert D. Hill, and Dr. Genyi Li for allowing me to access their equipments. Thank you to Bert Luit for the numerous technical supports and always being there throughout the whole project. Also thank you to Dr. Bowlaye Fofana for his technical help on the microarray data analysis.

I also want to express my thanks to other members in Dr. Vessey's lab including Dr. Houman Fei and Dr. Carla Zelmer for their help in my research and in aspects on my life outside the lab.

Also I would thank the technicians and support staff in the Plant Science Department for all they did for me!

Finally, I want to say thanks to my family for always being there to support me; and specially thank you, Kelly, I couldn't imagine what my life would've been in the past two years without you!

LIST OF TABLES

LIST OF FIGURES

Figure **page**

Figure **page**

Figure **page**

1.0 INTRODUCTION

Plants from the family Leguminosae (Fabaceae) when grown under nitrogen-limiting conditions can enter into a symbiotic relationship with bacteria from several families, collectively called rhizobia, to form a new root-borne organ, the nodule. In the nodule, the bacteria convert the atmospheric N_2 into ammonium and supply nitrogen to the plant, and in return, the plant supplies carbohydrates to the bacteria (Crespi and Galvez, 2000).

The presence of combined nitrogen negatively influences the establishment of symbiosis due to the comparably higher energy cost to develop, maintain and operate effective nodules than to directly assimilate the available combined nitrogen (Gan et al., 2004). Nitrate has been recognized to have inhibiting effects on legume-rhizobia symbiosis for a long time (Streeter, 1988) even at very low concentrations (e.g. 0.1 mM, Waterer and Vessey, 1993b). In contrast, it has been demonstrated that, NH_4^+ at static low concentrations between 0.1 mM and 2.0 mM (depending on the culture system) stimulates specific nodulation[1] (i.e., number of nodules per g root dry weight) in pea (*Pisum sativum*) and white clover (*Trifolium repens*) (Waterer et al., 1992; Gulden and Vessey, 1997; Fei and Vessey, 2003; Fei and Vessey, 2004).

The inhibitory effects of nitrate can manifest themselves at three levels: initiation of symbiosis, nitrogenase activity and nodule growth (Streeter, 1988). The effects on the initiation of symbiosis can be determined by the number of nodules on the plant root. There are several explanations of the possible mechanisms for the inhibiting

[1] Specific nodulation is a more informative parameter with regard to the legume-rhizobia symbiosis per se because low concentration of ammonium could promote whole plant nodulation simply by promoting overall root growth (i.e. providing more sites for infection), but not nodulation rate. Specific nodulation reflects nodulation per unit of root.

effect of nitrate on nodule initiation, such as reduction of production of flavonoids and isoflavonoids (molecular signals excreted by host roots to trigger the initial mutual recognition and signal exchanging between host legume and rhizobia) in roots (Wojtaszek, 1993), the inhibition of root hair growth (the infection site for rhizobia) (Munns 1968), decrease of lectin (necessary for the binding of the rhizobia to the root surface) production (Wojtaszek, 1993), and change of phytohormones level or ratios (Caba et al., 1998; Ferguson, 2003; Lee and LaRue, 1992). However, there are very limited explanations about the possible mechanisms of the significantly different impacts on nodulation between the two kinds of mineral N (NO_3^- and NH_4^+) at similar concentration levels (Fei and Vessey, 2003; Fei and Vessey, 2004).

To investigate the genes implicated in the differential effects of low concentration of ammonium and nitrate on the initiation of symbiosis, we chose a model organism for temperate legumes, *Medicago truncatula* (commonly known as 'barrel medic'), to conduct this research work. A variety of genomic tools have been developed (Cook, 1999) for *M. truncatula* and the whole genome sequencing focusing on the euchromatic regions is undergoing (www.medicago.org). Furthermore, the whole genome of the symbiotic partner of *M. truncatula, Sinorhizobium meliloti*, has been sequenced (Galibert, 2001).

The development of DNA microarray technology has enabled the detection of the transcript abundance of a large number of genes simultaneously at certain time points and in certain plant tissues. In collaboration with Dr. Helge Küster, (Department of Genetics, Institute of Genome Research, Bielefeld University, German) we were able to use the *M. truncatula Mt16kOLI1* microarrays produced in their institute, to investigate

the differential gene expression associated with the influence of ammonium and nitrate on the initiation of nodulation of *M. truncatula.*

1.1 Objectives

1. To compare the effects of NO_3^- and NH_4^+ at low concentration (0.1-1.0 mM) on nodulation, nitrogen fixation and growth of *M. truncatula*;

2. to determine the nodulation-promoting concentration(s) of NH_4^+ in *M. truncatula* and the effect of NO_3^- on nodulation at this concentration(s);

3. to determine the concentration level at which the differential effects of NO_3^- and NH_4^+ on nodulation are most distinguishing;

4. to identify genes regulated (induced or repressed) by inoculation at initial stages of nodulation utilizing *Mt16kOLI1* microarray;

5. to identify genes regulated (induced or repressed) by inoculation and NO_3^- (at concentration level identified as described in objective 3) at initial stages of nodulation utilizing *Mt16kOLI1* microarray technique;

6. to identify genes regulated (induced or repressed) by inoculation and NH_4^+ (at concentration level identified as described in objective 3) at initial stages of nodulation utilizing *Mt16kOLI1* microarray;

7. to identify nodulation-related genes (genes that were regulated by inoculation) that were differentially regulated by NO_3^- and NH_4^+.

2.0 LITERATURE REVIEW

2.1 Biological Nitrogen (N_2) Fixation

2.1.1 Introduction

Nitrogen (N) is an essential component for the production of amino acid and protein and consequently is one of the most required elements for the construction and maintenance of life. Although 78% of air is nitrogen (N_2), it is still a limiting nutrient for plant growth. This is due to the fact that plant can only metabolize the combined forms of N such as ammonium (NH_4^+) and nitrate (NO_3^-). Certain microorganisms, termed diazotroph, are capable of reducing (i.e., fixing) N_2 to ammonia (Hansen, 1994). This biological process is named biological nitrogen fixation (BNF) which contributes about 65% of the total annual yield of fixed nitrogen (Fisher and Newton, 2002).

This literature review starts with the description of three types of N_2-fixing relationships found in nature and the biochemical function of nitrogenase- the enzyme complex which reduces N_2 to ammonium. Concerning the legume-rhizobia symbiosis, the general features of the two symbiotic partners, the process of the establishment of symbiosis and several important molecules (e.g., flavonoid, Nod factors, lectin) involved in this process, several distinct structures and organs produced in the symbiosis (e.g. infection thread, nodules, symbiosomes, O_2-diffusion barrier), the transfer of fixed nitrogen from nodule to other parts of the plant, and the current development in *Medicago truncatula* research have been included. Furthermore, the influence of combined nitrogen on legume-rhizobia symbiosis has been described at the three levels: initiation of symbiosis (pre-infection and infection process), the nodule growth, and the

N_2-fixation process, with an extra section specially covering the interactions between mineral nitrogen and phytohormones in the nodulation process. Finally, several important features of real time qRT-PCR and DNA microarray techniques are explained.

2.1.2 Modes of BNF

Biological systems that are capable of fixing atmospheric N_2 can be generally classified into three groups: the free-living microorganisms, which fix nitrogen alone and do not normally, or necessarily, have a symbiotic partner such as a plant; the "associations", in which the diazotrophs colonize the rhizosphere and sometimes the interior surface of outer root cortical cells, or intercellular space (endophytes) of host plants; and the mutulistic symbiosis, in which plants harbor nitrogen-fixing bacteria within their tissue (Vessey, 2004; Postgate, 1998). However, it should be noted that differences between these three groups are not always clear-cut and a number of representatives may belong to two groups. Also the inclusion of endophytes in associations or mutulistic group is arguable due to the uncertainty about whether the fixed nitrogen in the endophytes is transferred to the plants by death and mineralization of diazotrophs or through a direct and rapid transfer as occurs in legumes nodules. The latter is an essential feature of mutulistic symbiosis (James, 2000).

2.1.3 Nitrogenase

All diazotrophs rely on the enzyme complex, nitrogenase, for the reduction of molecular nitrogen. The overall stoichiometry of biological N_2-fixation can be summarized in the following equation:

$$N_2 + 8H^+ + 8e^- + 16MgATP \rightarrow 2NH_3 + H_2 + 16MgADP + 16\ Pi$$

Although several different nitrogen-fixing enzymes exist, distributed among over 100 species of diazotrophs, it is useful to refer to the whole family of enzymes as 'nitrogenase' (Postgate, 1998).

2.1.3.1 Molybdenum Nitrogenase. The 'conventional' molybdenum nitrogenase complex consists of two metalloproteins, the iron (Fe) protein and the iron-molybdenum (FeMo) protein. The small, Fe protein (encoded by *nifH* gene) is a homodimer with a molecular mass of 60-64 kDa. The Fe protein transfers the electrons from electron donors (such as ferredoxin or flavodoxin) to the FeMo-protein at a cost of ATP. The FeMo protein is a heterotetramer ($\alpha_2\beta_2$) of approximate 230 kDa in molecular weight. The α subunit as a molecular mass of approximate 56kDa, encoded by the *nifD* gene while the β submit has a molecular mass of approximate 60kDa and encoded by the *nifK* gene. Each individual $\alpha\beta$-dimer of the FeMo protein contains two different metalloclusters: P-clusters and FeMo-cofactor. Whereas the P-cluster likely participates in inter-protein electron transfer, the FeMo-cofactor is the active site of substrate (such as N_2) binding and reduction (Fisher and Newton, 2002).

2.1.3.2 Alternative Nitrogenase. In addition to molybdenum nitrogenase, some alternative nitrogenases exist in some bacterial species. In these species, usually under Mo limiting environment, the Mo element in the FeMo protein of nitrogenase is replaced by V, and when V is also absent, Fe can take this place, and the enzyme thereby formed are referred to as V-nitrogenase and Fe-only nitrogenase, respectively (Vance, 2002). Comparing to the Mo-dependent enzymes, the two alternative nitrogenases have lower specific activities and less efficiency (Postgate, 1998).

2.1.3.3 A Novel Nitrogenase: *Streptomyces thermoautotrophicus* Nitrogenase. Although this newly identified nitrogenase also contains Mo, it has several unique features comparing to the conventional Mo nitrogenase (Gadkari, 2002). These include different encoding genes, different proteins, different *in vivo* electron donor and different spectrum of substrates. The uniqueness of this nitrogenase was also demonstrated by the fact that several potent inhibitors of the conventional nitrogenase activity, the O_2, CO, H_2 and MgADP, have no effect on its function at all (Fisher and Newton, 2002).

2.2 The Legume-Rhizobia Symbiosis

2.2.1 Introduction

Although there are many potential sources of fixed N in terrestrial ecosystems, symbiotic N_2-fixation by legume-rhizobia provides the largest input of N for agriculture with several hundred kg of fixed N/ha per year being commonly reported (People et al, 2002). This symbiosis relationship will be elucidated in detail in following section.

2.2.2 The Symbiotic Partners

2.2.2.1 The Macrosymbionts- the Legume Family. Leguminosae (Fabaceae) consists of more than 17,000 species which pertains to more than 200 genera, and is the third largest family of flowering plants. As important agricultural plants, legumes serve as food, forage and edible and industrial oil. Close to 60% of legume genera or approximately 20% of all legume species have been tested for nodulation with rhizobia, in which nodulation for approximately 90% of the species has been confirmed (Hansen, 1994).

2.2.2.2 The Microsymbiont- the Rhizobia. The symbiotic partners of legumes, belonging to six genera *Rhizobium, Bradyrhizobium, Sinorhizobium, Mesorhizobium*

Azorhizobium and *Allorhizobium,* are collectively referred to as rhizobia (Spain, 2000). They are motile, gram-negative, and rod-shape bacteria with dimension of approximate 0.5-0.8 μm by 1.3-3.0 μm. Rhizobia are able to invade the roots of their legume host plant where they trigger the formation of a new organ, the root nodule, in which N_2-fixation occurs (Vance, 2002).

2.2.3 Establishment of Symbiosis

In symbiotic N_2-fixation, plants benefit directly from the presence of the microsymbiont, since approximately 90% of the fixed N_2 is translocated from the bacteria to the plant (Hansen, 1994). Favorable conditions for N_2-fixation can be maintained by the structure and function of the symbiotic plant organs, the root nodules. The successful development of the root nodule involves several important steps, the pre-infection mutual recognition between the host legume and rhizobia, the infection by the rhizobia, and the induction of root cortical and pericycle cell divisions and their subsequent differentiation into a functional nodule.

2.2.3.1 Pre-infection Stage

It was demonstrated that the symbiotic relationship of legume/rhizobia can only develop if plants and bacteria are compatible, which implies the existence of a mutual recognition process (Hansen, 1994; Vance, 2002). This process clearly is a result of multiple activities occurring at several stages of the formation of symbiosis and between both partners of the symbiosis. Two classes of signal molecules are known to play crucial roles at the initiation of the symbiosis: the first are compounds excreted by the roots of the host and perceived by the bacteria, in general flavonoids; the second compound are

the lips-chito-oligosaccharides (LCOs), or so-called Nod factors, which are secreted by bacteria and perceived by the host plant.

2.2.3.1.1 Flavonoids. Flavonoids are implicated in the induction of rhizobial chemotaxis, which plays an important role in the root colonization process (Yost, 1998). However, the chemoattraction by flavonoids is probably not a determinant factor for host specificity since non-symbiotic bacteria respond also to the exudates of legumes (Hansen, 1994). Flavonoids also induce the transcription of bacterial nodulation genes (*nod* genes). One of these *nod* genes, *nodD*, is activated by certain flavonoid and then becomes a transcriptional activator of the other *nod* genes. The recognition between the *nodD* genes of certain rhizobia and the specific flavonoids secreted by certain legumes is believed to be the first level of host-specific recognition in the symbiosis (Vessey, 2004). The proteins encoded by these *nod* genes are involved in biosynthesis and secretion of the second class of signal molecules, Nod factors, which are perceived by plants (Mirabella, 2002). In *Sinorhizobium meliloti*, multiple isoforms of the *nodD* genes exist, which is thought to be an evolutionary adaptation of the bacteria to recognizing different groups of flavonoids and hence form symbiosis relationship with multiple hosts (Spaink, 2000).

2.2.3.1.2 Nod Factors. Nod factors are specific lipo-chito-oligosaccharides (LCOs). In general, they consist of a β-1,4-linked N-acetyl-D-glucosamine backbone with four or five residues. The non-reducing terminal sugar moiety is substituted at the C2 position with a fatty acid which generally has a length of 16 or 18 carbons. Additional substitution on both the reducing and non-reducing terminal sugars determine the host specificity of certain rhizobia (Mirabella, 2002). Identification of Nod factor receptors and following signaling transduction represents one of the recent highlights of plant biology research

(Riely et al., 2004). Several Nod factor receptors have been identified in the two model legumes *Medicago truncatula* (Limpens et al., 2003) and *Lotus japonicus* (Madsen et al, 2003; Radutoiu et al, 2003). The involvement of multiple plant receptors for Nod factors were suggested by Ardourel *et al.* (1994): a low stringency receptor which could be activated by the most basic Nod factor structure, the chitin oligomer, and induce the root-hair deformation and cortical cell division; and a high stringency receptor which recognize Nod factors with host-specific modifications and mediates the formation and maintenance of the infection thread and early nodulation-related gene (*ENOD*) expression (Riely et al., 2004).

2.2.3.1.3 Lectin and Attachment of Rhizobia to the Root Hair. Upon being chemoattracted to a legume rhizosphere by the root exudes, rhizobia attach to root hair via a lectin-mediated mode or a non-specific mode. Lectins of plant origin have been implicated to be involved in the recognition and attachment for a long time (Dazzo and Hubbell, 1975), due to their specific binding sites for certain saccharide moieties at the surface of rhizobia. Several experiments supported this hypothesis by introducing one legume's lectin gene into the other legume and consequently the transgenetic legume obtained the ability to form the symbiosis with the compatible rhizobia strains of the donor legume (Diaz et al., 1989; Van Rhijin et al., 1998, 2001). Besides the lectin hypothesis, Smit et al. (1992) presented a two-step attachment model, in which the first step is a non-specific attachment involving a bacterial secreted Ca^{2+}-binding protein, rhicadhesin. The second step of the attachment involving the plant lectins and/or bacterial appendages such as cellulose fibrils and fimbriae, leads to a firm attachment.

2.2.3.1.4 Infection Zone. Although rhizobia will attach to the root hairs in different developmental stages, the new, rapidly growing root hairs appear to be the most susceptible to infection (Vance, 2002). In vetch (*Vicia sativa*), the susceptible zone is about 2 mm long and encompasses young root hairs that have almost reached their mature state (Heidstra 1994).

2.2.3.2 Infection and Nodule Formation

2.2.3.2.1 Infection Thread. The root hair's curling can be induced by Nod factors and the bacteria attaching to the root hair are enclosed within the curled root hair tip. Then the growth of the root hair wall is reoriented to form the infection thread. The infection thread is a tunnel-like structure which provides a conduit for the bacteria to reach the root cortex and the developing nodule meristem (Vance, 2002).

2.2.3.2.2 Two Types of Nodules. Simultaneous (or prior) to the formation of infection threads, cortical cell division is triggered by the Nod factors and finally leads to nodule formation. Two major distinguished developing models of legume root nodules are determinate nodules and indeterminate nodules (Hansen, 1994).

Determinate Nodules. In spherical determinate nodules, such as those of soybean (*Glycine max* (L.) Merr.) and French bean (*Phaseolus vulgaris.* L.), a primary nodule meristematic region in the outer cortex, begins to divide and differentiates into a region housing the rhizobia. Later, a secondary meristematic region originates near the pericycle and eventually forms the vascular system of the nodule which is connected to the root vascular system and in charge of the transport of metabolistic substances between the two symbionts. Further growth of both meristematic regions leads to the

joining of the two. Subsequently, the cell enlargement results in a spherical nodule, which does not possess meristematic tissue upon maturation (Hansen, 1994; Vance, 2002).

Indeterminate Nodules. Meristem development in indeterminate nodules, such as those of pea (*Pisum sativum*), alfalfa (*Medicago sativa*) or white clover (*Trifolium repens*) are initiated only in the inner cortex adjacent to the pericycle and opposite the protoxylem. Cell division followed by cell enlargement results in an elongate cylindrical-shape nodule. Three regions are visually distinguishable for a mature indeterminate nodule: a white one on the nodule top, comprising of the apical meristem zone and the zone of infection thread invasion; a pink region (the N_2-fixing zone), due to the presence of leghemoglobins, contains the symbiosomes (see 2.2.3.3), and a green or brown region at the base of the nodule, contains cells that undergo senescence. Different from determinate nodules, an apical meristem still exists in mature indeterminate nodules (Hansen, 1994; Vance, 2002).

2.2.3.3 Symbiosomes. Infection threads continue growing to invade the nodule primordium where the bacteria are released into plant cell cytoplasm. The released bacteria are enclosed within a plant-derived membrane called the peribacteroid membrane (PMB). The bacteria and membrane surrounding them have been termed symbiosomes, in which the process of N_2-fixation occurs. The PMB prevents contact between the bacterium and host plant cytosol and is also the selective barrier regulating nutrient exchange between host cells and rhizobia (Vance, 2002).

2.2.3.4 the Oxygen Paradox. Oxygen is a paradox for all aerobic diazotrophs. On the one hand, their nitrogenase could be destroyed on contact with oxygen; on the other hand, oxygen is necessary for them to produce energy and reducing power to fuel their life

activities including N_2-fixation. Free living diazotrophs developed various strategies to exclude oxygen from the sites nitrogenase activity (Postgate, 1998), whereas for the rhizobia in the legume nodules, this job is done by the O_2-diffusion barrier in the inner cortex of nodule and the leghaemoglobin in the cytosol of the infected cells together. The O_2-diffusion barrier, comprising of a compact layer two to four cells in thickness, reduces the oxygen supply to the infection zone to a concentration harmless to nitrogenase. At the same time, transport of O_2 from the diffusion barrier to the sites of respiration by bacteriods is facilitated by the high affinity O_2-carrier, leghaemoglobin (Bergersen, 1997; Vance, 2002).

2.2.3.5 Transfer of Fixed N. Ammonium synthesized by nitrogenase is released from the bacteroid and transported via an ammonium-transporter (Kaiser et al, 1998) across the symbiosome membrane into the host cell cytoplasm where initial ammonium-assimilation into amino acids occurs through the concerted action of several enzymes such as GS (glutamine synthetase) and GOGAT (glutamine amide-2-oxoglutarate aminotransferase) etc. The forms of N compounds which are transported out of the nodule in the xylem sap to other plant organs for further N metabolism are amides (glutamine and asparagines) for most temperate legumes having indeterminate nodules, and ureides (allantoin and allantoic acid) for most tropical, determinate-nodule legumes (Vance, 2002).

2.2.3.6 Autoregulation. Autoregulation is defined by Rolfe and Gresshoff (1988) as that developing infection centers, prior to the onset of nitrogen fixation, trigger a general plant response that inhibits further cell division activity in newly developing root tissue. Autoregulation is considered as a way the legume plants control the number of nodules

on the root systems. Reciprocal-grafts between hypernodulating mutant and wild-type soybean indicate that shoot factors involved in regulation of nodulation (Abd-Alla, 2001; Ceatano-Anollès and Gresshoff, 1991). The gene (*GmNARK*) involved in the long-distance signal transduction of shoot controlling nodulation was isolated from the supernodulating mutants of soybean (Searle et al., 2003), which is a receptor-like protein. A gene encoding a distantly related protein of GmNARK in *M. truncatula* (TC77448) is present on the *Mt16kOLI1* microarray.

2.2.3.7 *Medicago truncatula* - A Model Organism for Temperate Legume. Legumes have several specific features which *Arabidopsis thaliana*, a model organism for plants, does not. These include their capability of forming symbioses with both rhizobia and arbuscular mycorrhizal fungi. The latter colonize roots of about 80% of vascular plants and improve their nutrient (especially phosphate) uptake (Newman and Reddell, 1987). To better exploit the symbiosis relationships between plants and these microbes, two legume species have been chosen as model plants for legume research, *Medicago truncatula* (Barker et al., 1990), representing legumes originated from temperate region and bear indeterminate nodules, and *Lotus japonicus* (Regel) K. Larsen (Handberg and Stougaard, 1992), representing legumes originated from tropical region and bear determinate nodules.

Medicago truncatula, commonly known as "barrel medic", has several advantages as genetic research material, including a short generation time (75-85 days), a comparably small diploid genome (450Mbp), autogamous genetics, and ease of transformation by *Agrobacterium* (Fedorova et al. 2002). Meanwhile, standardized *M. turncatula* DNA microarrays are available or under development at several research

institutions (Küster et al. 2004; Institute of Genome Research, Bielefeld University; *NSF Project #0109732:* Integrated Functional Genomics of Natural Products), and these allow high throughput analysis of gene expression profile. *M. truncatula* is a close relative to alfalfa (*Medicago sativa* L.), an important forage crop, and moreover, a comparison between soybean and *M. turncatula* revealed very high levels of microsynteny between the two genomes, which suggest that information derived about the *M. turncatula* genome has enormous implications even for soybean (Frugoli and Harris, 2001) and potentially for all other crop legumes. With 226,923 expressed sequence tags (ESTs; TIGR (The Institute for Genomic Research) *M. truncatula* Gene Index, Release 8.0, January 19, 2005) deposited in publicly accessible databases and the undergoing whole genome gene space sequencing (http://medicago.org/genome/about.php), *M. truncatula* is indisputably a perfect plant for identifying how the exogenous nitrate and ammonium differentially influence the gene networks that initiate the legume-rhizobia symbiosis.

2.3 Influence of Combined Nitrogen on Legume-Rhizobia Symbiosis

The presence of combined nitrogen (e.g. NH_4^+, NO_3^-, and urea) generally negatively influence symbiotic N_2 fixation due to the much higher energetic costs to develop, maintain and operate effective nodules comparing to absorbance and assimilation of the mineral nitrogen existing in the rhizosphere (Gan et al., 2004). The inhibitory effects of mineral nitrogen can manifest themselves at three levels: initiation of symbiosis (pre-infection and infection process), nodule growth and nitrogenase activity (Streeter, 1988).

2.3.1 Influence of Combined Nitrogen on Pre-infection Events

2.3.1.1 Host. The accumulation of flavonoids and isoflavonoids within roots, together with other phenolics, have been reported to be inhibited by mineral nitrogen (Wojtaszek et al. 1993; Cho 1991a, 1991b). Simultaneously, the exudation of flavonoids and isoflavonoids was also suppressed by mineral N, with higher concentration of nitrogen exerting a higher inhibitory effect (Wojtaszek et al., 1993). Recent research demonstrated that preinoculation of *Bradyrhizobium japonicum* with an isoflavonoid compound, genistein, a major Nod factor inducer in the *B. japonicum*, could partially overcome the inhibition of mineral N on soybean nodulation and N_2-fixation (Pan et al., 2000).

2.3.1.2 Bacteria. The presence of combined nitrogen in excess impairs several key rhizobial symbiotic activities (Lopez-garcia et al., 2001). It has been demonstrated that nitrogen (mainly ammonium) negatively regulates bacterial nod gene expression in *B. japonicum* and *S. meliloti* (Dusha et al., 1989; Wang and Stacey, 1990). Recent research proved that *B. japonicum* grown under the presence of 1 or 0.1 mM $(NH_4)_2SO_4$ displayed lower exopolysaccharide content, lower soybean lectin binding, lower expression level of the *nodC* gene, decreased nodule number per plant, and poorer competitive status compared to bacteria grown in an N-starvation medium (Lopez-garcia et al., 2001).

2.3.2 Influence of Combined Nitrogen on Infection Events

A series of infection steps are negatively affected by the existence of combined nitrogen, including a decrease in root hair deformation, a decrease in the number of rhizobia binding to root hairs, (Streeter, 1988; Hansen, 1994), an inhibitory effect on initial cortical cell divisions and the formation of infection thread (Carroll and Mathews, 1990), and inhibitory effects on some early nodulin genes (Charon et al., 1997).

It was also found that the effect of NH_4NO_3 on blocking the root hair deformation induced by Nod factor was confined only to the root hairs that developed in the presence of NH_4NO_3, whereas NH_4NO_3 was not able to block the deformation of the root hairs that developed before the addition of NH_4NO_3 (Heidstra et al., 1994).

The inhibitory effect of nitrate and ammonium on the infection process could also be evident by the decreased number of nodules produced on the legume root (Streeter, 1988). However, it was observed that ammonium, at the concentration range of 0.1-2.0 mM, stimulates the specific nodulation in pea (*Pisum Sativum*) in various culture systems including hydroponic culture system (0.1 and 0.5 mM, Waterer et al., 1992; 0.2 mM, Waterer and Vessey, 1993a; 1.0 mM, Bollman, 2002), sand culture system (2.0 mM NH_4^+, Gulden and Vessey, 1997), and solution flow-through growth-pouch system (0.5 and 2.0 mM, Fei and Vessey, 2003). Most recently, the same stimulating effect was observed in another temperate-origin legume, white clover (*Trifolium repens* cv. Haifa) (0.1 mM, Fei and Vessey, 2004).

Several specific features of this stimulating effect were found (Fei and Vessey, 2003). Firstly, this stimulating effect is concentration-dependent; higher concentration of ammonium, varying between 1.0 mM and 8.0 mM inhibits the specific nodulation (1.0 mM, Waterer and Vessey, 1993a; 2.0 mM, Bollman, 2002; 8.0 mM, Gulden, 1997; 2.5 mM, Fei and Vessey, 2004). Secondly, the stimulating effect is species-dependent; low concentration of ammonium inhibits specific nodulation in a tropical-origin legume, soybean (*Glycine max* [L.] Merr.) (0.5-2.0 mM, Gulden and Vessey, 1998). Thirdly, the stimulating effect is dependent upon the form of nitrogen; NO_3^- has been found to be

inhibitory to the specific nodulation at the concentration of 0.1 mM or above (Waterer and Vessey, 1993b; Bollman, 2002).

2.3.3 Influence of Combined Nitrogen on Nodule Growth

When combined N is added to nodulated roots, nodule growth is arrested and nodule endodermis grows to progressively surround the apical meristem, which becomes inactive. When the N source is removed, the apical meristem is reactivated, and thus nodule growth resumes (Patriarca et al., 2002). In another experiment with soybean, the increase in diameter of the nodules almost completely ceased after 1 d of supplying 5 mM NO_3^-, and the nodule growth quickly returned to the normal growth rate following withdrawal of nitrate from the nutrient solution (Fujikake, 2003). Nodule growth is more sensitive to nitrate addition than to additions of ammonium (Imsande, 1986).

2.3.4 Influence of Combined Nitrogen on Nitrogenase Activity

It has been long recognized that combined N inhibits the N_2-fixation function of legumes (Streeter, 1988) and the inhibitory effect is reversible (Fujikake, 2002).

Four hypotheses were put forward to explain the mechanism of this inhibitory effect: the carbohydrate deprivation hypothesis, the nitrite toxicity hypothesis (Streeter, 1988), the decreased O_2 diffusion into nodules hypothesis (Vessey and Waterer, 1992) and the feedback inhibition hypothesis (Bacanamwo and Harper, 1997).

The carbohydrate deprivation hypothesis proposed that when nitrate is supplied, its reduction and assimilation will demand large amounts of carbohydrate to supply the metabolic backbones and the reducing power, and hence the available carbohydrate and reducing power in the root nodules will decrease which caused the depressed nitrogenase activity. This hypothesis was supported by the observations that sugar, when supplied

together with nitrate to the plant, alleviated the inhibitory effect of nitrate on nitrogenase (Streeter, 1988). It was also supported by another experiment in which the amount of ^{14}C-labeled photosynthate transported into nodules is decreased by nitrate and ammonium (Fujikake, 2003). The biggest drawback of this hypothesis lies in the difficulties of determining cause and effect (Streeter, 1988) since the observed reduced supply of carbohydrate to the nodule tissue could also be an effect of a decreased requirement caused by an inhibition of nitrogenase activity.

The nitrite toxicity hypothesis is based on the observation that nitrite is a potent inhibitor of nitrogenase from a wide range of N_2-fixing organism and the assumption that when nitrate is supplied to the plant, the nitrate reductase (NR), existing in plant cytoplasm as well as in the bacteriod formed from some rhizobia strain, will covert the nitrate to nitrite and therefore increase the concentration of nitrite in bacteriod to inhibit the nitrogenase activity (Streeter, 1988) or the leghemoglobins activity (Arrese-Igor et al, 1997, 1998) . Since the nitrate reductase from the bacteroid was shown not to influence the inhibitory effect of nitrate on N_2-fixation (Garcia-Plazaola et al., 2000), attention has been paid to plant mutants which have lowered NR activity. The inhibition of nitrogenase by nitrate was alleviated in a NR-deficient mutant pea plant during a 2-day exposure to nitrate. However, long term exposure to nitrate resulted in severe inhibition of nitrogenase activity in the mutant plant, which might be due to toxic effect of the high amount of nitrate accumulated in the plant tissue (Walsh and Carroll, 1992).

The O_2 diffusion hypothesis proposes that the addition of nitrate, in some way, decreases the permeability of the O_2-diffusion barrier in the inner cortex of legume nodule, reduces the amount of available oxygen for producing enough energy and

reducing power which in turn limits the activity of nitrogenase. By using an indirect measuring method, the oxygen limitation coefficient, it was reported that nitrate exposure causes a greater oxygen limitation of nodule metabolism than in non-N controls (Vessey et al, 1988; Kaiser et al., 1997).

The feedback inhibition hypothesis suggests that the regulation of nitrogenase activity by nitrate may be through sensing change in the composition of the phloem supply to nodules. Two products of nitrate metabolism, glutamine (Neo and Layzell, 1997) and asparagines (Bacanamwo and Harper, 1997) have been suggested to be involved in the feedback regulation process.

2.4 NO_3^- and NH_4^+ Metabolism in Plants

2.4.1 Transporters

Physiological studies suggested three distinct nitrate uptake systems existing in plants (Forde and Clarkson, 1999). A constitutive low-affinity transport system (LATS), a constitutive and a nitrate-inducible high-affinity transport system (cHATS and iHATS). The NO_3^- concentration borderline between high- and low-affinity systems is species dependent and usually around 0.5 mM (Williams and Miller, 2001). Two protein families have been identified as nitrate transporter based on the substrates (besides NO_3^-) they are capable of transporting across the cell membrane: the nitrate-nitrite porters (NNP) and the peptide transporter (PTR). In accordance, two gene families, *NRT1* and *NRT2*, were recognized to encode these two protein families, PTR and NNR respectively. Although, the matches of HATS to *NRT2* and LAST to *NRT1* are generally accepted, their relationship appeares to be more complicated by the fact that an Arabidopsis nitrate transporter, *AtNRT1.1*, displayed dual-affinity (Liu et al., 1999).

The existence of both low- and high affinity ammonium transport systems in plants have also been revealed by physiological experiments (D'Apuzzo, 2004). In contrast to the nitrate transporter naming system, the genes encoding high- and low-affinity ammonium transporter are denoted as *AMT1* and *AMT2* respectively. The ammonium inducible *AMT1* was also observed in tomato and rice (Loque and von Wiren, 2004)

2.4.2 Metabolism.

In plant cells, nitrate is converted into ammonium via two enzymes, nitrate reductase and nitrite reductase. ammonium is then combined with glutamate to yield glutamine through the GS - GOGAT cycle. Depending on the species, the majority of the absorbed nitrate could be either assimilated in roots or translocated to the shoots and assimilated there, and ammonium, in contrast, is mainly assimilated in the root (Tobin and Yamaya, 2001). Glutamine as a major metabolic intermediate product of both nitrate and ammonium assimilation, has been suggested as a major metabolic trigger for the down-regulation of ammonium and nitrate uptake (Loque and von Wiren, 2004).

2.5 Interactions Between Mineral Nitrogen and Phytohormones in the Nodulation Process

There is abundant evidence for the involvement of plant hormones in the nodulation process. The information on three hormones, auxin, cytokinins and ethylene is most detailed and their involvement, as well as their interaction with nitrate, will be briefly discussed below.

The involvement of auxin in nodule development was supported by the fact that the auxin transport inhibitor N-(1-naphthyl) phthalamic acid induces the formation of

pseudo-nodules on the roots of different legumes (Patriarca et al., 2004). Mathesius et al. (1998) used a precise spot-inoculation method and a fused auxin-responsive *GH3:gusA* gene to show that IAA flowing from the shoot was blocked at the inoculation spot which led to a lower auxin level between the inoculation spot and root tip and higher auxin level immediately above the inoculation spot. They further observed high auxin activity in the progenitor cells of nodule primordia. It was suggested that nitrate's inhibition of nodulation could be imposed via its depressing effect on flavonoids accumulation in the root and flavonoids could function as auxin transport inhibitors (Coronado et al., 1995).

Cytokinins can mimic Nod factors' function in inducing the inner cortical cell divisions, amyloplast accumulation and expression of some early nodulin genes, which suggested the involvement of cytokinins in the early signaling events that leads to nodule initiation (reviewed by Mathesius et al., 2000). Recent research using the fused cytokinins responsive *ARR5*: *gusA* gene has suggested that cytokinins levels are up-regulated in the initially dividing cells in the cortex as well as in the deforming root hair cells (Lohar et al., 2004). Nitrate was found to inhibit the cytokinins-induced cortical cell division in white clover (Mathesius et al., 2000) and in alfalfa (Bauer et al., 1996) and was proposed to due to its inhibiting the cytokinins level or sensitivity in the inner cortex cell (Mathesius et al., 2000).

Based on available data, Mulder et al. (2005) hypothesized that cytokinins and auxin, both increase in the progenitor cells of the nodules primordial, may then act synergistically to initiate cell divisions and nodule primordial formation.

The stimulating effect of nodulation in pea by low concentration of ammonium was recently suggested to be related to the increased cytokinin: auxin ratio in roots (Fei

and Vessey, 2003). It was found that ammonium, at nodulation stimulating concentration in pea, increased the cytokinins (zeatin) concentration, but had not effect on root IAA concentration. The exogenous application of cytokinins (6-BAP) stimulated root nodulation in a similar pattern to a 0.5 mM NH_4^+ treatment, whereas IAA did not increase the nodulation level. Similar observations were also confirmed in white clover (Fei and Vessey, 2004).

Exogenous ethylene has been shown to inhibit nodulation in most legumes studied, including legumes producing indeterminate nodules such as *P. sativum, M. turncatula,* and *M. sativa* and legumes producing determinate nodules such as *L. japonicus* and *P. vulgaris* (Mulder et al., 2005). In another study, the inhibitory effect of endogenous ethylene on the initiation of cortical cell division was shown to determine the nodules positioning: nodules only developed at the position opposite to the protoxylem poles where ACC oxidase, which synthesizes the last step in the biosynthesis pathway of ethylene, was expressed at a very lower level (Heidstra et al., 1997). NO_3^-, at inhibitory concentration, increased the ethylene production by 5-d-old roots (Lee and LaRue, 1992). The proposal of the involvement of ethylene in mediating the inhibitory effect of nitrate on nodulation was also based on the findings that the ethylene synthesis or action inhibitors (AVG (aminoethoxy-vinylglycine) and Ag^+, respectively) could overcome nitrate's inhibition of nodulation (Ligero et al., 1991; Caba et al, 1998). Other support for the involvement of ethylene in nitrate regulation came from a nitrate-tolerant supernodulating soybean mutant *nts* which displayed tolerance to ethylene too (Caba et al., 1999).

2.6 Gene Expression Analysis

"Transcription is the first and main level of regulation of gene expression. Variations in the ensemble of the mRNA molecules of a cell, the transcriptome, are largely reflected in equivalent variations in the population of the cell protein" (Lorkowski and Cullen, 2003). Real time quantitative reverse transcription PCR (qRT-PCR) and DNA microarrays are two newly-developed methods to analyze differential gene expression.

2.6.1 Real time qRT-PCR

Real time qRT-PCR method, as its name implies, monitors the PCR reaction in the "real time" throughout the entire PCR process, or monitors the amount of target PCR product after each PCR cycle. The development of this method was prompted by the commonly recognized limitation of the conventional PCR method in determining the initial copy number of cDNA in a sample. In conventional PCR, because the process is allowed to proceed to saturation (usually 30 to 40 cycles), the final amount of PCR product cannot accurately reflect the initial amount of the cDNA. By using a combination of fluorescent dye and instruments that are capable of detecting fluorescence signal instantly, the relative amount of double strand amplicons (in the form of fluorescence density) at the end of each cycle could be monitored and determined in a real time PCR reaction. Therefore, the quantification of initial template DNA amount can be made by reverse extrapolating the amount of PCR product from the early exponential phase of the PCR reaction. Combined with reverse transcription, real time quantitative PCR is also used to quantify the amount of mRNA species (transcripts) existing in an RNA preparation. It has advantages over other commonly used transcripts-quantitative methods

such as Northern blotting, RNAse protection assay, and in situ hybridization in its comparatively high sensitivity (Bustin, 2000).

Real time PCR data analysis methods may be broadly classified as "absolute" or "relative" (Livak and Schmittgen, 2001). Absolute quantification involves the construction of a standard curve based upon known copy numbers of target sequence, whereas relative approaches involve determining the change in expression level relative to another set of experimental samples, typically the experimental control group (Peirson et al. 2003). Relative Real time RT-PCR is the most popular method to validate microarray results (Chuaqui et al., 2002).

There are generally two fluorescence-labeling methods for the amplicons. The first method involves the design of a specific probe which is labeled with a fluorescent dye molecule and a quencher molecule to quench the fluorescence signal of the probe. This probe is also complementary to one strand of the amplicon. Upon hybridization to the amplicon or hybridization first and then hydrolyses by the 5`-nuclease activity of the DNA polymerase, the fluorescence signal will be released from the quencher and can then be detected. The second method involves a non-sequence-specific double-strand DNA binding dye (SYBR Green). SYBR Green displays very low fluorescent signal when it's unbounded, yet once intercalated into the double-strand amplicon, it fluoresces much stronger. For both methods, the more amplicons produced, the higher the fluorescent signal intensity.

Since SYBR Green binds to any double-stranded DNA, it is not able to discriminate the desired (target) PCR product and the undesired (non-target) PCR product. Therefore, the detected fluorescence will not be able to reflect the actual copy

number of the desired PCR product if the designed primers allow the production of undesired PCR product(s). This problem can be detected by two validating methods following the PCR reaction. Firstly, a melt curve analysis can be run right after the end of PCR reaction by increasing the temperature of the reaction solution from 60 °C to 95 °C. Melt curve analysis is based upon observing the fluorescence of SYBR Green (bound to amplicons) continuously throughout a temperature cycle. PCR product denaturation can be observed as a rapid loss of fluorescence near its melting temperature (Tm) (Ririe et al., 1997). Since the Tm is set by GC/AT ratio, as well as the length of the PCR product, this method allows the discrimination between single PCR product and multiple PCR products. The melt curve of a single PCR product will be smooth; the melt curve of multiple PCR products will not. Secondly, the PCR product can be loaded onto an EtBr-agarose gel to examine whether a single band with designed length is produced.

2.6.2 DNA Microarray Technique

2.6.2.1 Introduction. The first research paper using high density DNA microarray (also called gene array or gene chips) was published in 1995 (Schena et al., 1995), and ever since that time, this technology has rapidly gained its popularity and now "comes to dominate many conferences and journals (Kohane et al., 2003)".

DNA microarray is a hybridization-based method, in which the single-stranded DNA fragment representing the complete or partial sequence of multiple genes (termed probes) are chemically fixed on a glass surface, and the mRNA or reversely-transcribed cDNA from certain tissue or cells (termed targets) will be labeled and incubated together with the targets (usually 14-18 hr) to allow the complementary probe and target sequence to anneal. Similar to the conventional gene expression analysis methods (such as

Northern blotting, RNase-protection etc.), the higher copy number of certain mRNA species exists in the experimental material, the higher signal intensity of the label (either in the form of fluorescence dye or radioactive isotope) will be captured. Thus, by comparing the relative difference of the signal intensity of the same mRNA (cDNA) from different treatments, the relatively differential expression level of this gene between the treatments can be determined. Unlike conventional gene expression analysis methods which describe only the expression level of one or a few desired genes, microarray method allows the investigation of the expression of thousands of genes (even all the genes of the genome) in a single hybridization and significantly improves the efficiency and productivity of differential gene expression analysis.

2.6.2.2 The *M. truncatula Mt16kOLI1* Microarray. The *Mt16kOLI1* microarrays were manufactured in the Department of Genetics, Institute of Genome Research, Bielefeld University, German. This microarray contains 16,086 70mer oligonucleotides, and each 70mer oligonucleotide is duplicately spotted on the array. The 16,086 70mer oligonucleotides, representing all 16,086 tentative consensus sequences (TCs)[2] from TIGR Gene Indices Database MtGI Release 5.0 (released on May 3, 2002), were designed and synthesized by Qiagen company (Medicago Genome Oligo Set Version 1.0). There are several features of these 70mer sequences: they were normalized to a melting temperature (Tm) 78°C+ 5°C, they were optimized using BLAST against all known *M. truncatula* genes to minimize cross-hybridization, and they were designed within 1000 bases of 3' end of each gene to facilitate working with cDNA obtained by

[2] TCs (Tentative Consensus) are consensus sequences based on two or more ESTs (Expressed Sequence Tag, obtained by single-pass sequencing either end of a cDNA clone) that overlap for at least 40 bases with at least 94% sequence identity. The best hits annotation for TC's were assigned by searching the TC set against a non-redundant amino acid database(nraa) using BLAT. (Cited from The Institute of Genomic Research (TIGR) website).

oligo-dT priming (Product introduction of Medicago Genome Oligo Set Version 1.0). The slides used to produce the microarray are the QMT Epoxy slides (Quantifoil).

2.6.2.3 The Probe Labeling Method and The Common Reference Experiment Design Method. Two probe labeling methods are commonly used in microarray work: the single color labeling method and the dual color labeling method (Jordan, 2001). In the dual color labeling method, two dyes (typically green (Cy3) and red (Cy5)) are used to label the two probe pools from two samples (treatments) which are to be hybridized on the same microarray slide.

Two major designs are used in the dual color microarray experiments involving the comparison of gene expression spanning time course or between multiple treatments: direct comparison and indirect comparison (Speed, 2003). Direct comparison uses a so-called loop design which compares the gene's expression between samples from certain treatments and time points directly on the same slide. Indirect comparison, in contrast, uses a common reference sample, in which one of the treatment samples and one common reference sample are hybridized on the same slide, and the gene expression comparison between treatment samples is conducted in an indirect way by using the expression level of common reference sample as the common denominator. An ideal common reference should provide a signal in all spots on the array (i.e. be able to hybridize to all the targets to be investigate in the experiment), so as to assure that no information is lost when the ratios are calculated. Pooling part of the RNA of all the samples used in the experiment has been reported to be effective in achieving the ideal common reference (Eisen and Brown, 1999).

3.0 MATERIALS AND METHODS

3.1 Introduction of General Approach

To fulfill all the objectives listed in 1.0 Introduction, a series of experiments were conducted. First, two experiments were conducted in a nutrient solution flow-through sand culture system to investigate the effect of ammonium (NH_4^+) and nitrate (NO_3^-) separately at concentration range 0.1-1.0 mM on growth, nodulation and nitrogen fixation, respectively. Secondly, one experiment was conducted in a nutrient solution flow-through growth pouch culture system to compare the effects of NH_4^+ and NO_3^- (at 0.1 and 0.5 mM levels) in the same experimental system at the same time. Various parameters were measured in these two experiments including dry weight (DW) of the plant parts, nodule number, total nitrogen, and ^{15}N abundance. Thirdly, one experiment aiming at identifying the genes regulated by the three treatments (inoculation-only, inoculation plus 0.1 mM NH_4^+ and inoculation plus 0.1 mM NO_3^-) at three time points (6 hpi (hours post inoculation), 12 hpi and 24 hpi) was conducted by utilizing *Mt16kOLI1* microarrays. In addition, a small experiment using real time qRT-PCR technique was conducted to monitor several marker genes which were known to be regulated by ammonium or nitrate in order to test the reliability of the mRNA population of the samples and to compare the differential expression of three specific marker genes to the microarray results.

3.2 Biological Materials

Medicago truncatula cv. Jemalong, Line 17, in which a variety of genomic tools have been developed (Cook, 1999), and the microsymbiont, *Sinorhizobium meliloti* 2011, the genome of which has been sequenced recently (Galibert, 2001), were used in this experiment. The *M. truncatula* was the courtesy of INRA-SGAP laboratory in Toulouse, France and the inoculant was provided by Dr. Hani Antoun, University of Laval.

3.3 Physiological Characterization of the Differential Effects of NH_4^+ and NO_3^- on Growth, Nodulation and N_2-fixation of *M. truncatula*

3.3.1 Experiment 1a and 1b: Using A Nutrient Solution Flow-through Sand Culture System

Two experiments were conducted using a nutrient solution flow-through sand culture system. Experiment 1a (Exp. 1a) investigated the effects of four concentrations (0.0 mM, 0.1 mM, 0.5 mM and 1.0 mM) of NH_4^+ on plant growth, nodulation and N_2-fixation respectively, and Experiment 1b (Exp. 1b) investigated the effects of the same four concentrations of NO_3^-. In both experiments, plants treated with N-free nutrient solution were used as controls.

3.3.1.1 Seed Germination. Before germination, the seeds of *M. truncatula* were picked out of the pods, scarified by rupturing the seed coat slightly with fine sand paper, checked under a dissecting microscope for the integrity of cotyledon, sterilized by immersing seeds in 25% commercial bleach for 2 min and then thoroughly rinsed with sterilized distilled H_2O (sdH_2O) for 3 min. Seeds were imbibed for 6 h in sdH_2O and then germinated in autoclaved seed growth pouches (CYG™, Mega International, West St.

Paul, MN, USA; 15.5×14.5 cm) in the dark. Twenty ml of sdH_2O was added to each pouch and the growing direction of the radicle was adjusted to vertical 24 h after germination if necessary.

3.3.1.2 Plant Growth. When the radical length reached 5-7 cm (usually within 3 days), seedlings were transferred into 2-L pots filled with coarse silica sand of one plant per pot. The 2-L pot was constructed from polyvinyl chloride pipe (10 cm in diameter and 26.0 cm in height) with a drain hole located 25mm from the bottom. Plants were first supplied with an N-free common nutrient solution (see below) for 48 h, and then each of the plants was inoculated with 3 ml of *S. meliloti* 2011 (10^8 cfu/ml) 20 min before applying the nutrient solutions. In Exp. 1a, the treatments were 0.0, 0.1, 0.5 or 1.0 mM 1%^{15}N-enriched NH_4^+ (prepared from a 1 M $(NH_4)_2SO_4$ stock solution) in a common nutrient solution. In Exp. 1b, the treatments were 0.0, 0.1, 0.5 or 1.0 mM 1%^{15}N-enriched NO_3^- (prepared from a 1 M KNO_3 stock solution) in a common nutrient solution.

The basic composition and concentrations of mineral nutrients in the common nutrient solution were the same as previously described (Waterer, 1993) except that the concentration of $H_2PO_4^-$ was changed to 0.75 mM and K^+ was changed to 1.0 mM in accordance. The initial concentrations of other nutrients were 0.25 mM Ca^{2+}, 0.25 mM Mg^{2+}, 19 μM $B(OH)_4^-$, 3.7 μM Mn^{2+}, 7.2 μM Cl^-, 0.3 μM Zn^{2+},0.13 μM Cu^{2+}, 0.05 μM MoO_4^-, and 10 μM Fe^{3+} as 300 Fe-Sequestrene (Ciba-Geigy Corp., Research Triangle Park, NC, USA). In Exp. 1a, the concentration of SO_4^{2-} varied between 0.5 mM to 1.0 mM, and the variation of SO_4^{2-} at this range has been shown previously not to differentially affect growth in our culture system. In Exp. 1b, the concentration of K^+ varied from 1.0 mM to 2.0 mM.

The common nutrient solution was made up in a 200-L tank. Twenty-L carboys were used to make up nitrogen-containing nutrient solutions by adding the appropriate amount of NH_4^+ and NO_3^- stock solutions into the common nutrient solutions. At the last harvest date, NH_4^+ and NO_3^- concentrations in the reservoirs as well as residual amounts drained from the pots were determined with a Dionex Ion Chromatograph (model 4000, Dionex Corp., Sunnyvale, CA, USA) using a CS12A column (for NH_4^+) and an AS4A separator column (for NO_3^-). The original concentrations (concentration in the carboy reservoirs) of the two forms of nitrogen were ranging from 97% to 105% of desired concentrations whereas the nitrogen concentrations in the drain solution were ranging from approximately 30% to 75% of original concentration. This proved that during the whole experiment period, the plant roots were exposed to approximately 30% or higher of desired mineral nitrogen concentrations.

A high precision multi-channel dispenser (model CE ISM1-B, Labortechnik-Analytik, Glattbrug, Switzerland) pumped the appropriate nutrient solution into the top of each pot at a constant speed of 1 ml/min; the nutrient solution passed through the root area and then flowed out of the drain hole at the bottom of the pot. A circle of landscape cloth was placed on the top of sand to prevent the growth of algae.

Plants were grown in a controlled-environment cabinet set at 25/20°C (day/night) temperature and 16/8 h (light/dark) photoperiod and exposed to a photon flux density of 300 ± 50 μmol m^{-2} s^{-1} provided by a combination of Cool White VHO and Grolux fluorescent lamps (Sylvania Inc., Drummonville, Québec, Canada) at a ratio of 3:1. A completely randomized experimental design was employed.

3.3.1.3 Plant Harvest and Analysis. Six randomly selected plants from each treatment were harvested at 10 days after inoculation (DAI) and the remaining 6 plants were harvested at 20 DAI. Plants were separated into shoots and roots and the sand surrounding the roots was gently rinsed away with dH_2O. Plant parts were stored at -80°C, and thawed on ice at a later date when nodules were picked off the roots and counted. Shoot, root and nodules of each plant were then dried for 4 days in a freeze dryer (Model Freeze Dryer 7, Labconco Inc., Kansas, MO, USA) and weighed. The component parts from each plant were then combined, pulverized and analyzed for total nitrogen content by a dry combustion method using a Leco nitrogen analyzer (Model NS-2000, Leco Corp., St. Joseph, MI, USA) and for ^{15}N abundance by using an ANCA-MS nitrogen determinator/mass spectrometer (Europa Scientific, Crewe, U.K.) in the Stable Isotope Laboratory, University of Saskatchewan. The percentage of nitrogen derived from the fertilizer (%NDFF) is calculated using the formula (Gulden, 1997):

$$\%NDFF = \left(\frac{\%^{15}N_{treatment} - \%^{15}N_{reference}}{\%^{15}N_{fertilizer} - \%^{15}N_{reference}}\right) \times 100$$

Plants treated with N-free nutrient solution were the reference. This formula is based on the classical equation for calculating %NDFF in field studies (Hardarson, 1993), but modified for our culture system. In our system, the only available nitrogen source for reference plant is the atmospheric N_2 and the only two available nitrogen sources for treatment plants are the mineral nitrogen in the nutrient solution (fertilizer) and the atmospheric N_2. The amount of nitrogen stored in the cotyledon was negligible (the average weight of individual seed is around 3 mg) and not considered. The percentage of nitrogen derived from the atmospheric N_2 (%NDFA) was calculated by subtracting %NDFF from 100. The total plant NDFF was determined by multiplying the %NDFF by

the total plant N content and the total plant NDFA was determined by subtracting the total plant NDFF from total plant N content.

3.3.1.4 Statistical Analysis. The two experiments were analyzed separately. All the data of each experiment were subjected to a one-way ANOVA analysis by using the SAS program (SAS Institute Inc., Cary, NC, USA). Where significant differences were detected ($P \leq 0.05$), differences among means were detected using the Fisher protected least significant difference test (LSD).

3.3.2 Experiment 2: Using A Nutrient Solution Flow-through Growth Pouch Culture System

Experiment 2 (Exp. 2) was conducted in a nutrient solution flow-through growth pouch culture system to investigate the effects of two concentrations (0.1 mM and 0.5 mM) of NH_4^+, the same two concentrations of NO_3^- on growth, nodulation and N_2-fixation in *M. truncatula* in the same experiment. Plants treated with an N-free nutrient solution were used as the control. Only the details of the experiment procedures that were different from what was described in the sand culture experiment are described below.

3.3.2.1 Seed germination. Seeds were chemically sacrificed and sterilized by immersing into concentrated sulfuric acid for 13 min, and then imbibing in sdH_2O for 6 h. Around 50 seeds were then transferred into a Petri dish with two layers of sdH_2O-saturated filter paper. The Petri-dishes were first placed at 4°C for 48 h to synchronize the seeds and then invertedly placed in dark at 22°C to allow seeds' germination. When the radicles reached 1 cm (usually after 24 h), seven seedlings were transferred into each autoclaved seed growth pouch where the radicles reached 5-7 cm within 3 days in dark.

3.3.2.2 Plant growth. Seedlings with 5-7cm radicles were then transferred to large growth pouches (H45cm×W20 cm) formulated of a nylon/polyethylene film (VAK-4-R film, WinPak Ltd., Winnipeg, Manitoba, Canada) with 2 drain holes at the bottom of each pouch as described in Fei and Vessey (2004). The growth pouch was hung in a black container and the root area was covered by a black plastic paper to prevent light from reaching the roots. One plant was grown in each growth pouch. All the plants were first supplied with the N-free common nutrient solution for 48 h before the application of inoculants and appropriate nutrient solutions. The nitrogen concentrations in the drain nutrient solution were 28% to 60% of the original concentrations at 48 h harvest time. The nutrient solution delivering methods, the plants growth conditions, and the composition and concentration of the four nitrogen-containing nutrient solutions (0.1 and 0.5 mM 1%^{15}N-enriched NH_4^+ and NO_3^-) and the N-free nutrient solution were as described in Exp 1a. A complete randomized experimental design was employed.

3.3.2.3 Plant harvest and analysis. Nine plants of each treatment were harvested at 20 DAI and assessed for root, shoot and nodule dry weight, nodule counts, and total N content and ^{15}N abundance as described in Exp 1a and 1b.

3.3.2.4 Statistics analysis. A one-way ANOVA analysis and Fisher's protected least significant test (LSD) were employed as described in Exp 1a and 1b.

3.4 Analysis of Differential Gene Expression During the Initiation of Symbiosis With and Without the Presence of NH_4^+ and NO_3^- by Utilizing *Mt16kOLI1* Microarrays

3.4.1 Experimental Design

The most distinguishing effects between ammonium and nitrate on nodulation were observed at 0.1 mM level in the physiological study (Fig. 4.4). So this concentration was used for investigating the genes implicated by the inoculation treatment as well as the genes implicated in the effects of ammonium and nitrate on the initiation of nodulation by utilizing DNA microarray technique. The complete experiment design is described in Table 3.1.

Table 3.1 Experimental design for *Mt16kOLI1* microarray analysis

Treatment[1]	Inoculants	Nutrient solution	Harvest time (Name of sample[2])
Control	-	Without N	0 h (0h0N), Before inoculation
Inoculation-only	+	Without N	6 hpi[3] (6h0N), 12 hpi (12h0N), 24 hpi (24h0N)
Inoculation/NH	+	With 0.1 mM NH_4^+	6 hpi (6hNH), 12 hpi (12hNH), 24 hpi (24hNH)
Inoculation/NO	+	With 0.1 mM NO_3^-	6 hpi (6hNO), 12 hpi (12hNO), 24 hpi (24hNO)

1. Inoculation/NH: inoculation plus 0.1 mM NH_4^+; Inoculation/NO: inoculation plus 0.1 mM NO_3^-
2. Name of sample indicating the treatments and harvesting time, e.g. 6h0N, 6hNO, and 6hNH representing samples harvested at 6 hpi from inoculation-only treatment, inoculation/NO treatment and inoculation/NH treatment.
3. hpi, hours post inoculation

An indirect comparison method with a common reference which comprised of the pool of all the ten samples in equal portions was used in the microarray experiment design. The gene expression comparisons between samples were conducted through an indirect way by using the expression level of common reference sample as the common denominator.

3.4.2 Plant Growth and Harvest.

To accumulate enough seedling root material for total RNA preparation, the same experiment was conducted twice. The root material harvested in the first experiment was used as sample (as named in Table 3.1) and the root materials harvested in the second experiment were used as the common reference in the microarray experiment.

3.4.2.1 Seed Germination. Seed germination methods were the same as described in Exp 2. After seedling radicles reached 1 cm in the Petri dishes, they were transferred into the autoclaved seed growth pouch (CYG™, Mega International, West St. Paul, MN, USA, 15.5×14.5 cm). To maximize the amount of root material for RNA extraction, twenty-eight seedlings were grown in each pouch, with each of the two sides of the paper insert holding fourteen seedlings. The growth pouches were held vertical by sitting them in aluminum stands (Mega International, West St. Paul, MN, USA). Plant seedlings were kept in the growth pouch in the dark for 4 days for elongation of their radicles.

3.4.2.2 Plant Growth. The aluminium stands together with growth pouches were moved into growth chamber and the growth condition was as described in Exp. 1a and 1b. Seedlings were allowed to grow for another 48 h with the supply of N-free nutrient solution to build up their photosynthesis system. Thereafter six pouches of seedlings (0h0N sample) were harvested, N-free nutrient solution supply was stopped and 10 ml *S. meliloti* 2011 (10^8 cfu/ml) was added into each pouch. After plants were inoculated for 20 mins, nutrient solutions containing zero nitrogen, 0.1 mM NH_4^+, and 0.1 mM NO_3^- were applied. The basic composition and concentration of the nutrient solution, the nutrient solution delivery methods were as described in Exp 1a and 1b. The only difference was that the nutrient solution-delivering speed was set to 2 ml/min in stead of 1 ml/min. The

nitrogen concentrations in the drain solution were approximate 0.05 mM for NO_3^- and 0.07 mM for NH_4^+ at the last harvesting date.

3.4.2.3 Plant Harvest. Six pouches of seedlings roots from sample 0h0N (control) were harvested immediately before inoculants were added. Thereafter, six pouches of seedling roots from each treatment were harvested at each of the three harvesting time points (6, 12 and 24 hpi). Roots of the seedlings were separated from shoots, and then carefully and quickly removed from the surface of the paper insert and immediately immersed into liquid nitrogen. Each harvest was finished within 25 min. 0 h and 24 h harvests were started at 3 h into the light period to eliminate variation as a result of gene expression change in related to night/day alternation. After each harvest, roots were kept at -80°C until RNA extraction.

3.4.3 DNA Microarray Experiment

3.4.3.1 Introduction of General Procedure. The common reference was prepared at one time. Specifically, 40 μg purified total RNA from each of the ten samples were combined together and aliquoted to 20 portions (20 μg per portion). Each proportion was then subjected to one labelling reaction with a vial of Cyanine-3 (Cy3) fluorescence dye (Amersham Biosciences Corp., Piscataway, NJ, USA). All of the twenty Cy3-labelled cDNA samples were then again mixed together and after quantification by spectrophotometry, were aliquoted to 20 portions of 50 pmol Cy3-labeled cDNA each, and stored at -20°C.

The sample cDNA was prepared immediately before microarray hybridization. Specifically, cDNA prepared from 40 μg total RNA of each sample was labelled with Cyanine-5 (Cy5) fluorescence dye (Amersham Biosciences Corp., Piscataway, NJ, USA)

as described below, then divided into two equal portions (50 mmol Cy5 each portion, calculating method see Appendix A), and each portion was then hybridized to one microarray, so there were two technical replicates (microarrays) for each sample.

During microarray hybridizations, one portion of the Cy3-labelled common reference cDNA and one portion of the Cy5-labelled sample cDNA were combined together and applied on the same microarray.

Due to the complexity of the DNA microarray protocols, only the most important procedures are described below. A much more detailed protocol used for the experiment is included in Appendix C.

3.4.3.2 RNA Extraction and Purification. Total RNA was extracted from seedling roots using TriReagent® (Sigma-Aldrich Canada Ltd., Oakville, Ontario, Canada) following the manufacturer's protocol. One hundred mg root material was homogenized into 1 ml TriReagent® solution. Each 10 µg total RNA were then subjected to 1 unit DNase I treatment (Ambion, Inc., Austin, TX, USA) for 30 min to get rid of genomic DNA contamination. DNase I was then deactivated by incubation at 75°C with addition of EDTA to a final concentration of 5 mM. Thereafter, a Microcon-30YM column (Millipore Inc., Billerica, MA, USA) was used to desalt and concentrate total RNA. In summary, 50 µg DNase I-treated total RNA was applied onto each Microcon-30YM column membrane. The total RNA was rinsed three times, each by adding 500 µl Nuclease-free water (Ambion, Inc., Austin, TX, USA) into the column followed by 13,000g centrifugation for 10 min. After the last washing step, further 1-2 min centrifugation was used to reduce the volume of RNA solution to 15 µl. One µl of purified total RNA was then run on a 1.2% formaldehyde-denatured agarose gel to

examine entirety of mRNA and another 1 µl was subjected to spectrophotometer for quantification before used for reverse transcription

3.4.3.3 cDNA Target Labelling. An "Amino Allyl cDNA Labelling Kit" (Ambion, Inc., Austin, TX, USA) was used, and the manufacturer's protocol was followed, to label the cDNA probes. In summary, each reverse transcription was carried out in a 20 µl reaction volume at 37°C for 2h. In each RT reaction, 20 µg purified total RNA, 200 units of M-MLV reverse transcriptase, 0.4 unit of RNase inhibitor, 0.4 mM dNTPs (the ratio of dTTP to Amino Allyl-coupled dUTP was 1:1) and 4 µM Oligo $(dT)_{18}$ were added in a 20 µl reaction volume µg. After reverse transcription, RNA was hydrolyzed by the addition of NaOH and then incubation at 65°C for 15 min. HEPES was added to neutralize the solution before recovering the cDNA by ethanol precipitation. One vial of CyDye Post Labelling Reactive Dyes (Cy3 or Cy5, Amersham Biosciences Corp., Piscataway, NJ, USA) was used to label the cDNA produced from each RT reaction. Dye coupling reaction was conducted in the presence of sodium bicarbonate (pH=9.0) for 1h and terminated by addition of hydroxylamine and incubating at room temperature for 15 min. Each labelled cDNA sample was purified by passing through a NucAway® column (Ambion, Inc., Austin, TX, USA) and then recovered by ethanol precipitation. One tenth of each labelled cDNA sample was loaded on a 1% agarose gel to roughly examine the size distribution of cDNA. The rest of the sample was diluted into 300 µl and the amount of cDNA recovered and the amount of coupled Cy3 or Cy5 dye was determined by spectrophotometry. The formulas to calculate the amount of coupled Cyanine dye and the cDNA recovered is listed in the Appendix A. After spectrophotometer quantification, 50 pmol Cy3-labelled cDNA (one portion from the common reference) and 50 pmol Cy5-

labelled cDNA (one portion from one of the samples) were completely dried under a speed vac system (Heto Vacuum Centrifuge and Heto Cooling Trap, Rose Scientific Ltd., Edmonton, Alberta, Canada) for 40 min.

3.4.3.4 Slides Processing, Hybridization, Washing and Imaging.

Slides Processing. Before applying Cy-labelled cDNA samples onto the microarray slides, a slide processing step is required to completely block the free epoxy groups coating the surface of the microarray (these epoxy groups fix the probe DNA onto the surface of the slides). Blocking those active DNA-coupling chemical groups can eliminate non-specific binding of DNA and hence reduce the background signal. Each microarray was processed according to the protocol supplied by Dr. Küster (University of Bielefeld, Germany, see detailed steps in Appendix C).

Hybridization. Dried cDNA from one of the ten samples (labelled with Cy5) and from one portion of the "Common Reference" (labelled with Cy3) were dissolved and combined in 70 µl DIG Easy Hyb (Roche Diagnostics Inc., Laval, Québec, Canada), denatured for 5 min at 65°C and then immediately applied onto the DNA-spotted side of the microarray slide. A plastic cover slip (hybrid-slips™, Sigma-Aldrich Canada Ltd., Oakville, Ontario, Canada) was put on the top of hybridization solution to spread the solution to cover the entire DNA spotted area. Each microarray slide was placed in a hybridization cassette (Monterey Industries Inc., Richmond, CA, USA) and the cassette was placed into a hybridization incubator (Model 2000, Robbins Scientific, Sunnyvale, CA, USA) and the hybridization was conducted at 42°C for 16-18h.

Washing. Each microarray was washed to eliminate unspecific hybridization. The washing steps and the composition and concentration of the serials of washing

solutions are described in Appendix C. After washing, slides were centrifuged to dryness and kept in the dark.

Imaging. The microarrays were scanned by using the GenePix® scanner (Axon Instruments, Molecular Devices Corp. Union, CA, USA). One or two pre-scans were used to determine the best gains of the PMT (photomultiplier tubes) for each channel so that the ratio of the fluorescence intensities of the spots from both channels was close to 1.0.

3.4.3.5 Microarray Data Processing and Analysis Strategy

After flagging the bad spots due to regional contamination using Genepix® software, the microarray data were imported into Acuity® software (Axon instruments, Molecular Devices Corp. Union, CA, USA) for data analysis. In Acuity, the data of the 20 microarrays were normalized together using a Global Lowess[3] normalization method supplied by the software. After passing through a SNR>2 (Signal-noise ratio) data filter, 16021 probes out of the total number of 16,513 remained. To have good confidence on the final dataset, only probes that gave signals across all 20 microarrays were considered for subsequent analysis. The justification for this criterion is that there were only two replicate microarrays for each treatment, hence if a signal is lost on any one of the two replicates for any signal data point within a treatment, no conclusion can be drawn on that data point. However, due to an experiment accident in the 12hNH treatment, only one slide was available for analysis in this treatment. After applying this criterion, 3016 probes were left for subsequent analysis.

---

[3] Global Lowess (Locally weighted scatter plot smoothing) normalization method attempts to correct some systematic variation caused by the different labelling efficiencies of different dyes, separate reverse transcription and labelling of the two samples etc. This method is based on the assumption that (1) only a small portion of genes on the microarray will vary significantly in expression between the two samples; (2) there is symmetry in the up- and down-regulated genes.

These 3016 probes were exported into Excel. A1.5 fold change cut-off relative to the expression level in 0h0N treatment was used to define differentially expressed genes as was used in Yahyaoui *et al.* (2004). Each individual spot was used as a replicate, so we have 4 replicates for each gene on the DNA microarray. A student t-test with probability of 0.05 was used to calculate the significance of all the identified differentially expressed genes.

The focus of our analysis was on those probes that were continuously up-/down-regulated relative to 0h0N across all three time points and displayed higher than 1.5 fold up-/down-regulation level with statistics significance at least on two time points. The rationales behind this selection are that those probes are easier to be confirmed and used for the following work than those transiently-regulated probes and also that basing on more than one significant data points we can have better confidence on the results we got.

3.4.4 Validation of Reliability of the mRNA Population and Three Marker Genes Using Real Time qRT-PCR

3.4.4.1 Introduction. As a way to validate the reliability of the mRNA population of the samples to be used for microarray work, real time quantitative reverse transcription PCR (real time qRT-PCR) method was used to monitor three marker genes whose transcript levels are known to be up-regulated by ammonium and/or nitrate treatments. A putative *M. truncatula* high affinity nitrate transporter gene, *Nrt2*, (TC78158 in the TIGR *M. truncatula* gene index), has been chosen as a marker gene for nitrate-induced gene expression alteration (Amarasinghe, 1998). For ammonium-induced gene expression change, a gene encoding cytosolic glutamine synthetase of *M. truncatula*, *MtGsb* (TC85222) mRNA was chosen, whose expression was induced to 2-3 fold increase by 10

mM NH_4^+ during 4-48 h post treatment comparing to nitrogen-starved plants (Stanford et al. 1993). The expression level of a partial sequence of a putative cytokinin receptor gene *Cre1b* (TC80422) (Brandstatter, 1998; Inoue, 2001) was also investigated as a complementary research to a previous research conducted in our lab in which the endogenous cytokinin level (BAP) was found to be positively related the stimulating effect of ammonium on nodulation and exogenously applied BAP at certain concentration was able to mimic the effect of low concentration ammonium (Fei and Vessey, 2004). An endogenous control, glyseraldehyde-3-phosphate dehydrogenase (*GAPDH*), was used to normalize the initial amount of cDNA as the real time PCR template.

3.4.4.2 Total RNA Extraction and Purification. The methods used to extact and purify total RNA are the same as described in the DNA microarray experiment. The effect of *DNase I* was proved by real time PCR method. When using the total RNA which was not treated by *DNase I* as template and primers of *GAPDH* in a PCR cycle, a specific PCR product having similar melting temperature (~84°C) to *GAPDH* was produced. This is evidence that genomic DNA contamination containing the sequence of *GAPDH* was present in the total RNA preparation. In contrast, when using the *DNase I*-treated total RNA as template in the same PCR reaction, only primer-dimmer was produced based on it melting temperature close to 77°C (data not shown).

3.4.4.3 Reverse Transcription and Real Time PCR Reaction. Two μg purified total RNA was reverse transcribed with 100 units of M-MLV reverse transcriptase, 0.5 unit of RNase inhibitor, 0.5 mM each of the dNTPs and 5 μM Oligo $(dT)_{18}$ in a 20 μl reaction volume. Reverse transcription was conducted in a thermal cycler (Genius, Techne Inc., Burlington, NJ, USA). For each sample, 0.25 μl RT products were used in each real time

PCR reaction. A specific thermal cycler for fluorescence real time PCR, the Smart Cycler® (Cepheid Inc., Sunnyvale, CA, USA), was used for the quantitative RT-PCR (qRT-PCR) reaction and the fluorescent signal detection. The final concentration of each PCR components in the 25 μl reaction volume were: 0.4 μM forward and reversed primers, 3.5 mM Mg^{2+}, 0.75XSyBR Green (Molecular probe, Eugene, OR, USA), and 100 μM each of the dNTPs. To minimize the pippetting error, the *PuRe Taq Ready-To-Go* PCR beads (Amersham Biosciences Corp., Piscataway, NJ, USA) were used which contained DNA polymerase, dNTPs, 1.5 mM Mg^{2+} and PCR buffer salt. PCR condition were: 94°C initial hold for 150 sec followed by 15 sec at 94 °C for denaturation and 40 sec at 60°C for both annealing and extension. Melt curves were determined immediately following the last cycle of PCR amplification and the PCR product was also run on a 4% agarose gel to determine whether a single PCR product produced. The threshold of fluorescent signal of the PCR product was set as 30, which was based on the fact that this fluorescence intensity value always fell in the linear range of the PCR amplification curves.

The primers of the four genes were: *Nrt2*, forward primer, CGC GGC AGC ACC TTT AGT, reverse primer, CGT TAC CAA CGT CGG ATT TTG; *MtGsb*, forward primer, GAA GGC AAC GAG CGT AGG TT, reverse primer, CAA CAC CCC ATA AGA AGG TGT TAA; CRE1, forward primer, TGC TTC TAC GCA CGG AAT TG, reverse primer, AGC CTT CCC ACA TGC TTG AG; *GAPDH*, forward primer, ACA AAC ATG GGA GCA TCC TTA CTA G, reverse primer, GTT TTT ACC GAC AAG GAC AAA GCT. These primers were designed by the ABI PRISM Primer Express

program (Applied Biosystem) with the help of Dr. Genlou Sun, Saint Mary's University. The sequences used to design primers were these genes' TC sequences in TIGR database.

3.4.4.4 General Procedure For Calculating the Relative Expression Level of Genes Using Fluorescence Real Time qRT-PCR

With the threshold cycle number of a specific PCR product (e.g. *Nrt2*) in a sample determined in the primary PCR amplification curve (Fig. 3.1) and the standard curve of certain PCR product (Fig. 3.2), log value of the "relative concentration" could be calculated (Fig. 3.2). The unit of the relative concentration is the concentration of the specific PCR product (e.g. *Nrt2*) in the 1/64 dilution of the RT reaction product used for creating the standard curve. The calculated relative concentration of the specific cDNA in a sample was further divided by the relative concentration of *GAPDH* in the same sample, so the expression level of specific cDNA (e.g. *Nrt2*) in a sample is as units of the cDNA (e.g. *Nrt2*) per unit of *GAPDH*. It can be expressed as following formula:

Expression level = (Relative concentration of target cDNA) / (Relative concentration of *GAPDH*)

The calculated expression level of the marker genes in the 9 treatment samples were then divided by their expression level in 0h0N control to get their relative expression level.

Several important results produced in real time PCR methods and how they were used in the calculation of the relative expression level of certain genes were described in the following sections.

Primary Curve. Fig. 3.1 is a sample of the primary curve of real time PCR reaction. The threshold cycle number is determined by the cycle number at which the

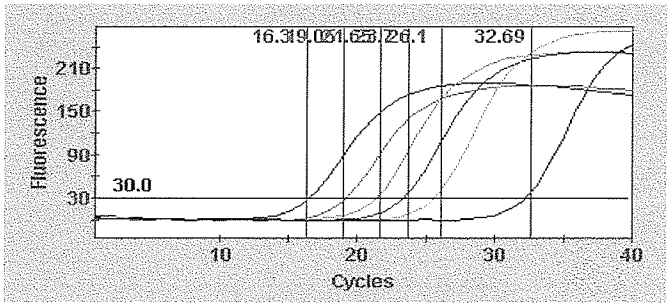

Fig. 3.1 Primary curve of real time qRT-PCR. Blue curve--1μl original concentration of RT product, azure curve—1/4 dilution, orange curve--1/16 dilution, green curve--1/64 dilution, yellow curve--1/256 dilution and brown curve--H_2O control. The number besides the vertical red lines describes the threshold cycle number—the cycle number at which the fluorescence produced by PCR product crosses the threshold fluorescence line 30. Graph was retrieved from Smart Cycler® software.

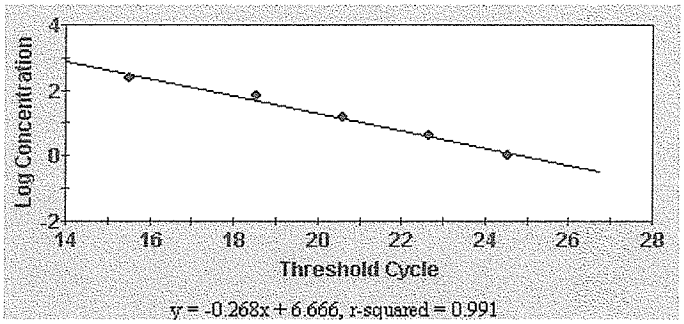

Fig. 3.2 Standard curve of *GAPDH* cDNA. Graph was retrieved from Smart Cycler® software.

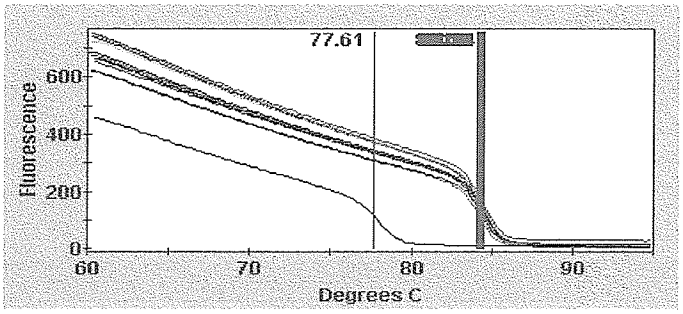

Fig. 3.3 Melting curves of *GAPDH*. Each curve except the lowest one represents the *GAPDH* PCR product in one of the PCR reactions. The vertical red lines represent the melting temperature of the PCR product. The lowest (grey) curve represents the melting curve of the non-specific PCR product in a H_2O control reaction. Graph was retrieved from Smart Cycler ® software.

fluorescence produced by PCR product crosses the threshold fluorescence line, implying the number of amplification cycle one sample needs to reach the certain copy number of a specific PCR product corresponding to fluorescence value of 30.

A H_2O control was used in each batch of PCR reaction, the primer-dimmer was sometimes observed to form in the water control reaction (Fig.3.1, brown curve). However, fluorescence produced by the primer-dimmer consistently did not increase above the background fluorescence after 30 cycles of PCR reaction, whereas all the threshold cycle number of our specific PCR product is lower than 26 cycles. Moreover, the existence of cDNA template could inhibit the formation of primer-dimmer by competition. Hence the noise produced by primer-dimmer and its amplification will not affect the experimental results.

Standard Curve. A serial dilution of 1, 1/4, 1/8, 1/16, 1/64 of 1 μl cDNA solution reversely-transcribed from 2 μg total RNA of 12hNO treatment in a 20 μl reaction volume was used to create the standard curve (Fig. 3.2). The r-squared values for all four cDNA species investigated in this experiment were between 0.99 and 1, indicating good linearity correlations between the threshold cycle numbers and log relative concentrations.

Melting Curve. Due to the non-specific binding property of SyBr Green dye, a melt curve analysis was conducted right after each PCR reaction to determine whether a single PCR product is produced. Fig. 3.3 is an example melting curve of *GAPDH* in all ten treatments. A close gathering of melting temperatures of *GAPDH* in different samples around 84°C proved the reliable of using melting curve to recognize single PCR product. The blue melting curve which displayed a lower melting temperature (77.61°C) was from

a H_2O control, and this melting temperature is due to the formation of primer dimmer (Gibellini, 2003).

Agarose Gel Documentation Determining the Production of Single PCR Product. Fig. 3.4 is a sample image of agarose gel documentation of the real time PCR products, in this case is the sequences of *GAPDH* cDNA. Single PCR product could be seen in all twelve samples and no PCR product was observed in H_2O control reaction (First lane on the left). Four each of all the genes tested in this experiment, there were always only one PCR product was detected by both melting curve and agarose gel results.

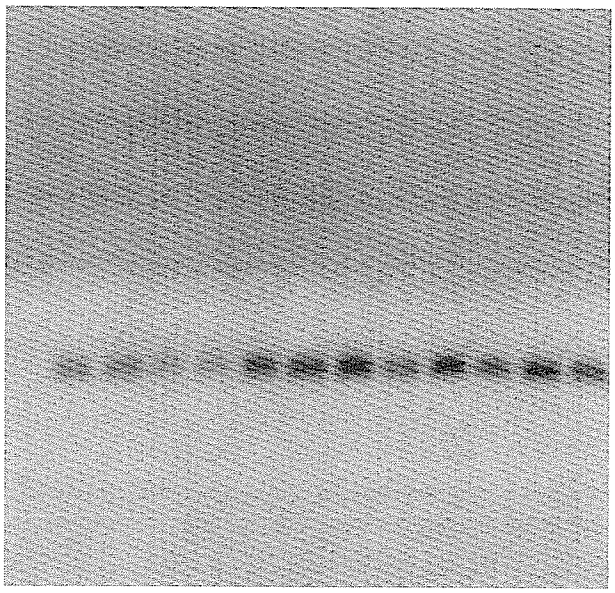

Fig. 3.4 Real time PCR product of *GAPDH* on 4% agarose gel. First lane on the left is the H_2O control.

4.0 RESULTS

4.1 Physiological Characterization of the Differential Effects of NH_4^+ and NO_3^- on Growth, Nodulation and N_2-fixation of *M. truncatula*

As described in the Material and Methods, three experiments were conducted to investigate the effect of ammonium and nitrate on growth and nodulation of *M. truncatula*. In the sand culture experiments, plants were harvested twice (10 and 20 day after inoculation, DAI) and in the growth pouch experiment, plants were harvested only at 20 DAI. Results of the two sand culture experiments were put under the subtitle of Exp. 1a (NH_4^+ experiment) and Exp. 1b (NO_3^- experiment) and result from growth pouch culture experiment was put under the subtitle of Exp. 2.

4.1.1 Plant Growth

4.1.1.1 Dry Weight (DW) Accumulation

Exp. 1a and 1b

In Exp. 1a, none of the three ammonium treatments had any significant effect on DW compared to 0.0 mM NH_4^+ (control) plants at 10 DAI (Fig. 4.1.A). At 20 DAI, the total DW of ammonium-treated plants were all higher than control plants, and the DW accumulation increased with increasing concentrations of ammonium.

Whole plant DW was generally lower in plants exposed to 0.0 mM NO_3^- than those exposed to 0.1, 0.5 and 1.0 mM NO_3^- (Fig. 4.1.B). At 10 DAI, 0.5 mM and 1.0 mM NO_3^- plants accumulated higher DW than other two treatments. At 20 DAI, all three levels of NO_3^- significantly enhanced the accumulation of whole plant DW and the enhancing effect was positively related to NO_3^- concentration.

Although DW accumulation shared the same trends between the two experiments at 20 DAI, the magnitude of the promoting effects of nitrate was quite larger than that of ammonium. At the same concentration range, approximately 2.4 to 7.6-fold increases in DW were observed in nitrate-treated plants (Fig. 4.1.A) relative to the control while only 1.4 to 2.3-fold increases were seen in ammonium-treated plants relative to the control (Fig. 4.1.B).

Exp. 2

At 20 DAI (Fig. 4.1.C), nitrate-treated plants accumulated more DW than either ammonium-treated plants or control, and there was a trend of higher DW with increasing nitrate concentration. However, both levels (0.1 mM and 0.5 mM) of NH_4^+ did not significantly increase total DW compared to the control. As to the mean values, DWs of 0.1 and 0.5 mM NH_4^+ plants were 127% and 187% of that of the control respectively, whilst the nitrate-treated plants at the same two concentrations accumulated the DWs equal to 314% and 515% of that of the control in.

4.1.1.2 Root/shoot Ratio

Exp. 1a and 1b

In Exp. 1a, the root/shoot ratio was higher in ammonium-treated plants than in control plants at 10 DAI and there were no significant difference within the three ammonium treatments ((Fig. 4.2.A). At 20 DAI, there was no difference between treatments and control plants.

In Exp. 1b, the root/shoot ratio was higher in 0.5 mM NO_3^- treatment than control plants at 10 DAI, and at 20 DAI both 0.5 and 1.0 mM NO_3^- treatments had the lowest root/shoot ratio (Fig. 4.2.B).

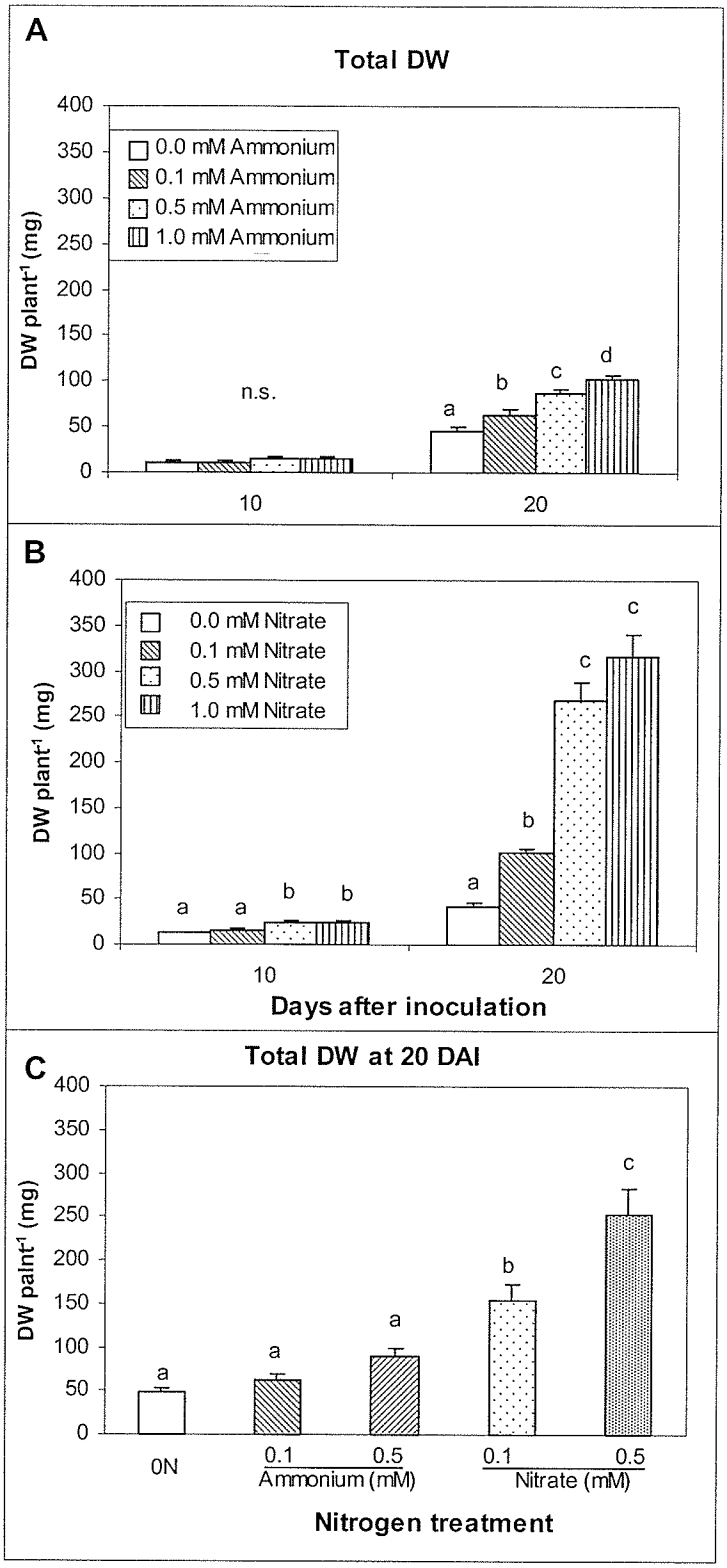

Fig. 4.1 Whole-plant DW of *M. truncatula* plants grown in different concentrations of NH_4^+ (A) and NO_3^- (B) in a flow-through sand culture system and in a flow-through growth pouch culture system (C). Bars indicate S.E. Significant differences among treatments are indicated by different letters above the bars ($P \leq 0.05$).

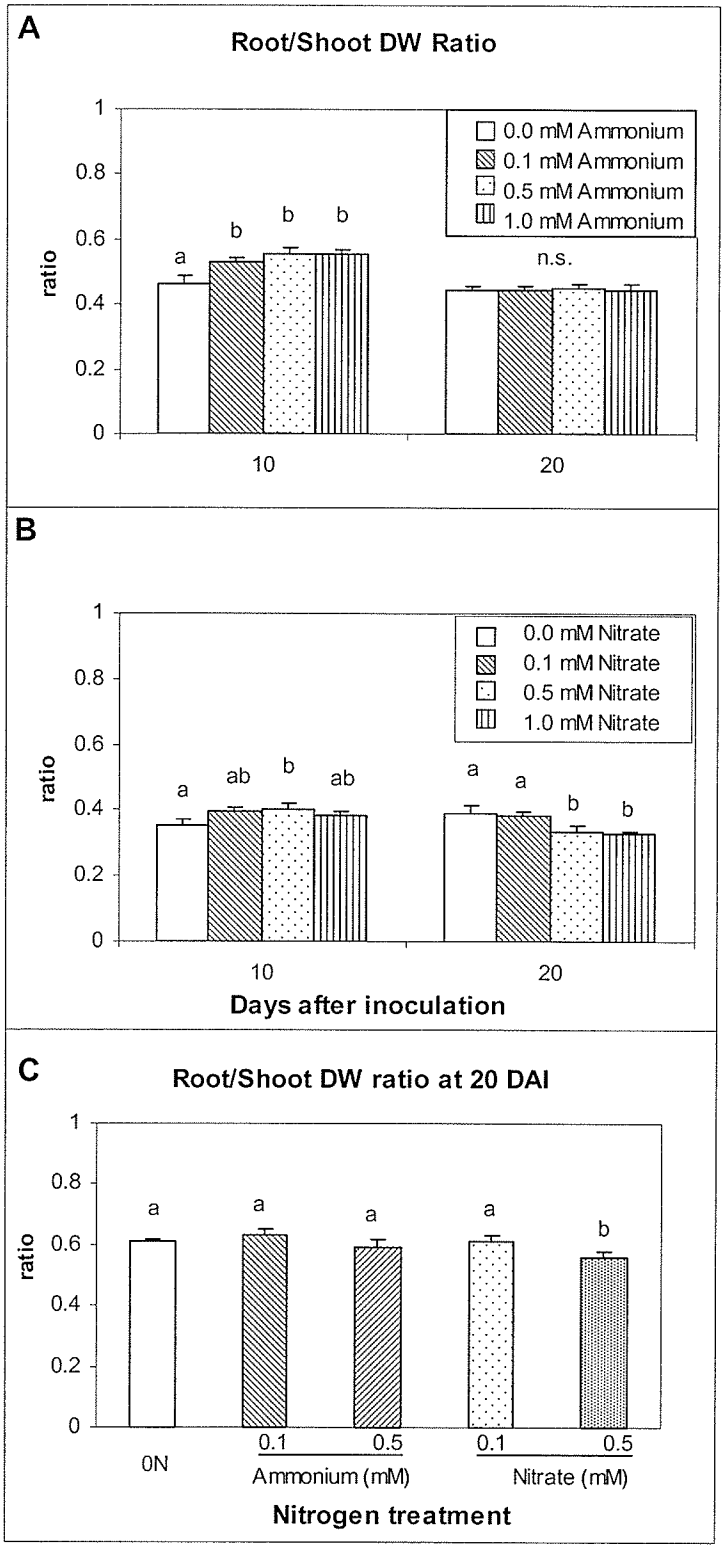

Fig. 4.2 Root/shoot DW ratio of *M. truncatula* plants grown in different concentrations of NH_4^+ (A) and NO_3^- (B) in a flow-through sand culture system and in a flow-through growth pouch culture system (C). Bars indicate S.E. Significant differences among treatments are indicated by different letters above the bars ($P \leq 0.05$).

Exp. 2

The root/shoot ratio was not significantly different between control plants, ammonium-treated plants and 0.1 mM nitrate-treated plants, and 0.5 mM nitrate-treated plants had significantly lower ratio than all other treatments and the control.

4.1.2 Nodulation

4.1.2.1 Total Nodule Number Per Plant

Exp. 1a and 1b

ammonium-treated plants did not display any significant difference in total nodule number relative to the control plants (0.0 mM) at 10 DAI (Fig. 4.3.A). The 1.0 mM NH_4^+ plants had more nodules than control (approximately 100% more) and 0.1 mM NH_4^+ plants at 20 DAI and a general trend of higher NH_4^+ concentration promoting more nodules could be observed.

At 10 DAI (Fig. 4.3.B), control plants (0.0 mM NO_3^-) bore more nodules than treatment plants (0.1, 0.5 and 1.0 mM NO_3^-), whereas at 20 DAI the trend was reversed when both 0.5 and 1.0 mM NO_3^- plants produced approximately 150% more nodules than control and the nodule number per plant increased with increasing of nitrate concentration.

The magnitude and trend of the promoting effect of ammonium and nitrate on nodule numbers were quite similar.

Exp. 2

At 20 DAI (Fig. 4.3.C), *M. truncatula* plants exposed to 0.1 and 0.5 mM NO_3^- had significantly higher nodulation than control and ammonium-treated plants, which possessed 2.5 and 2.1 times the number of nodules observed on control plants,

respectively. In contrast, plants treated with 0.1 and 0.5 mM NH_4^+ did not possess significantly more nodules than the control.

4.1.2.2 Specific Nodulation

Exp. 1a and 1b

All the ammonium treatment had fewer nodules per g root DW than control at 10 DAI (Fig 4.4.A). However, no significant differences were observed between the ammonium-treated plants and the control plants at 20 DAI. Considering the mean values of all the treatments, the 0.1 mM NH_4^+ plants and the control plants had very similar specific nodulation (2080 and 2070 nodules per unit root DW, respectively), whereas both 0.5 mM and 1.0 mM NH_4^+plants had around 85% of the specific nodulation of control plants at 20 DAI.

The specific nodulation was lower in all the nitrate-treated plants than the control plants at 10 DAI (Fig. 4.4.B). At 20 DAI, the similar trend was observed; both 0.5 and 1.0 mM NO_3^- inhibited specific nodulation significantly to 41% and 38% of that of the control plants. Specifically, although the inhibitory effect of 0.1 mM NO_3^- plants on specific nodulation was not significant at 0.05 probability level at 20 DAI, it was significant at the probability level of 0.059 and it had 80% of the control's specific nodulation.

In summary, when compare to their respective control plants, all three levels of nitrate generally inhibited specific nodulation whereas none of the three ammonium concentrations displayed significant effects on specific nodulation.

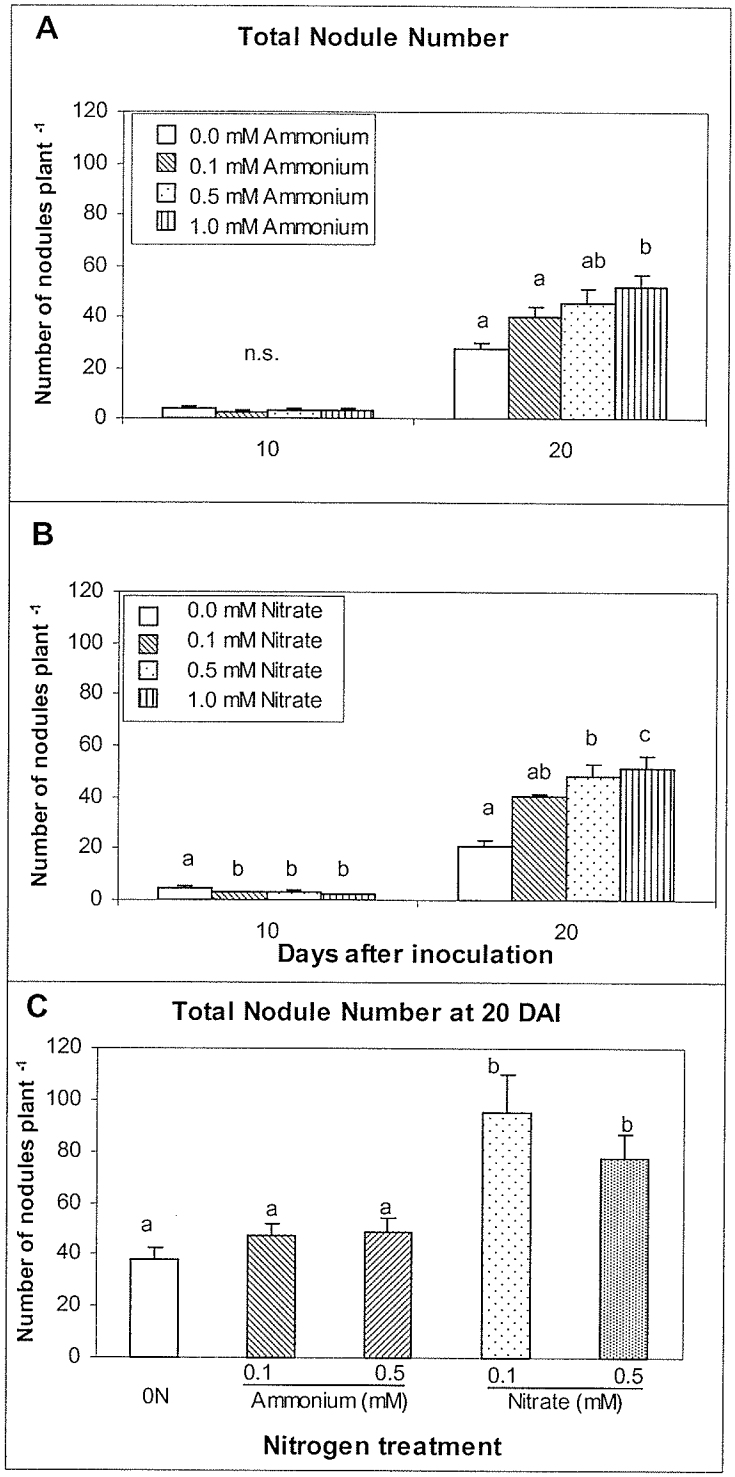

Fig. 4.3 Total nodule number on the root of *M. truncatula* plants grown in different concentrations of NH_4^+ (A) and NO_3^- (B) in a flow-through sand culture system and in a flow-through growth pouch culture system (C). Bars indicate S.E. Significant differences among treatments are indicated by different letters above the bars ($P \leq 0.05$).

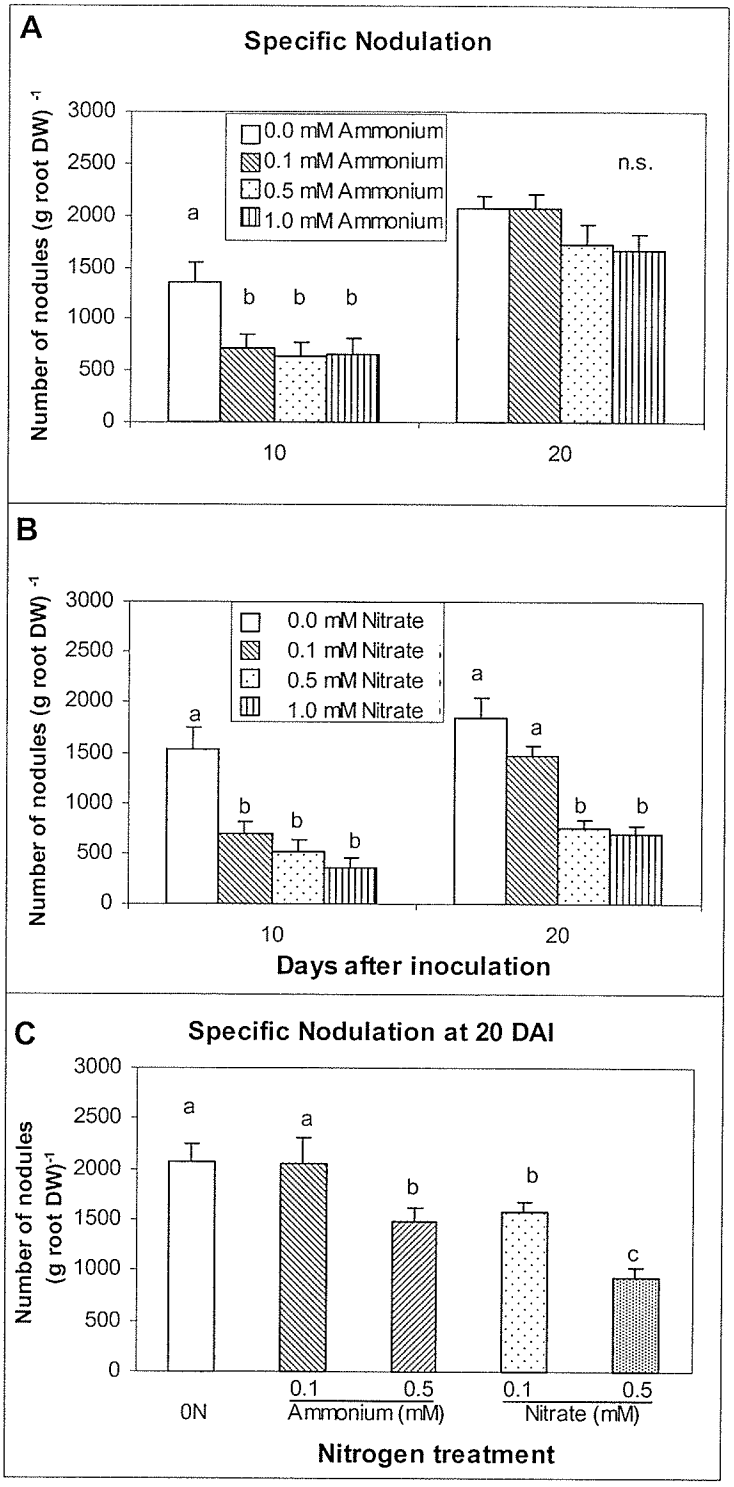

Fig. 4.4 Specific nodulation of *M. truncatula* plants grown in different concentrations of NH_4^+ (A) and NO_3^- (B) in a flow-through sand culture system and in a flow-through growth pouch culture system (C). Bars indicate S.E. Significant differences among treatments are indicated by different letters above the bars ($P \leq 0.05$).

Exp. 2

In the growth pouch experiment, specific nodulation was generally lower in nitrogen-treated plants than the control plants with the only exception of 0.1 mM NH_4^+, which displayed almost the same level of specific nodulation (99.5%) as the control plants (Fig 4.4.C). The 0.5 mM NH_4^+, 0.1 mM NO_3^- and 0.5 mM NO_3^- treatments had 71%, 76% and 45% of the control plants' average specific nodulation. The inhibitory effect of NO_3^- on specific nodulation is significantly more than ammonium at both 0.1 and 0.5 mM levels.

4.1.2.3 Individual Nodule DW

Only nodule DW at 20 DAI was measured and analyzed for both sand culture experiments as the nodule mass at 10 DAI was negligible.

Exp. 1a and 1b

At all three levels of ammonium, treated plants had nodules with lower mass than the control plants (Fig. 4.5.A). However, there were no differences on nodule weight among the three ammonium treatments and they all bore nodules approximately half the size of the control on average.

In Exp. 1b, the average individual nodule DW was highest in the control plants at 20 DAI. A continuous decrease of average nodule DW with the increase of nitrate concentration was observed (Fig. 4.5.B). The 0.1 mM NO_3^- plants had nodules approximately half the size of those on control plant roots, 0.5 mM NO_3^- plants had approximately one fourth of the size and 1.0 mM NO_3^- plants had about one fifth of the size.

Both ammonium and nitrate decreased nodule size. At the 0.1-1.0 mM concentration range, the inhibitory effect increased with the concentration of nitrate while held constant among ammoniumtreatments.

Exp. 2

In contrast to the observation in Exp 1a and 1b, only plants exposed to 0.5 mM NO_3^- had on average smaller nodules than the control (Fig. 4.5.C), which accounted for approximately 2/3 of the size of nodules of control plants. Both levels of NH_4^+ and 0.1 mM NO_3^- did not exert a significant influence on individual nodule mass in growth pouch culture system.

4.1.2.4 Total Nodule DW Per Plant

Exp. 1a and 1b

The total nodule DW was not influenced by any of the three levels of NH_4^+ (Fig 4.6.A). In contrast, the 0.1 mM NO_3^- plants had the highest total nodule mass (Fig. 4.6.B), 0.0 mM NO_3^- and 0.5 mM NO_3^- had the second highest total nodule mass and 1.0 mM NO_3^- had the lowest total nodule mass.

Exp. 2

M. truncatula exposed to 0.1 mM NO_3^- had the higher total nodule DW than control plants and the ammonium-treated plants (Fig. 4.6.C). There was no significant difference in total nodule mass between the other treatments (0.1 mM NH_4^+ and 0.5 mM NH_4^+ and 0.5mM NO_3^-) and the control.

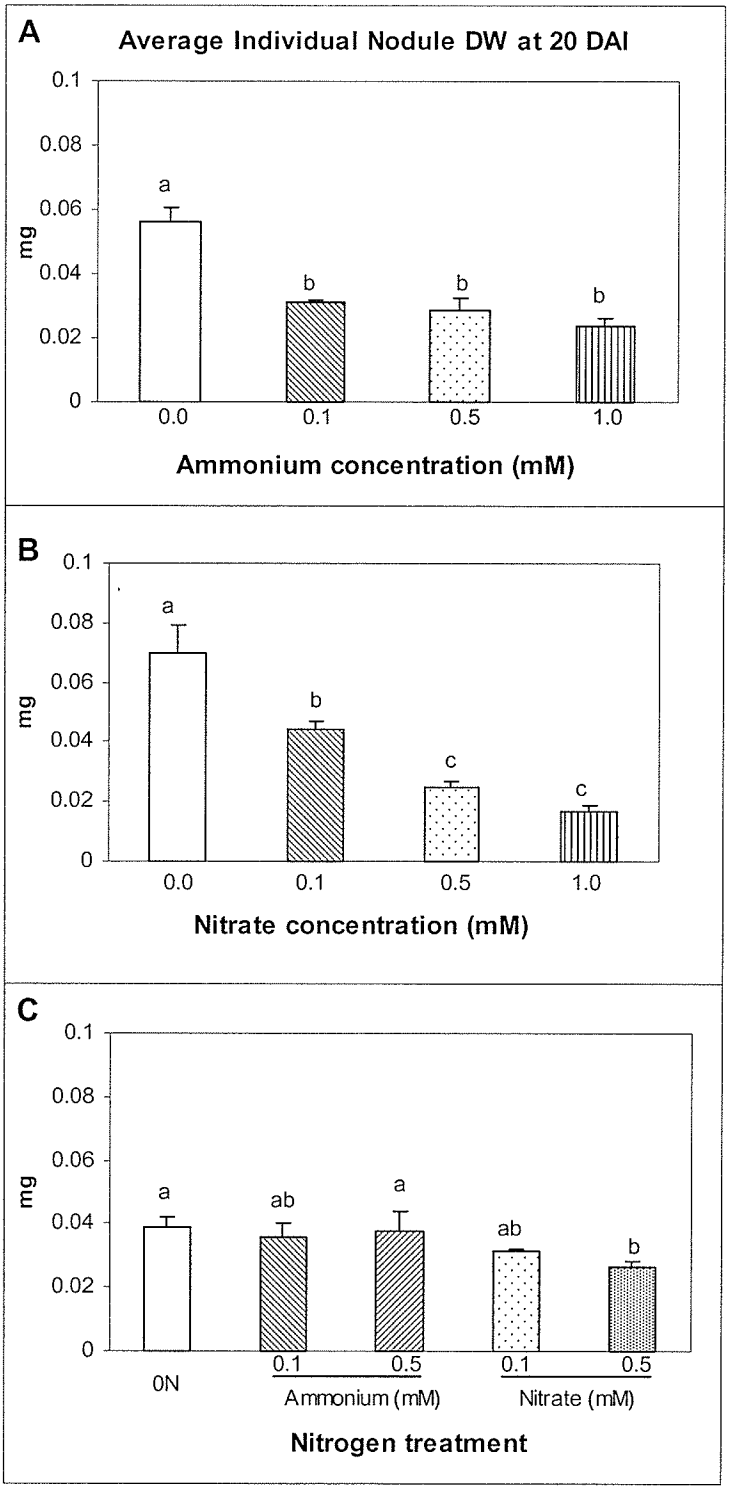

Fig. 4.5 Average DW of individual nodule of *M. truncatula* plants grown in different concentrations of NH_4^+ (A) and NO_3^- (B) in a flow-through sand culture system and in a flow-through growth pouch culture system (C). Bars indicate S.E. Significant differences among treatments are indicated by different letters above the bars ($P \leq 0.05$).

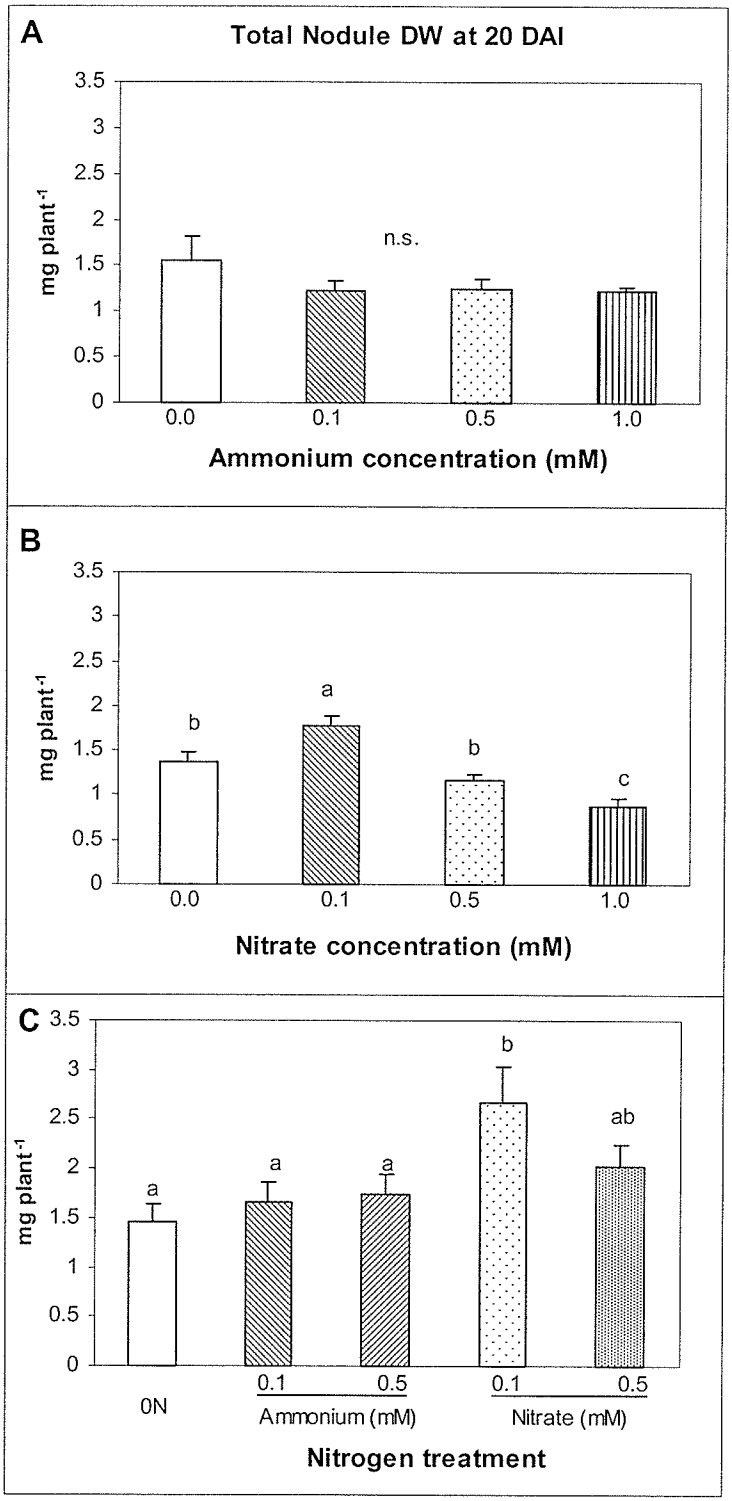

Fig. 4.6 Whole plant nodule DW of *M. truncatula* plants grown in different concentrations of NH_4^+ (A) and NO_3^- (B) in a flow-through sand culture system and in a flow-through growth pouch culture system (C). Bars indicate S.E. Significant differences among treatments are indicated by different letters above the bars ($P \leq 0.05$).

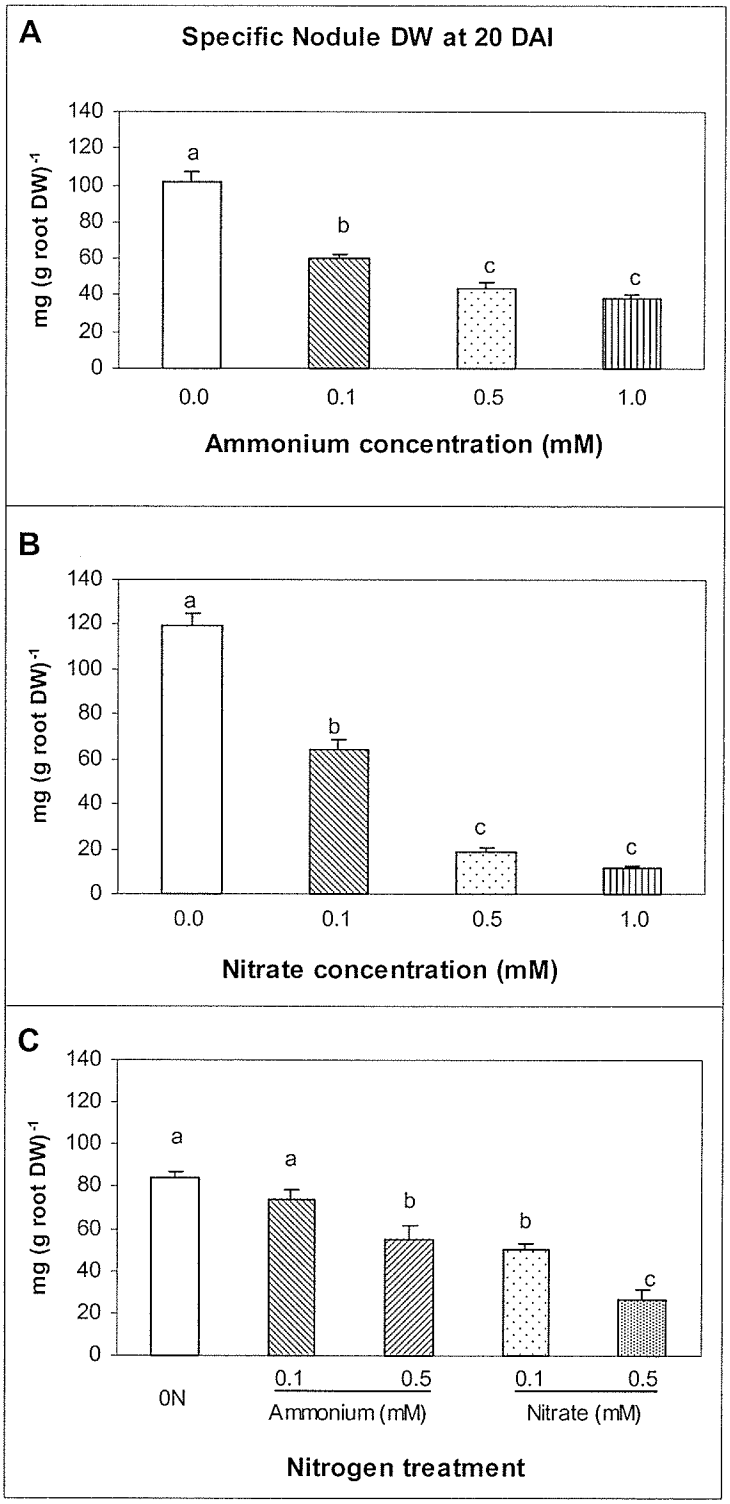

Fig. 4.7 Specific nodule DW of *M. truncatula* plants grown in different concentrations of NH_4^+ (A) and NO_3^- (B) in a flow-through sand culture system and in a flow-through growth pouch culture system (C). Bars indicate S.E. Significant differences among treatments are indicated by different letters above the bars ($P \leq 0.05$).

4.1.2.5 Specific Nodule DW

Exp. 1a and 1b

The specific nodule DW [mg nodule DW (g root DW)$^{-1}$] of control plants was highest in both experiments (Fig. 4.7.A and Fig. 4.7.B). The inhibitory effect of both nitrate and ammonium is positively related to their concentration although nitrate displayed a much stronger inhibitory effect on the specific nodule mass than ammonium at the 0.5 and 1.0 mM level. The 0.1, 0.5 and 1.0 mM NO_3^- inhibited the specific nodule DW to 60%, 44% and 38% of that of the control plants while the three concentration of ammonium reduced the specific nodule mass to 53%, 15% and 9% of that of the control plants.

Exp. 2

Different from Exp. 1a, the inhibitory effect of 0.1 mM NH_4^+ on the specific nodule was not significant although the general trend is the same (Fig. 4.7.C); whereas similar as Exp. 1b, 0.1 mM NO_3^- reduced the specific nodule DW significantly to 61% of that of the control. At 0.5 mM, both forms of mineral nitrogen inhibited the specific nodule mass with a significantly higher inhibitory effect observed in the nitrate treatment, which reduced the specific nodule DW to 65% of that of the control plants, than in the ammonium treatment, which reduced the specific nodule DW to 32% of the control.

4.1.3 Nitrogen Accumulation and Fixation

4.1.3.1 Whole Plant Nitrogen Content

Exp. 1a and 1b

In both Exp. 1a and 1b, total nitrogen content increased with the increasing of mineral nitrogen concentration at both harvesting dates (Fig. 4.8.A and Fig. 4.8.B).

However, when compare to their respective control plants, the magnitude of the increase in total nitrogen content by nitrate is much larger than that of the ammonium treatment. Specifically, 0.1, 0.5 and 1.0 mM NH_4^+ accumulated 66%, 136% and 186% more nitrogen than the control respectively; whereas the three levels of nitrate-treated plants accumulated 235%, 960% and 1220% more nitrogen than the control plants respectively.

Exp. 2

Although the general trend is similar to Exp. 1a for ammoniumtreatments, neither of the two treatments accumulated significantly more nitrogen than the control (Fig. 4.8.C). In contrast, 0.1 and 0.5 mM NO_3^- plants had significant high nitrogen content than control plants, which accumulated 407% and 847% more nitrogen comparing to the control.

4.1.3.2 Whole Plant Nitrogen Concentration

Exp. 1a and 1b

The whole plant nitrogen concentration was lowest in the control plants in both experiments and increased with the concentration of mineral nitrogen (Fig. 4.9.A and Fig. 4.9.B). However, more significant improvement in nitrogen concentration was observed in nitrate than ammonium treatments comparing to their respective control plants. At 20 DAI, 0.1, 0.5 and 1.0 mM NH_4^+-treated plants had 5%, 24% and 25% higher nitrogen concentration than control plants, respectively (Fig. 4.9.A); whereas NO_3^- treatments had 42%, 81% and 103% higher concentration at 10 DAI, and 37%, 66% and 74% higher at 20 DAI (Fig 4.9.B). The data for total nitrogen concentration at 10 DAI of Exp. 1a is not available due to a technical problem.

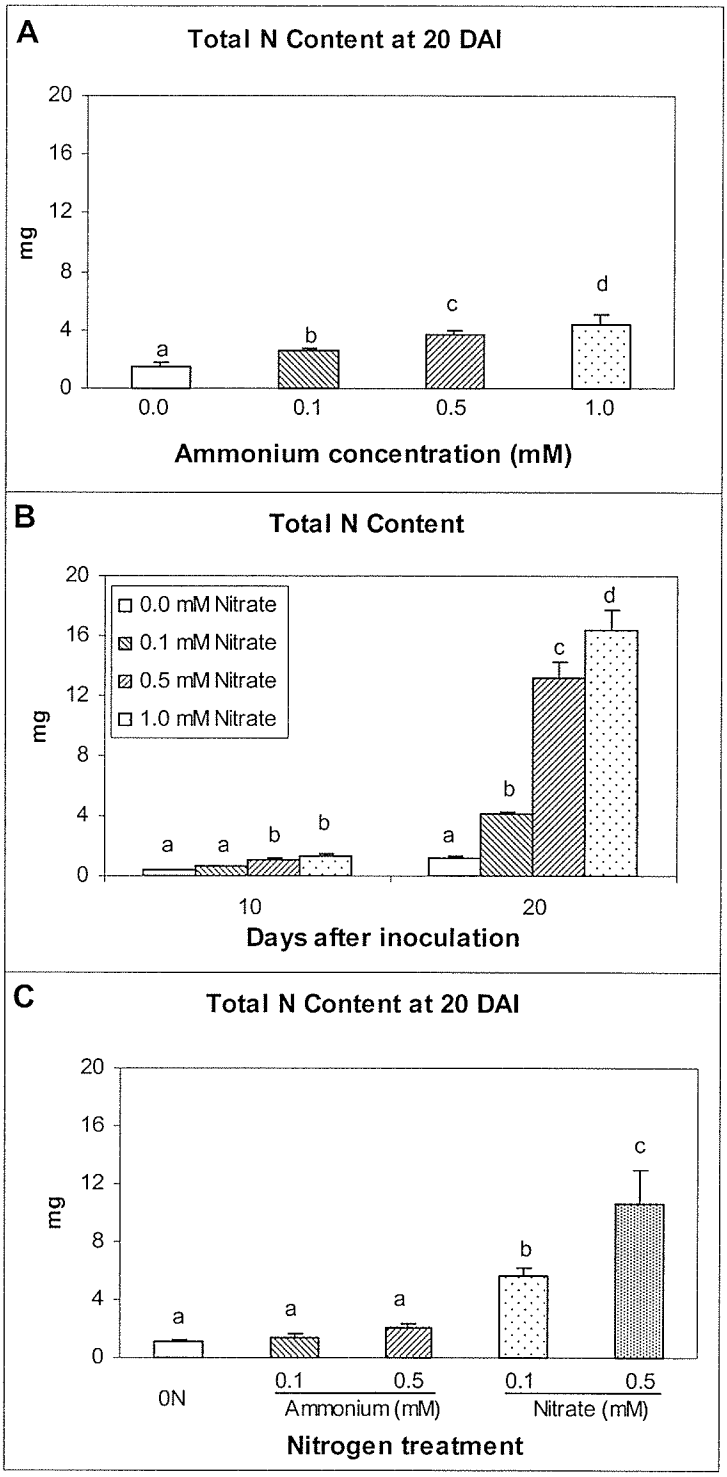

Fig. 4.8 Whole plant nitrogen content of *M. truncatula* plants grown in different concentrations of NH_4^+ (A) and NO_3^- (B) in a flow-through sand culture system and in a flow-through growth pouch culture system (C). Bars indicate S.E. Significant differences among treatments are indicated by different letters above the bars ($P \leq 0.05$).

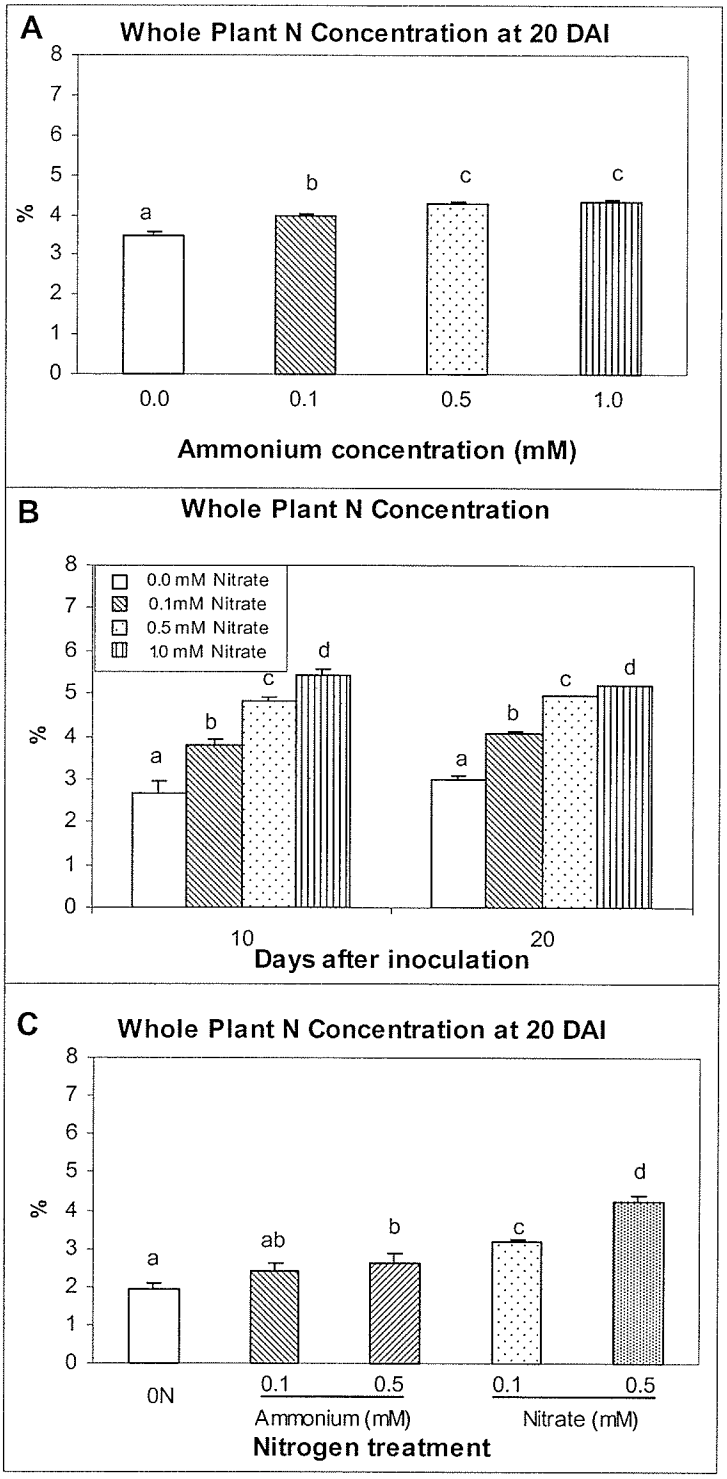

Fig. 4.9 Whole plant nitrogen concentration of *M. truncatula* plants grown in different concentrations of NH_4^+ (A) and NO_3^- (B) in a flow-through sand culture system and in a flow-through growth pouch culture system (C). Bars indicate S.E. Significant differences among treatments are indicated by different letters above the bars ($P \leq 0.05$).

Exp. 2

The control plants (0.0 mM N) had the lowest nitrogen concentration, and 0.5 mM NH_4^+ and both levels of NO_3^- (0.1 and 0.5 mM) had significantly higher nitrogen concentration than the control plants (Fig. 4.9.C). At either of the two nitrogen concentration levels, nitrate-treated plants accumulated higher nitrogen concentration than ammonium-treated ones. Specifically, the 0.1 and 0.5 mM NH_4^+-treated plants had 24%, 32% higher nitrogen concentration than control plants respectively, whereas nitrate treatments had 64 and 117% higher N concentration.

4.1.3.3 Percentage of Nitrogen Derived From Atmosphere (NDFA %)

Exp. 1a and 1b

The %NDFA decreased with increases in mineral nitrogen levels in both the nitrate and ammonium treatments (Fig. 4.10.A and Fig. 4.10.B). All three ammonium treatments had higher %NDFA than nitrate at same levels. Specifically, at 0.1 mM level, ammonium-treated plants obtained almost half of their nitrogen from the atmosphere whereas nitrate-treated plants received less than 1/3 of their nitrogen from fixation. The %NDFA was marginal in NO_3^- treatments at 0.5 and 1.0 mM levels, which were 6% and 5% respectively. In contrast, fixed nitrogen still accounted for a fairly large portion of total nitrogen concentration in ammonium treatments at these two levels, which were around 30% and 20%, respectively.

Exp. 2

Similar to the observation in Exp. 1a and 1b, the %NDFA decreased with increases in mineral nitrogen concentration (Fig. 4.10.C). At both concentrations, nitrogen fixation accounted for much less of the total nitrogen accumulation in nitrate-

treated plants (35% and 5%, respectively) than those of ammonium-treated plants (50% and 27%, respectively).

4.1.3.4 Total NDFA

Exp. 1a and 1b

The total NDFA in Exp. 1a was significantly higher in control plants than in the ammonium-treated plants; however, no significant differences were observed among the three levels of ammonium, which fixed 27% (0.1 mM), 32% (0.5mM) and 43% (1.0 mM) less nitrogen than control plants (Fig. 4.11.A).

In Exp. 1b, 0.1 mM NO_3^- had almost the same amounts of nitrogen fixed from the atmosphere as the control plants and their total NDFA are significantly higher than that of the other two treatments. No difference was observed between 0.5 and 1.0 mM NO_3^- treatments and they both fixed approximately 60% of the amount of nitrogen fixed by control plants (Fig. 4.11.B).

Exp. 2

The highest total NDFA was observed in 0.1 mM nitrate-treated plants which fixed 34% more nitrogen than control plants (Fig. 4.11.C). The total NDFA of control plants were higher than 0.5 mM NO_3^- treatment and both of the two ammonium treatments. There were no significant differences between 0.5 mM NO_3^- treatment and two ammonium treatments, which accounted for approximately 50% to 60% of the total NDFA in control plants.

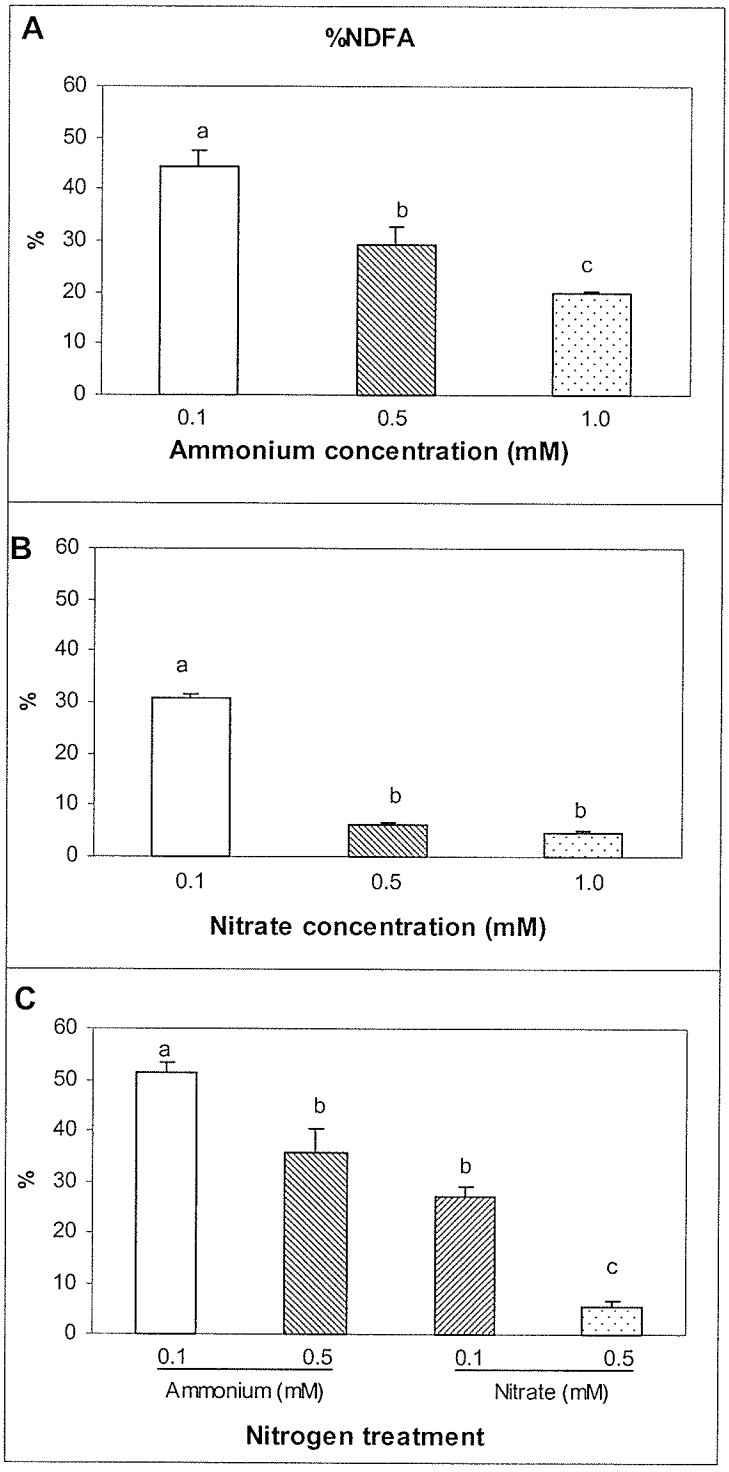

Fig. 4.10 Percentage of nitrogen derived from atmosphere (%NDFA) of *M. truncatula* plants grown in different concentrations of NH_4^+ (A) and NO_3^- (B) in a flow-through sand culture system and in a flow-through growth pouch culture system (C). Bars indicate S.E. Significant differences among treatments are indicated by different letters above the bars ($P \leq 0.05$).

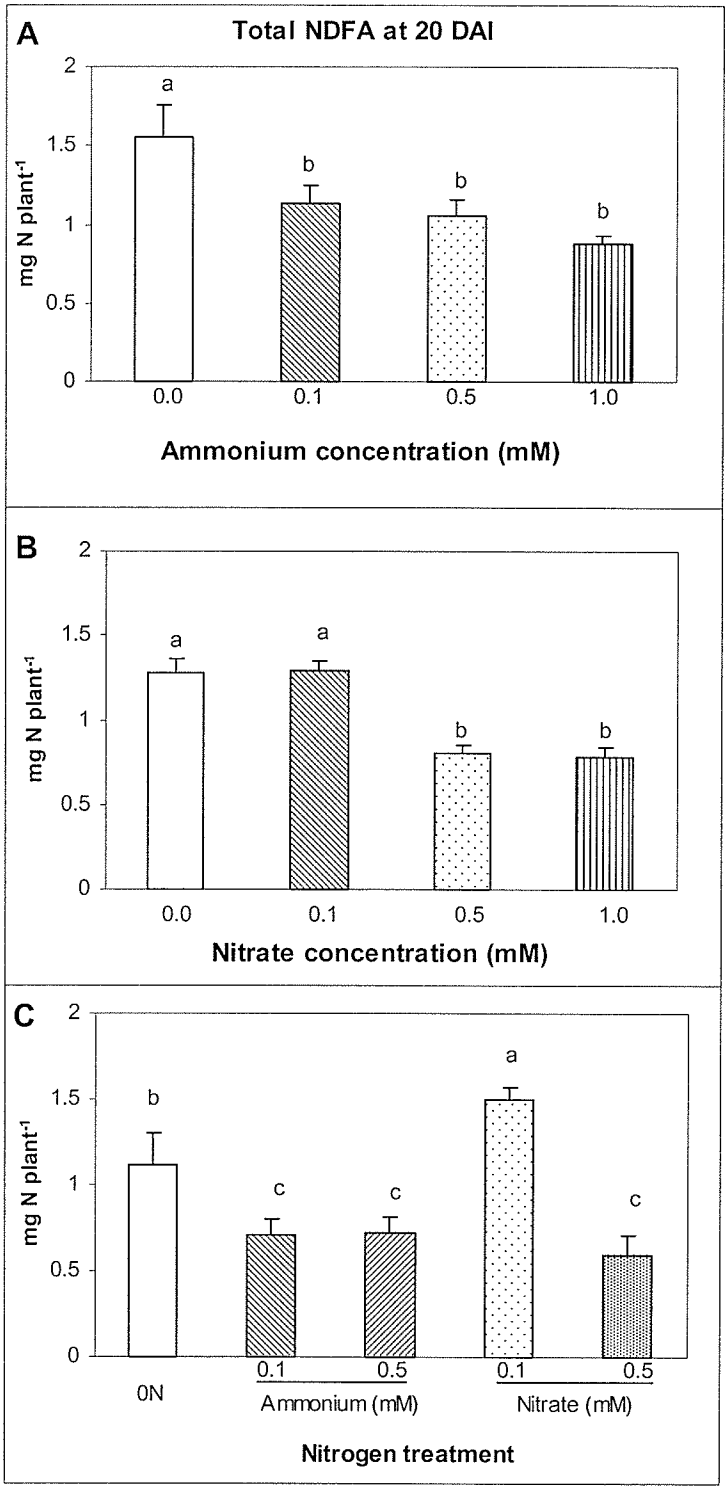

Fig. 4.11 Total nitrogen derived from atmosphere (NDFA) of *M. truncatula* plants grown in different concentrations of NH_4^+ (A) and NO_3^- (B) in a flow-through sand culture system and in a flow-through growth pouch culture system (C). Bars indicate S.E. Significant differences among treatments are indicated by different letters above the bars ($P \leq 0.05$).

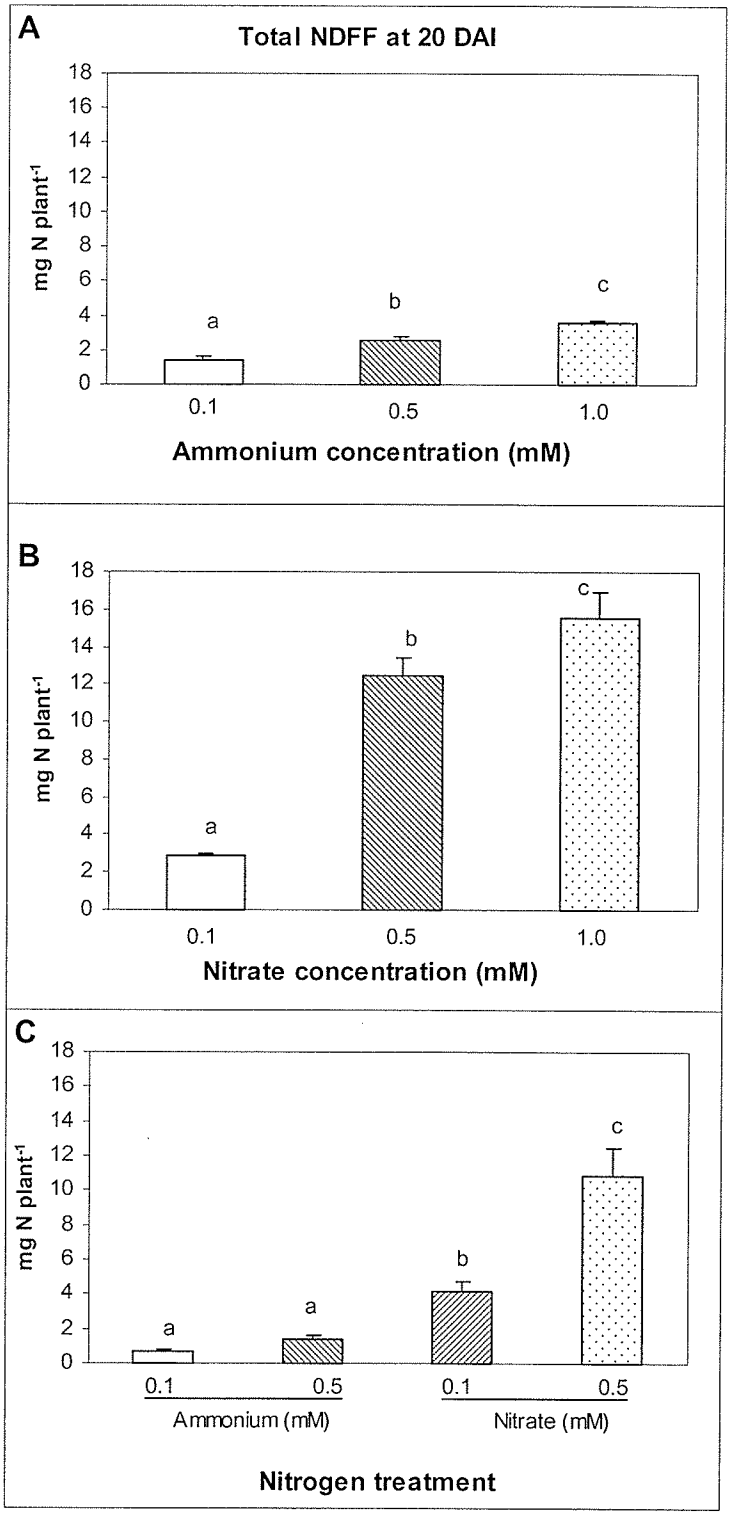

Fig. 4.12 Total nitrogen derived from fertilizer (NDFF) of *M. truncatula* plants grown in different concentrations of NH_4^+ (A) and NO_3^- (B) in a flow-through sand culture system and in a flow-through growth pouch culture system (C). Bars indicate S.E. Significant differences among treatments are indicated by different letters above the bars ($P \leq 0.05$).

4.1.3.5 Total NDFF

Exp. 1a and 1b

The total NDFF increased with the concentration of mineral nitrogen in both experiments (Fig. 4.12.A and Fig. 4.12.B). However, much higher amounts of nitrogen came from the nitrate fertilizer than the ammonium fertilizer at same concentration level. At 0.1 mM concentration level, approximately 1.5 mg nitrogen came from ammonium-containing nutrient solutions and almost 3 mg N was from nitrate-containing nutrient solutions. At 0.5 and 1.0 mM levels, three times and four times more nitrogen mass came from nitrate-containing nutrient solutions than ammonium-containing solutions, respectively.

Exp. 2

Both the 0.1 mM and 0.5 mM NO_3^- treatments obtained significantly more nitrogen from the nutrient solution than NH_4^+ treatments (Fig. 4.12.C). Specifically, at 0.1 mM and 0.5 mM, nitrate-treated plants accumulated 2 times and 4 times more nitrogen from fertilizer than ammonium-treated plants, respectively.

4.2 Analysis of Differential Gene Expression During the Initiation of Symbiosis With and Without the Presence of NH_4^+ and NO_3^- by Utilizing *Mt16kOLI1* Microarrays

4.2.1 Pre-hybridization Measurements

DNase I-treated and column-purified total RNA was loaded on 1.2% formaldehyde -denatured agarose gel to determine the quality of RNA, and only those showed no signs of degradation (Fig. 4.13.) and had a 260/280 ratio higher than 1.8 was used for reverse transcription.

Fig. 4.14 is an example gel documentation of the Cy3/Cy5-labeled cDNA after the last step of cDNA labeling process, the NucAway®-column purification. Although the double-strand DNA ladder loaded by the side of samples can not accurately determine the size distribution of Cyanine-labeled single-strand cDNA, a rough estimation can be made. The cDNA smear was visible from approximately 100 bp to 2kb with most intense region above approximately 500 bp. The light smear starting from gel loading well ending at the upper line of intense region is believed to be due to the residue uncoupled Cy3/Cy5 dye.

A spectrophotometer scanning (190-750 nm) was also used to quantify the amount of cDNA and cDNA-coupled Cyanine dye (Fig. 4.15). The absorbance peak of Cy3 is 550 nm and absorbance peak of Cy5 is 650 nm. The small peak joined with the peak at 650/550 nm is an important indicator of labeling quality; if both peaks have nearly similar intensity, fluorescence signal quenching, caused by over-labeling of the cDNA, can occur. In our experiment, over-labeling was never observed. Labeling density could be calculated from the absorbance data using the formula listed in Appendix A. A

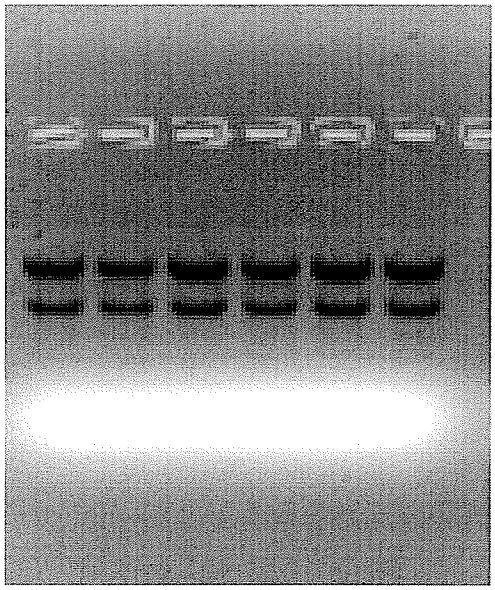

Fig. 4.13 Total RNA on a 1.2% formaldehyde -denatured agarose gel. Total RNA was extracted by TriReagent®, then treated with *DNase I* and passed through Microcon-30YM column before loaded on the gel.

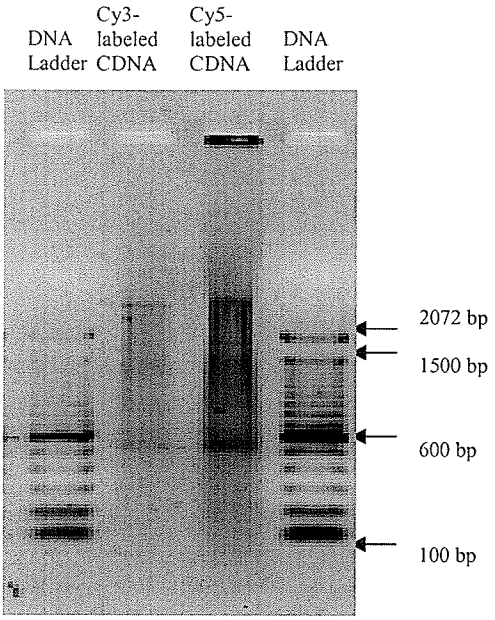

Fig. 4.14 Cyanine-labelled cDNA on a 1.2% agarose gel.

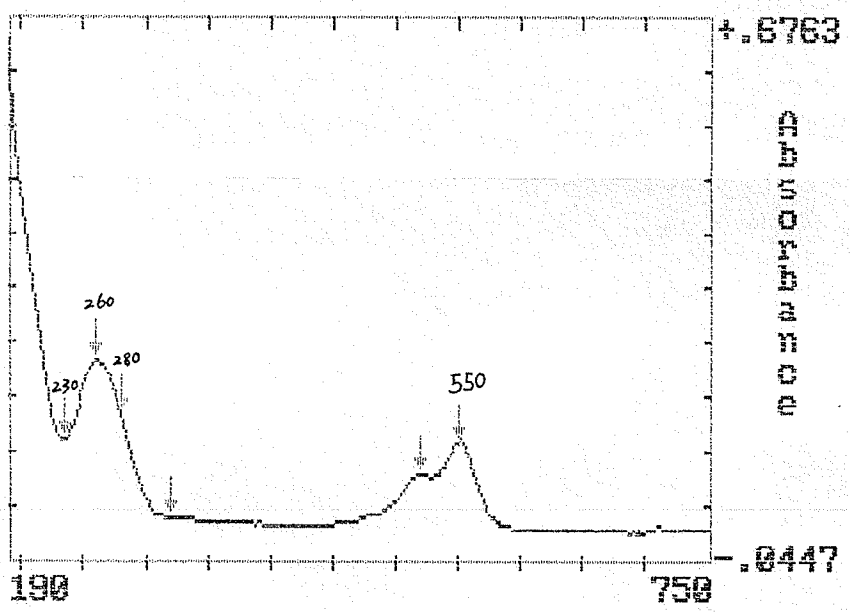

Fig. 4.15 Absorbance scans of Cy3-labeled cDNA in H_2O.

value of 20-50 nt (nucleotides) per dye molecular is generally thought a good labeling density (Ambion on-line technical source) and 30 pmol coupled cyanine dye for each of the two samples could produce good signal on a glass microarray (Microarray handbook, Amersham on-line technical source). In our experiment, 50 pmol cDNA-coupled Cy3/Cy5 dye with labeling density within the range of 20-50 nt per dye molecular were used for each hybridization.

4.2.2 Examination of the fidelity of Microarray Data

4.2.2.1 Visual Inspection of the Microarray Image

The consistency of hybridization across the whole microarray could be roughly judged by observing the equality of the signals produced on two replicate spots for each probe (Fig. 4.16). Duplicate spots were arranged within one block, as displayed in Fig. 4.16. For example, spots in column 14 are the replicate of spots in column 1; column 26 is the duplicate of column 13, and so on. By visually comparing the signal pattern between the two half of one block, a general good agreement was observed.

4.2.2.2 Hierarchical Clustering All the Microarrays

To determine the reproducibility between the two replicate microarrays used for each sample, a hierarchical clustering method was applied on all the probes that passed the SNR$\geq$2 criterion. If replicate arrays do not cluster together, the variation among supposedly identical arrays is greater than the variation among different samples, and therefore the data extracted from the microarray will not be reliable[4]. From the clustering result (Fig. 4.17), it can be observed that except for the three replicates of 12h0N sample, all other replicate microarrays were clustered together.

---

[4] Verdnik Damian. Guide to Microarray analysis. Acuity 4.0 software Application note. Axon Instruments Inc.

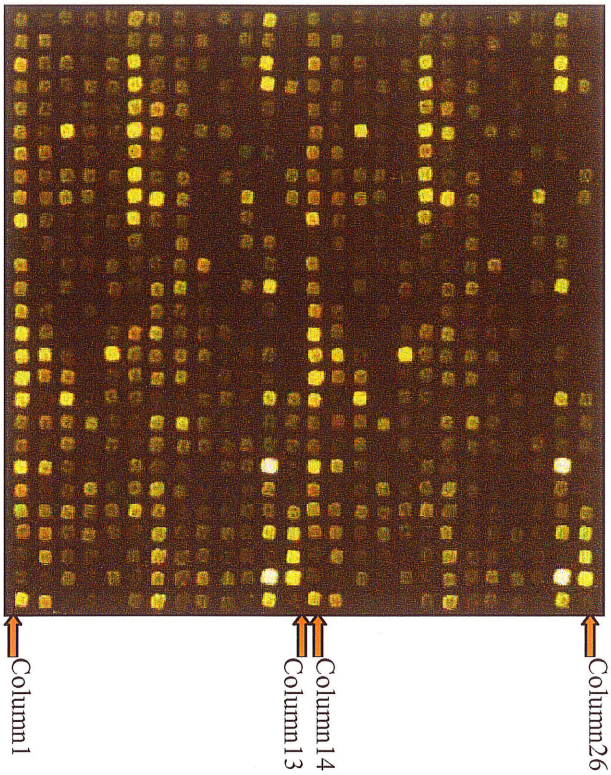

Fig. 4.16 Image of the fluorescence signals of one block region of the *Mt16kOLI1* microarray after hybridization and scanning.

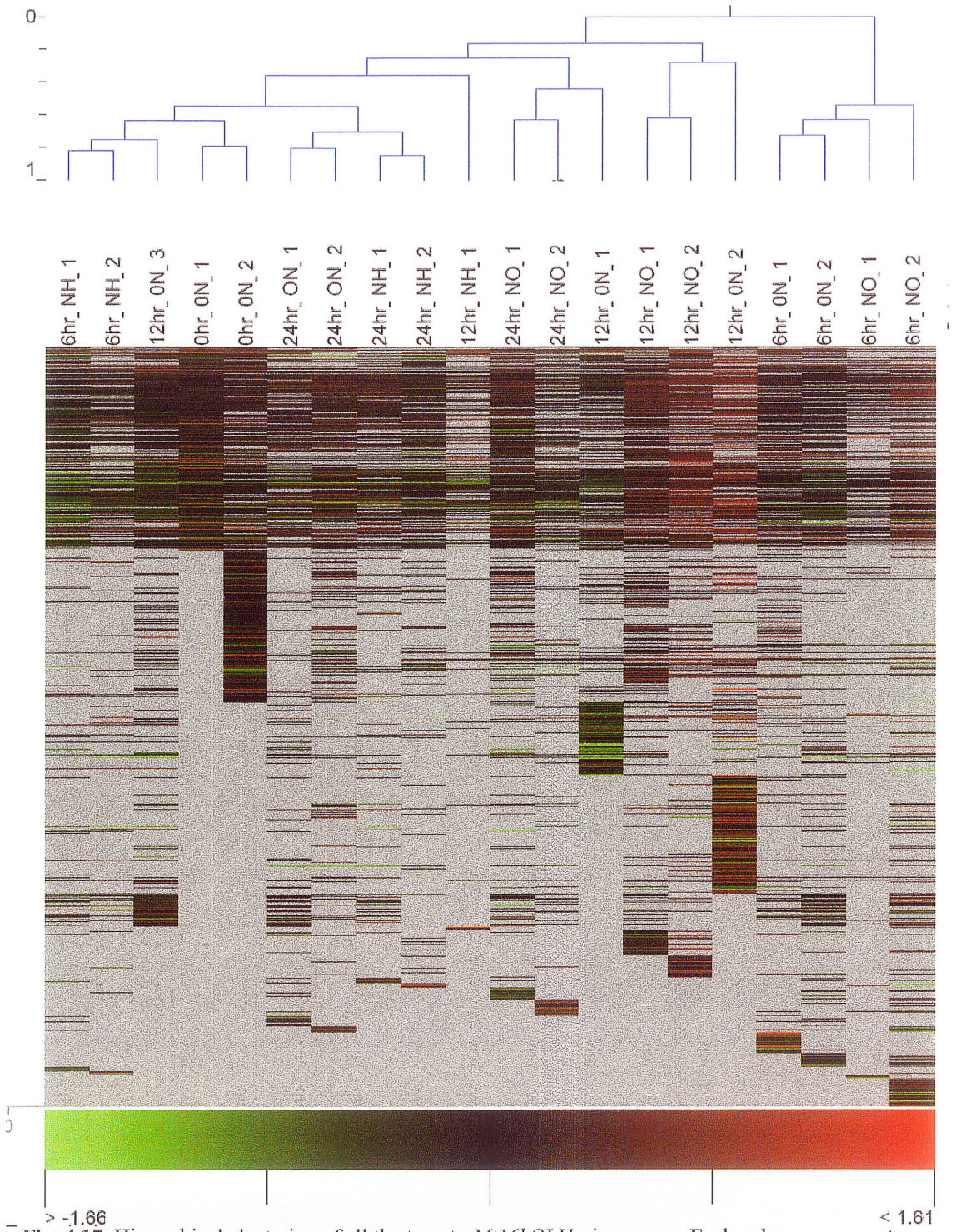

Fig. 4.17 Hierarchical clustering of all the twenty *Mt16kOLI1* microarrays. Each column represents one microarray and each row represents one probe. The name of each microarray is on the top of each column, which indicates the samples hybridized on it. The color of each cell indicates the ratio of the Cy5 signal to Cy3 signal, green indicating a higher signal on Cy3-labeled sample (common reference), red color indicating a higher signal on Cy5-labeled sample, black color indicating equal signal intensity between two channel and gray color cells representing the missing data points. Graph retrieved from Acuity 4.0 software).

4.2.2.3 Monitoring the Expression of the House Keeping Gene *GAPDH*

On the *Mt16kOLI1* microarrays, the complete sequence of *GAPDH* is divided into three probes representing 3' region (1111-1179bp), center region (649-717bp), and 5' (99-167bp) region of the mRNA with 8-16 replicates for each probe. Fig. 4.18 presents the regulation pattern of all those replicate probes. The replicate probes were not averaged and presented in the figure because these replicates were distributed across the whole microarray, and therefore the equality of ratios of the replicates is another indication of the hybridization consistency across the whole microarray. At almost all the nine time points, the detected ratios between the replicates for each probe as well as between the three probes that representing different regions of the cDNA are quite similar. The only exception was the 12hNH sample, in which the ratio of the probe corresponding 3' region of *GAPDH* mRNA is highest, and the ratio of the probe representing 5' region of *GAPDH* mRNA was lowest. Furthermore, the relative expression level of all *GAPDH* probes is below the cut-off ratio 1.5 ($2^{0.4}$=1.3 fold).

4.2.2.4 Validation of the Three Marker Genes by Real Time qRT-PCR

Real time qRT-PCR is one of the commonly used methods to validate the results of DNA microarray. Although real time qRT-PCR method was not used as post microarray validation method in this experiment, it was used to test three marker genes before microarray work started.

Concerning the detected expression of the three chosen genes, the nitrate transporter *Nrt2* was increased almost 50 fold by nitrate treatment comparing to other two treatments (Fig. 4.19), and the cellular transcript level of cytosolic glutamine synthetase was promoted by both ammonium and nitrate comparing to non-nitrogen treatment as

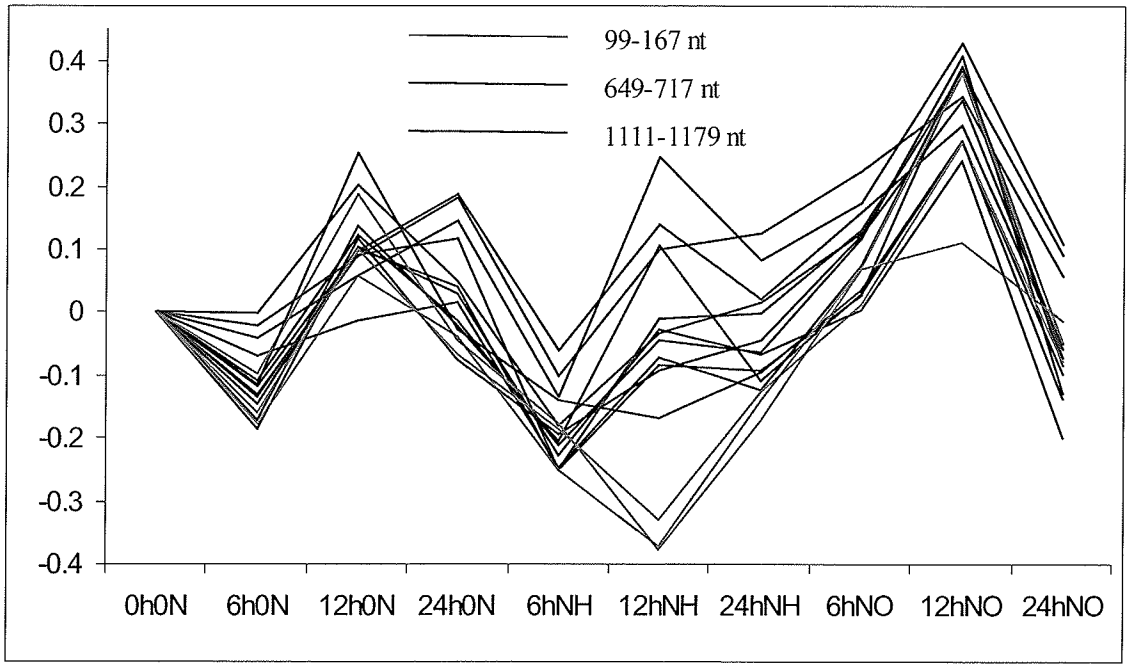

Fig. 4.18 Expression level of three probes representing three regions of *GAPDH* mRNA. The expression levels of 4-8 replicates for each probe were put in the graph to display the general tendency.

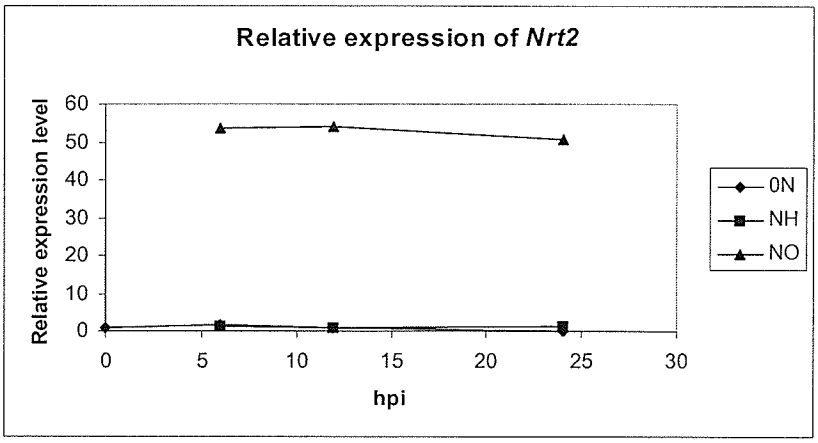

Fig. 4.19 Real time qRT-PCR result of nitrate transporter gene *Nrt2*. hpi, hours post inoculation; 0N, nitrogen-free treatment; NH, 0.1 mM NH_4^+ treatment; NO, 0.1 mM NO_3^- treatment.

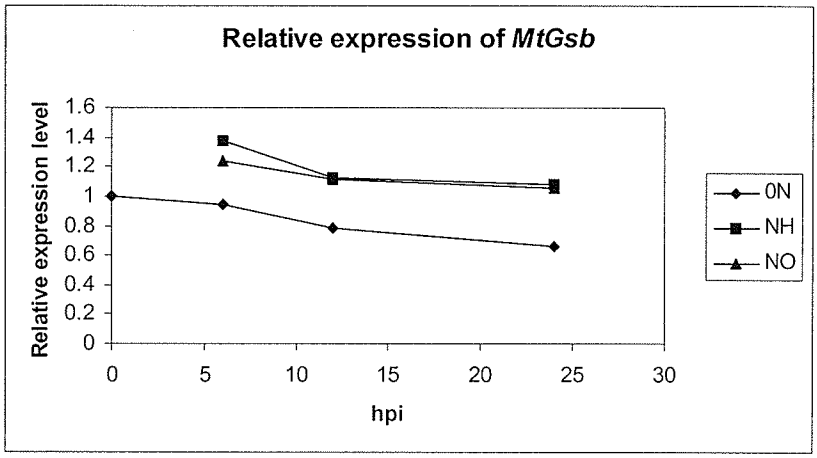

Fig. 4.20 Real time qRT-PCR result of Cytosolic Glutamine synthetase gene *MtGsb*.

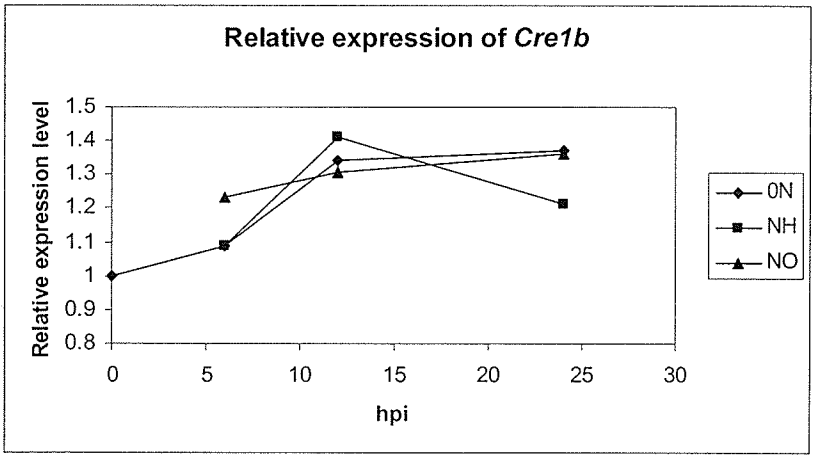

Fig. 4.21 Real time qRT-PCR result of Cytokinin receptor gene *Cre1b*.

expected (Fig. 4.20). However, for the cytokinin receptor gene, no consistent up/down regulation throughout the 24 h period by any of the treatments was observed, although an up-regulation relative to non-inoculated roots were generally observed (Fig. 4.21).

A comparison on the detected expression level of the three genes at all the treatments and time points in relative to 0h0N by microarray method and real time qRT-PCR method was conducted (Table 4.1). Probes on microarray corresponding to *Nrt2*, *Cre1b* and *GAPDH* were found based on the TC number, probes corresponding to *MtGsb2* are found based on sequence similarity by using the *MtGsb2* sequence from NCBI to blast against *Medicago truncatula* sequence database in TIGR. *Cre1b* (TC80422) did not pass the SNR>2 criterion and its expression levels were retrieved from the original microarray data sheet. In summary, despite the fact that some probes' expression level is higher in real time qRT-PCR, and others are higher in DNA microarray, the general tendency are similar between these two methods (Table 4.1). The expression level of *Nrt2* in nitrate treatments was detected to be up-regulated more than 2 fold in both methods, albeit 5-20 fold difference on the exact ratios obtained from different techniques. The result of *Cre1b* on microarray is not reliable due to its very low SNR.

4.2.3 Summary of the Microarray Data

The number of probes that were significantly changed more than 1.5 or 2 fold for each sample relative to 0h0N treatment is summarized in Table 4.2. In the inoculation-only and inoculation/NO treatments, the total number of down-regulated probes at the 1.5 fold cut-off (285 and 176 probes respectively) was smaller than that of up-regulated

Table 4.1 Detected Relative Expression Levels of Three Marker Genes by Real Time qRT-PCR Method and *Mt16kOLI1* DNA Microarrays

Samples	*Cre1b*		*MtGsb*		*Nrt2*	
	Microarray	qRT-PCR	Microarray	qRT-PCR	Microarray	qRT-PCR
0h0N	1	1	1	1	1	1
6h0N	3.587553	1.101045	1.138394	0.941565	0.800515	1.576462
12h0N	2.015773	1.369479	1.180993	0.783774	0.656561	0.868772
24h0N	0.866637	1.369873	0.911933	0.663568	0.230206	0.76
6hNH	2.399943	1.0702	1.220947	1.378689	0.852044	1.423606
12hNH	1.315399	1.439516	1.007654	1.119758	no data	0.858934
24hNH	2.832351	1.338956	0.860353	1.076937	0.965267	1.460311
6hNO	1.3463	1.087497	1.409321	1.235339	10.98909	53.77316
12hNO	3.333413	1.260496	1.215037	1.112282	8.134197	54.17996
24hNO	3.42594	1.431722	1.039579	1.060164	2.869899	50.4324

Table 4.2 Summary of the Significance Analysis of Differentially-expressed Genes

Treatment[1]	Cut-off	Significantly regulated Probes			
		6h	12h	24h	Total
		Up/down	Up/down	Up/down	Up/down
Inoculation-only	1.5	247/73	84/48	83/93	383/285
	2	67/18	32/11	30/13	104/48
Inoculation/NO	1.5	430/45	542/40	109/125	772/176
	2	130/17	135/11	49/25	205/37
Inoculation/NH	1.5	31/154	143/222	67/98	216/396
	2	12/18	47/54	10/6	63/70

1. Inoculation/No: Inoculation plus 0.1 mM NO_3^-; Inoculation/NH: Inoculation plus 0.1 mM NH_4^+.

probes (383 and 772 probes respectively). In contrast, in inoculation/NH treatment, the total number of down-regulated probes at 1.5 fold cut-off (396 probes) was higher than that of up-regulated gene (216 probes). Also, it is noteworthy that the numbers of up-regulated probes in inoculation/NO treatment are much higher than those in other treatments across all three time points and at both fold change cut-offs. For example, at 1.5 fold cut-off there were totally 772 up-regulated probes in inoculation/NO treatment, while 383 and 216 up-regulated ones in inoculation-only and inoculation/NH treatment respectively. When using the more stringent 2 fold cut-off, all of the above tendencies can also be observed. A complete list of all these probes annotation and expression level is in appendix B.

4.2.4 Analysis of the Differentially Regulated Genes Detected by *Mt16kOLI1* Microarrays

All the probes that were continuously up-/down- regulated relative to 0h0N across all three time points and displayed higher than 1.5 fold up-/down-regulation level with statistics significance at least on two time points were grouped into the functional categories defined by Journet et al. (2002) and their annotation was based on the MENS (Medicago EST Navigation System) database. The probes from the three functional categories: secondary metabolism and hormone metabolism (Category VI.), defense and cell rescue (Category XII. A.), and abiotic stimuli and development (category XII.B.) were paid the most attention in the analysis. Other probes that may be related to nodulation or nitrate/ ammonium metabolism were also analyzed.

The three treatments, inoculation-only treatment (Table 4.3 and 4.4), inoculation/NO treatment (Table 4.5 and 4.6), and inoculation/NH treatment (Table 4.7

Table 4.3 List of 35 Probes Detected to be Up-regulated by Inoculation-only Treatment by *Mt16OLI1* Microarray

Oligo ID	TIGR ID	Functional Group[1]	Annotation[2]	6h0N	P[3]	12h0N	P	24h0N	P
MT013418	TC92778	V.	UDP-glucose glucosyltransferase-like protein	0.61	0.0008	0.60	0.0195	0.48	0.0013
MT007207	TC85631	V.	Respiratory-chain NADH dehydrogenase, subunit 1	1.54	0.0009	0.84	0.0761	0.59	0.0490
MT014651	TC78310	V.	NADPH:quinone oxidoreductase	0.20	0.3659	0.65	0.0096	0.64	0.0241
MT007350	TC77094	V.	Lipase, class 3 3.1.1.3	0.80	0.0073	0.74	0.0082	0.51	0.0474
MT000172	TC85552	V.	Hydroxymethylglutaryl-coenzyme A reductase	0.14	0.5964	1.38	0.0009	2.95	0.0000
MT015276	TC85679	V.	ATP citrate lyase	0.24	0.0387	0.60	0.0085	0.87	0.0000
MT015146	TC85138	VI.	Naringenin-chalcone synthase 2.3.1.74	0.84	0.0001	1.17	0.0005	1.50	0.0000
MT015145	TC76767	VI.	Naringenin-chalcone synthase (EC 2.3.1.74)	0.57	0.0003	1.08	0.0005	1.64	0.0000
MT015080	TC85174	VI.	Naringenin-chalcone synthase	0.10	0.8575	1.21	0.0007	1.49	0.0001
MT015147	TC76769	VI.	Naringenin-chalcone synthase	0.16	0.4972	0.92	0.0029	1.06	0.0008
MT015144	TC76770	VI.	Naringenin-chalcone synthase	0.13	0.6335	0.68	0.0421	0.88	0.0346
MT015059	TC85161	VI.	Lipoxygenase, LH2 domain 1.13.11.12	0.61	0.0105	0.24	0.1783	0.99	0.0007
MT010049	TC85194	VI.	Lipoxygenase, LH2 domain 1.13.11.12	0.53	0.1691	0.70	0.0017	0.82	0.0009
MT015627	TC79321	VI.	Gibberellin regulated protein	0.20	0.4027	0.79	0.0029	1.39	0.0015
MT015188	TC85328	VI.	Gibberellin regulated protein	0.29	0.1878	0.60	0.0149	1.56	0.0000
MT015149	TC76765	VI.	Chalcone synthase 2.3.1.74	0.24	0.2095	0.98	0.0018	1.84	0.0001
MT014682	TC89001	VIII.	RNA-binding region RNP-1	0.74	0.0064	0.60	0.0182	0.10	0.6327
MT015105	TC76514	VIII.	RNA-binding region RNP-1	1.16	0.0000	0.61	0.3442	0.33	0.0377
MT014204	BQ14378	VIII.	mRNA capping enzyme-like protein	1.15	0.0000	1.58	0.0000	1.16	0.0001
MT000176	TC85529	VIII.	K+ channel tetramerisation; BTB/POZ domain	0.79	0.0066	1.16	0.0001	1.68	0.0001
MT013424	TC92311	VIII.	HMG1/2 \(high mobility group\) box	1.78	0.0010	0.75	0.0905	1.12	0.0305
MT015213	TC76652	IX.	Granulin; Papain cysteine protease \(C1\)	0.61	0.0111	0.69	0.0180	0.29	0.0657
MT009165	TC79619	X.	Ras small GTPase, Rab type	1.05	0.0059	0.65	0.0243	0.39	0.2217
MT009590	TC88987	X.	Putative phospholipase C	0.88	0.0284	0.39	0.3202	0.93	0.0204
MT007617	TC86303	X.	Calcium-binding EF-hand	0.23	0.1199	0.70	0.0006	1.16	0.0000

Table 4.3 List of 35 Probes Detected to be Up-regulated by Inoculation-only Treatment by *Mt16OLI1* Microarray (Continued)

Oligo ID	TIGR ID	Functional Group[1]	Annotation[2]	6h0N	P[3]	12h0N	P	24h0N	P
MT015051	TC85153	XII.	Haem peroxidase 1.11.1.7	1.50	0.0079	1.00	0.0361	2.11	0.0001
MT000812	TC77754	XII.	Zn-finger, modified RING	0.75	0.0357	0.92	0.0251	0.29	0.4199
MT010227	AL38128	XII.	Putative albumin/Leginsulin	0.66	0.0196	0.60	0.0259	1.53	0.0001
MT006913	TC82952	XII.	Probable albumin/Legisulin	0.65	0.0055	0.71	0.0070	0.44	0.0552
MT003548	TC80587	XII.A.	Probable *rip-1* peroxidase gene product (3'UTR) [nodulin]	0.32	0.3702	0.70	0.0217	1.36	0.0017
MT015465	TC77767	XII.A.	Heavy metal transport/detoxification protein	0.55	0.0439	0.88	0.0026	1.73	0.0000
MT015537	TC78576	XII.A.	Heavy metal transport/detoxification protein	0.63	0.0356	0.49	0.0340	0.73	0.0052
MT000326	TC85855	XII.A.	Heavy metal transport/detoxification protein	0.68	0.0064	0.82	0.0233	1.40	0.0002
MT007980	TC78144	XII.B.	Probable cold and water-stress induced portein-like protein	0.19	0.3619	0.65	0.0420	0.68	0.0416
MT004212	TC81363	XII.B.	No apical meristem \(NAM\) protein	1.54	0.0002	0.83	0.0458	0.37	0.2373

1. Functional groups: I. Cell Wall; II. Cytoskeleton; III. Membrane transport; IV. Vesicular trafficking secretion and protein sorting; V. Primary metabolism; VI. Secondary metabolism and hormone metabolism; VII. Chromatin and DNA metabolism; VIII. Gene expression and RNA metabolism; IX. Protein synthesis and processing; X. Signal transduction/post-translational regulation; XI. Cell division cycle; XII. Miscellaneous; XII.A. Defense and cell rescue; XII.B. Abiotic stimuli and development; XII.C. Unknown function; XIII. No homology.
2. Annotation was derived from the latest MENS (*Medicago truncatula* EST navigation system) database or TIGR *Medicago* Gene Indices.
3. Calculated probability of Type I error.

Table 4.4 List of 24 Probes Detected to be Down-regulated by Inoculation-only Treatment by *Mt16OLI1* Microarray

Oligo ID	TIGR ID	Functional Group[1]	Annotation[2]	6h0N	P[3]	12h0N	P	24h0N	P
MT005666	TC83381	I.	Caffeic acid O-methyltransferase	-0.79	0.0064	-0.92	0.0061	-0.04	0.8602
MT015103	TC85301	I.	Extensin-like protein; Proline-rich region	-1.00	0.0026	-0.78	0.0091	-0.67	0.0154
MT006734	TC90867	III.	Probable natural resistance-associated macrophage protein	-1.68	0.0308	-2.73	0.0055	-2.70	0.0053
MT007028	TC76540	IV.	Protein transport protein MIP family;	-0.75	0.0000	-1.04	0.0000	-0.03	0.5502
MT014721	TC80862	IV.	Protein transport	-0.78	0.0003	-0.80	0.0265	-0.61	0.0065
MT003897	TC82820	IX.	60S ribosomal protein L32 RP49	-0.80	0.0086	-0.83	0.0151	-0.17	0.4416
MT014263	TC85392	IX.	Heat shock protein Hsp70	-1.85	0.0010	-1.05	0.0160	-0.51	0.1537
MT009448	TC88937	V.	Glycoside hydrolase, family 32 3.2.1.26	-1.00	0.0000	-0.71	0.0007	-0.78	0.0000
MT008479	TC87442	V.	Putative glutenin	-0.63	0.0058	-1.05	0.0003	-1.14	0.0008
MT007766	CA98961	V.	Glyoxalase/Bleomycin resistance protein/dioxygenase domain	-0.16	0.4967	-1.01	0.0062	-1.22	0.0064
MT015314	TC85491	V.	Plastocyanin-like	-1.16	0.0004	-0.49	0.0411	-0.80	0.0002
MT014220	TC85388	VI.	S-adenosylmethionine decarboxylase	-1.56	0.0000	-1.72	0.0000	-0.53	0.0003
MT014223	TC85382	VI.	S-adenosylmethionine decarboxylase	-0.98	0.0050	-0.94	0.0031	-0.21	0.2571
MT014222	TC85380	VI.	S-adenosylmethionine decarboxylase	-1.30	0.0002	-1.29	0.0000	-0.51	0.0709
MT014219	TC85379	VI.	S-adenosylmethionine decarboxylase proenzyme	-1.44	0.0002	-1.40	0.0001	-0.52	0.0362
MT000126	TC85379	VI.	S-adenosylmethionine decarboxylase proenzyme	-1.18	0.0000	-1.16	0.0000	-0.31	0.0017
MT014813	TC82572	X.	Leucine-rich repeat, plant specific	-0.77	0.0020	-0.59	0.0230	-1.14	0.0138
MT007297	TC76955	X.	Putative phosphatase	-0.61	0.0022	-0.68	0.0011	-0.20	0.0582
MT014697	TC79658	X.	Serine/Threonine protein kinase;	-0.70	0.0175	-0.82	0.0060	-0.75	0.0286
MT000511	TC77262	XII.	Lectin-related polypeptide	-0.38	0.0186	-0.63	0.0063	-1.04	0.0002
MT014114	TC85431	XII.	Plant lipid transfer/seed storage/trypsin-alpha amylase inhibitor	-0.66	0.1135	-0.86	0.0036	-0.93	0.0016
MT015278	TC76902	XII.	Plant lipid transfer/seed storage/trypsin-alpha amylase inhibitor [NODULIN MtN5]	-1.33	0.0152	-1.24	0.0027	-0.25	0.2609
MT013646	TC80377	XII.A.	Haem peroxidase	-1.35	0.0006	-1.53	0.0007	-2.18	0.0288
MT015128	TC76538	XII.B.	Cold acclimation responsive protein BudCAR5	-0.63	0.0070	-0.82	0.0023	-0.65	0.0077

1. Functional groups: I. Cell Wall; II. Cytoskeleton; III. Membrane transport; IV. Vesicular trafficking secretion and protein sorting; V. Primary metabolism; VI. Secondary metabolism and hormone metabolism; VII. Chromatin and DNA metabolism; VIII. Gene expression and RNA metabolism; IX. Protein synthesis and processing; X. Signal transduction/post-translational regulation; XI. Cell division cycle; XII. Miscellaneous; XII.A. Defense and cell rescue; XII.B. Abiotic stimuli and development; XII.C. Unknown function; XIII. No homology.
2. Annotation was derived from the latest MENS (*Medicago truncatula* EST navigation system) database or TIGR *Medicago* Gene Indices.
3. Calculated probability of Type I error.

Table 4.5 List of 127 Probes Detected to be Up-regulated by Inoculation/NO Treatment by *Mt16OLI1* Microarray

Oligo ID	TIGR ID	Functional Group[1]	Annotation[2]	6hNO	P[3]	12hNO	P	24hNO	P
MT007386	TC76891	I.	Expansin 45, endoglucanase-like domain	0.88	0.0000	0.78	0.0147	0.54	0.0015
MT006840	TC81720	I.	Cellulose synthase	1.03	0.0172	1.43	0.0004	1.26	0.0060
MT002072	TC87235	I.	Pectinacetylesterase	0.82	0.0216	0.48	0.2204	0.91	0.0330
MT004096	TC89665	I.	Expansin 45, endoglucanase-like domain	1.08	0.0000	1.00	0.0007	0.27	0.0324
MT003497	TC81141	II.	Tubulin/FtsZ protein	0.65	0.0003	0.61	0.0008	0.03	0.8103
MT010140	TC82929	III.	General substrate transporter	0.79	0.0394	0.91	0.0004	0.63	0.0065
MT010002	TC86605	III.	Probable hexose transporter	0.63	0.0088	0.73	0.0049	0.20	0.2617
MT009589	TC78157	III.	Probable high affinity nitrate transporter	2.56	0.0001	2.32	0.0002	1.91	0.0028
MT001067	TC86825	III.	UDP-glucoronosyl/UDP-glucosyl transferase	0.89	0.0087	0.62	0.0019	0.43	0.0801
MT008435	TC78391	III.	ABC transporter, transmembrane region;	0.73	0.0001	0.69	0.0000	0.06	0.3261
MT004310	TC90046	III.	Mitochondrial substrate carrier	1.64	0.0001	2.81	0.0002	1.29	0.0003
MT008364	TC87009	III.	Photosystem I psaA and psaB	1.46	0.0002	1.53	0.0001	0.78	0.0522
MT001235	TC86779	IV.	Target SNARE coiled-coil domain	1.01	0.0003	0.94	0.0005	0.59	0.0208
MT000612	TC77500	IV.	Probable Nuclear Transport Factor 2 (NTF2) domain containing protein	0.79	0.0223	1.17	0.0051	0.78	0.0546
MT001967	TC78950	V.	5-formyltetrahydrofolate cyclo-ligase	1.16	0.0018	0.83	0.0046	0.10	0.6610
MT005603	TC83747	V.	Anthranilate synthase component I and chorismate binding protein	1.05	0.0039	1.61	0.0008	1.05	0.0021
MT007932	TC86624	V.	Fatty acid desaturase family; Cytochrome b5	0.88	0.0792	1.14	0.0384	1.03	0.0461
MT002178	TC79701	V.	Homoserine dehydrogenase	0.83	0.0451	0.81	0.0104	0.72	0.0346
MT015535	TC78440	V.	Patatin	0.55	0.0138	0.96	0.0005	0.62	0.0513
MT014279	BE324669	V.	Photosystem I assembly Ycf4 protein	0.72	0.0001	1.11	0.0002	0.68	0.0004
MT014285	TC85612	V.	Photosystem I reaction centre subunit VI	1.02	0.0010	0.66	0.0129	0.48	0.1524
MT015090	TC76497	V.	Photosystem II protein	0.78	0.0025	0.96	0.0003	0.17	0.4770
MT015091	AL381395	V.	Photosystem II protein	0.61	0.0351	0.94	0.0050	0.28	0.2621
MT001418	TC87436	V.	Pyruvate decarboxylase	0.96	0.0076	0.67	0.0110	0.36	0.1990
MT014829	AW683462	V.	Carbohydrate kinase, PfkB	1.28	0.0005	0.82	0.0114	0.18	0.4923
MT007206	TC85631	V.	Respiratory-chain NADH dehydrogenase, subunit 1	0.71	0.0791	0.78	0.0131	0.51	0.0396
MT000172	TC85552	V.	Hydroxymethylglutaryl-coenzyme A reductase	1.66	0.0002	0.99	0.0015	0.78	0.0028
MT001528	TC87405	V.	6-phosphogluconate dehydrogenase	0.76	0.0004	1.05	0.0000	0.68	0.0035
MT010457	TC80150	V.	Acylphosphatase 3.6.1.7	1.08	0.0000	0.61	0.0037	0.24	0.0450
MT015324	TC85881	V.	Putative esterase; Esterase/lipase/thioesterase, active site 3.1.1.1	0.94	0.0000	0.86	0.0000	0.31	0.1075
MT014001	TC85484	V.	Transketolase, N terminal 2.2.1.1	0.27	0.1727	0.75	0.0103	0.63	0.0022

Table 4.5 List of 127 Probes Detected to be Up-regulated by Inoculation/NO Treatment by *Mt16OLI1* Microarray (Continued)

Oligo ID	TIGR ID	Functional Group[1]	Annotation[2]	6hNO	P[3]	12hNO	P	24hNO	P
MT015597	TC87789	V.	Probable UDP-Glucose transferase 2.4.1.-	0.73	0.0513	1.51	0.0001	1.01	0.0082
MT015828	TC91498	V.	Probable UDP-Glucose transferase 2.4.1.-	0.79	0.0070	0.90	0.0010	0.39	0.0632
MT015750	TC80009	V.	Probable UDP-Glucose transferase 2.4.1.-	0.84	0.0182	1.88	0.0007	0.31	0.1614
MT006225	TC87302	V.	UDP-glucoronosyl/UDP-glucosyl transferase	0.83	0.0009	0.94	0.0009	0.29	0.1675
MT000707	TC86358	V.	O-methyltransferase, family 2; Generic methyltransferase	1.13	0.0007	0.57	0.0265	0.68	0.0389
MT010603	TC90084	V.	Glycoside hydrolase, family 14 3.2.1.2	1.07	0.0017	0.67	0.0355	0.25	0.1333
MT007680	TC77576	V.	Adenylate kinase	0.97	0.0114	0.93	0.0023	0.89	0.0151
MT015374	TC86097	V.	Adenylate kinase;	0.75	0.0275	1.16	0.0006	0.56	0.0145
MT015170	TC76593	V.	Aldehyde dehydrogenase	0.73	0.1153	1.25	0.0186	1.26	0.0257
MT014926	TC84885	V.	Esterase/lipase/thioesterase, active site	0.75	0.0019	0.84	0.0001	0.05	0.6519
MT015442	TC77578	V.	Glutamate dehydrogenase	0.92	0.0272	0.96	0.0054	1.14	0.1667
MT007207	TC85631	V.	Respiratory-chain NADH dehydrogenase, subunit 1	1.54	0.0112	1.88	0.0001	1.93	0.0001
MT015147	TC76769	VI.	Naringenin-chalcone synthase	0.82	0.0196	1.16	0.0025	0.31	0.1428
MT015148	TC76766	VI.	Naringenin-chalcone synthase	0.61	0.0413	0.76	0.0086	0.36	0.1161
MT015149	TC76765	VI.	Chalcone synthase 2.3.1.74	0.92	0.0552	1.34	0.0057	0.78	0.0019
MT015145	TC76767	VI.	Probable chalcone synthase 2.3.1.74	1.07	0.0043	1.37	0.0000	1.00	0.0002
MT015146	TC85138	VI.	Naringenin-chalcone synthase 2.3.1.74	1.31	0.0000	1.42	0.0000	0.82	0.0014
MT015072	TC85146	VI.	Naringenin-chalcone synthase 2.3.1.74	0.97	0.0114	1.19	0.0002	0.32	0.1435
MT015080	TC85174	VI.	Naringenin-chalcone synthase	1.13	0.0042	1.41	0.0001	0.53	0.0157
MT007309	TC77009	VI.	Ferritin	0.69	0.0017	0.64	0.0055	0.13	0.3783
MT004509	TC91410	VI.	Cytochrome P450	0.66	0.0368	0.89	0.0015	0.53	0.0418
MT014041	TC80193	VI.	Cytochrome P450	0.95	0.0005	0.71	0.0081	0.29	0.1630
MT015607	TC87455	VII.	Histone H4	0.69	0.0022	0.95	0.0008	0.22	0.2027
MT000741	TC86183	VII.	Histone-fold/TFIID-TAF/NF-Y domain; Histone H4	0.88	0.0005	0.76	0.0012	0.43	0.0328
MT015593	TC86259	VII.	Histone-fold/TFIID-TAF/NF-Y domain; Histone H4	0.63	0.0033	1.05	0.0003	0.32	0.1490
MT015298	TC85723	VII.	Histone H1/H5	1.04	0.0144	0.86	0.0001	0.08	0.5936
MT005469	TC83455	VII.	Putative DNA polymerase A family protein	1.10	0.0053	1.15	0.0150	0.53	0.1398
MT014682	TC89001	VIII.	RNA-binding region RNP-1 \(RNA recognition motif\)	1.01	0.0005	0.94	0.0013	0.13	0.4325
MT000176	TC85529	VIII.	K+ channel tetramerisation	0.97	0.0006	0.84	0.0005	0.64	0.0030
MT013424	TC92311	VIII.	HMG1/2 \(high mobility group\) box	1.96	0.0016	2.02	0.0005	1.31	0.0096
MT007685	TC86401	VIII.	Zn-binding protein, LIM	0.70	0.0325	0.84	0.0191	0.02	0.9743

Table 4.5 List of 127 Probes Detected to be Up-regulated by Inoculation/NO Treatment by *Mt16OLI1* Microarray (Continued)

Oligo ID	TIGR ID	Functional Group[1]	Annotation[2]	6hNO	P[3]	12hNO	P	24hNO	P
MT007620	TC77388	VIII.	RNA-binding region RNP-1 \(RNA recognition motif);	0.94	0.0003	0.78	0.0013	0.46	0.1635
MT009606	TC80157	VIII.	CCAAT-binding transcription factor, subunit B	0.86	0.0001	0.69	0.0000	0.01	0.8865
MT005020	TC91909	VIII.	DNA-directed RNA polymerase	0.67	0.0271	1.02	0.0048	0.40	0.0406
MT013096	TC91070	VIII.	Eukaryotic translation initiation factor 3 subunit 10, putative	1.33	0.0001	0.74	0.0007	0.13	0.3465
MT007320	TC85835	VIII.	Hyaluronan/mRNA binding protein	0.69	0.0049	0.73	0.0235	0.47	0.0208
MT005580	TC92185	VIII.	Squamosa promoter binding protein 1	0.87	0.0763	1.34	0.0056	1.01	0.0385
MT006494	TC93832	VIII.	Translation factor EF-1 alpha-like protein	1.45	0.0006	0.88	0.0136	0.33	0.2218
MT012096	TC91885	IX.	Clp protease	1.41	0.0001	1.74	0.0000	1.11	0.0043
MT015213	TC76652	IX.	Granulin; Papain cysteine protease \(C1\)	0.95	0.0053	0.82	0.0038	0.34	0.1688
MT015350	TC77201	IX.	Ribosomal protein S27E	0.72	0.0003	1.06	0.0000	0.19	0.1134
MT015351	TC77201	IX.	Ribosomal protein S27E	0.74	0.0014	1.00	0.0006	0.18	0.3178
MT001314	TC87412	IX.	P Ubiquitin-activating enzyme	0.64	0.0359	0.69	0.0000	0.37	0.0355
MT015281	TC85672	IX.	Ribosomal protein L4/L1e	0.69	0.0004	1.17	0.0003	0.11	0.5051
MT009624	TC88821	IX.	Cell division protein FtsH protease-like	0.80	0.0051	0.73	0.0001	0.23	0.1781
MT007919	TC86609	IX.	Chaperonin Cpn60/TCP-1	0.70	0.0025	0.52	0.0020	0.77	0.0004
MT011430	TC82177	IX.	Putative tripeptidyl peptidase II.	1.21	0.0029	0.67	0.0459	0.38	0.1219
MT010501	TC79962	X.	Protein phosphatase 2A, regulatory B subunit \(B56 family\)	1.38	0.0023	1.37	0.0054	1.26	0.0016
MT003590	TC79857;	X.	Leucine-rich repeat	0.63	0.0340	0.82	0.0073	0.21	0.6413
MT006604	TC91913	X.	Response regulator receiver	1.75	0.0002	1.27	0.0002	0.41	0.1089
MT008442	TC78374;	X.	Leucine-rich repeat	0.75	0.0167	0.90	0.0099	0.50	0.2059
MT003241	TC81525	X.	Serine/Threonine protein kinase	0.89	0.0000	0.82	0.0010	0.53	0.0050
MT014973	TC84313	X.	Protein kinase	1.27	0.0018	1.17	0.0065	0.19	0.2727
MT009879	TC88728	X.	NAF domain	1.68	0.0001	1.48	0.0001	1.22	0.0007
MT007850	TC86616	X.	GTP-binding protein	0.66	0.0057	0.57	0.0608	0.60	0.0053
MT009590	TC88987	X.	Putative phospholipase.	1.85	0.0005	2.43	0.0002	2.08	0.0009
MT001419	TC78433	X.	Pyrophosphate-dependent phosphofructokinase beta subunit	0.81	0.0005	0.65	0.0009	0.37	0.0174
MT011055	TC80378	X.	Ras GTPase superfamily;	1.20	0.0150	0.92	0.0228	0.39	0.3070
MT005462	TC90987	X.	Receptor-like kinase RHG4	1.22	0.0013	0.63	0.0001	0.49	0.0025
MT015654	TC91708	XI.	Cyclin-dependent kinase, regulatory subunit	0.66	0.0462	1.12	0.0015	0.13	0.4519
MT015105	TC76514	XI.	Probable NUM1-Like protein	1.41	0.0006	1.88	0.0000	1.25	0.0000

Table 4.5 List of 127 Probes Detected to be Up-regulated by Inoculation/NO Treatment by *Mt16OLI1* Microarray (Continued)

Oligo ID	TIGR ID	Functional Group[1]	Annotation[2]	6hNO	P[3]	12hNO	P	24hNO	P
MT015100	BG448933	XI.	Probable NUM1-Like protein	1.40	0.0001	1.69	0.0000	1.03	0.0009
MT007683	TC86261	XI.	Cullin	1.20	0.0003	1.16	0.0003	0.32	0.2213
MT000009	BF519896	XII.	18S RIBOSOMAL RNA	1.05	0.0047	1.34	0.0014	0.48	0.0650
MT002201	TC88116	XII.	Alpha/beta hydrolase fold; Esterase/lipase/thioesterase, active site	1.45	0.0010	0.69	0.0038	0.73	0.0189
MT003928	TC78336	XII.	Meprin/TRAF-like MATH; BTB/POZ domain	1.22	0.0007	0.93	0.0012	0.40	0.1033
MT000048	TC85428	XII.	Plant lipid transfer/seed storage/trypsin-alpha amylase inhibitor	0.79	0.0059	0.62	0.0195	0.51	0.0798
MT008761	TC79154	XII.	Thymidylate synthase	1.87	0.0000	1.92	0.0001	1.29	0.0000
MT008328	TC78046	XII.	Calreticulin	1.03	0.0587	1.73	0.0016	1.21	0.0065
MT011119	TC89930	XII.	Lectin-like receptor kinase	1.21	0.0006	0.68	0.0076	0.29	0.2083
MT010049	TC85194	XII.	Lipoxygenase, LH2 domain 1.13.11.12	0.76	0.0017	1.10	0.0001	1.09	0.0010
MT015051	TC85153	XII.	Haem peroxidase 1.11.1.7	1.51	0.0088	2.25	0.0016	2.27	0.0002
MT010227	AL381280;	XII.	Putative albumin / Leginsulin	1.43	0.0007	2.26	0.0000	2.36	0.0000
MT000812	TC77754	XII.	Zn-finger, modified RING	1.05	0.0137	0.84	0.0266	0.56	0.1178
MT007617	TC86303	XII.	Calcium-binding EF-hand	0.70	0.0016	0.41	0.0024	0.79	0.0002
MT007000	TC85164	XII.	Haem peroxidase;	0.70	0.0026	0.82	0.0002	0.67	0.0016
MT015106	TC76511	XII.A.	Bet v I allergen	1.28	0.0002	0.67	0.0003	0.29	0.4407
MT015662	TC88533	XII.A.	Probable ABC transporter	0.71	0.0122	1.42	0.0008	0.57	0.0435
MT003859	TC88124	XII.A.	ABC transporter	0.81	0.0020	0.72	0.0012	0.26	0.1960
MT014204	BQ143785	XII.A.	mRNA capping enzyme	1.43	0.0000	2.05	0.0000	0.84	0.0006
MT003548	TC80587;	XII.A.	Probable rip-1 Peroxidase gene product (3'UTR) [NODULIN]	0.55	0.1778	1.38	0.0021	0.92	0.0318
MT015537	TC78576	XII.A.	Probable heavy metal transport/detoxification protein	0.83	0.0053	0.66	0.0113	0.61	0.0373
MT015536	TC78577	XII.A.	Heavy metal transport/detoxification protein	0.78	0.0295	0.73	0.0257	0.12	0.6764
MT015465	TC77767	XII.C.	Heavy metal transport/detoxification protein	1.07	0.0043	0.81	0.0062	0.67	0.0600
MT000326	TC85855	XII.A.	Copper chaperone homolog CCH	0.39	0.2405	1.25	0.0003	1.37	0.0013
MT015612	TC87724;	XII.A.	Disease resistance protein RGA2 (RGA2-blb) (Blight resistance proteinRPI).	1.94	0.0009	2.30	0.0000	2.03	0.0003
MT009182	TC79735;	XII.A.	Disease resistance protein-like protein MsR1.	1.13	0.0030	0.70	0.0294	0.29	0.2551
MT015842	TC86227	XII.A.	NB-ARC domain; TIR domain	0.84	0.0118	0.92	0.0037	0.13	0.4545
MT010752	TC81627	XII.A.	Putative disease resistance protein RGA3 (RGA1-blb) (Blight resistanceprotein B149)	1.29	0.0016	1.20	0.0015	0.93	0.0077
MT015581	TC77728	XII.A.	TIR domain	1.19	0.0338	1.14	0.0102	0.41	0.2566

Table 4.5 List of 127 Probes Detected to be Up-regulated by Inoculation/NO Treatment by *Mt16OLI1* Microarray (Continued)

Oligo ID	TIGR ID	Functional Group[1]	Annotation[2]	6hNO	P[3]	12hNO	P	24hNO	P
MT014405	TC86109	XII.B.	Seed maturation protein	1.16	0.0011	1.02	0.0094	0.58	0.0210
MT007980	TC78144	XII.B.	Dehydrin	0.40	0.0834	1.04	0.0012	1.01	0.0016
MT015188	TC85328	XII.B.	Gibberellin regulated protein	0.95	0.0001	1.32	0.0000	1.21	0.0024
MT015525	TC78048	XII.B.	Gibberellin regulated protein	0.15	0.6279	0.96	0.0001	0.62	0.0009
MT015627	TC79321	XII.B.	Gibberellin regulated protein	0.98	0.0006	1.47	0.0001	1.77	0.0016
MT004212	TC81363	XII.B.	No apical meristem \(NAM\) protein	1.90	0.0004	1.24	0.0002	1.08	0.0042

1. Functional groups: I. Cell Wall; II. Cytoskeleton; III. Membrane transport; IV. Vesicular trafficking secretion and protein sorting; V. Primary metabolism; VI. Secondary metabolism and hormone metabolism; VII. Chromatin and DNA metabolism; VIII. Gene expression and RNA metabolism; IX. Protein synthesis and processing; X. Signal transduction/post-translational regulation; XI. Cell division cycle; XII. Miscellaneous; XII.A. Defense and cell rescue; XII.B. Abiotic stimuli and development; XII.C. Unknown function; XIII. No homology.
2. Annotation was derived from the latest MENS (*Medicago truncatula* EST navigation system) database or TIGR *Medicago* Gene Indices.
3. Calculated probability of Type I error.

Table 4.6 List of 17 Probes Detected to be Down-regulated by Inoculation/NO Treatment by *Mt16OLI1* Microarray

Oligo ID	TIGR ID	Functional Group[1]	Annotation[2]	6hNO	P[3]	12hNO	P	24hNO	P
MT007738	TC76889	I.	Cell wall-associated hydrolase	-1.01	0.0005	-0.90	0.0006	-1.60	0.0004
MT006734	TC90867	III.	Probable natural resistance-associated macrophage protein	-1.88	0.0201	-2.66	0.0070	-1.60	0.0383
MT010255	TC81000	V.	UDP-glycose:flavonoid glycosyltransferase	-0.44	0.0863	-0.96	0.0155	-0.62	0.0202
MT004260	TC82099	V.	UDP-glucose glucosyltransferase	-0.50	0.1817	-1.06	0.0153	-1.44	0.0041
MT003394	TC89683	V.	Probable nitrate transporter	-0.94	0.0000	-0.78	0.1353	-0.83	0.0065
MT008479	TC87442	V.	Glutenin	-0.30	0.0458	-0.85	0.0026	-1.02	0.0062
MT000390	TC85975	V.	Fructose-bisphosphate aldolase, class-I	-0.72	0.0012	-0.11	0.2423	-1.16	0.0000
MT000126	TC85379	VI.	S-adenosylmethionine decarboxylase proenzyme (EC 4.1.1.50)	-1.17	0.0000	-1.03	0.0000	-0.55	0.0045
MT014219	TC85379	VI.	S-adenosylmethionine decarboxylase proenzyme	-1.53	0.0003	-1.26	0.0004	-0.73	0.0147
MT014220	TC85388	VI.	S-adenosylmethionine decarboxylase	-1.37	0.0002	-1.44	0.0000	-0.55	0.0071
MT014222	TC85380	VI.	S-adenosylmethionine decarboxylase	-1.17	0.0010	-1.31	0.0000	-0.40	0.0421
MT014223	TC85382	VI.	S-adenosylmethionine decarboxylase	-0.84	0.0011	-0.76	0.0102	-0.23	0.2563
MT000432	TC77184	VI.	Isoflavone reductase 1.3.1.-	-0.75	0.0003	-0.21	0.0354	-0.74	0.0604
MT011201	TC89470	XII.	Zn-finger, RING	-0.57	0.0121	-0.65	0.0086	-0.75	0.0630
MT000511	TC77262	XII.	Legume lectin	-0.62	0.0126	-0.35	0.0216	-0.67	0.0018
MT000708	TC86430	XII.A.	Haem peroxidase	-0.67	0.0029	-0.66	0.0358	-0.18	0.2322
MT013646	TC80377	XII.A.	Haem peroxidase	-1.03	0.0050	-1.55	0.0008	-1.58	0.0003

1. Functional groups: I. Cell Wall; II. Cytoskeleton; III. Membrane transport; IV. Vesicular trafficking secretion and protein sorting; V. Primary metabolism; VI. Secondary metabolism and hormone metabolism; VII. Chromatin and DNA metabolism; VIII. Gene expression and RNA metabolism; IX. Protein synthesis and processing; X. Signal transduction/post-translational regulation; XI. Cell division cycle; XII. Miscellaneous; XII.A. Defense and cell rescue; XII.B. Abiotic stimuli and development; XII.C. Unknown function; XIII. No homology.
2. Annotation was derived from the latest MENS (*Medicago truncatula* EST navigation system) database or TIGR *Medicago* Gene Indices.
3. Calculated probability of Type I error.

Table 4.7 List of 13 Probes Detected to be Up-regulated by Inoculation/NH Treatment by *Mt16OLI1* Microarray

Oligo ID	TIGR ID	Functional Group[1]	Annotation[2]	6hNH	P[3]	12hNH	P	24hNH	P
MT002072	TC87235	I.	Pectinacetylesterase	0.76	0.0443	0.12	0.7166	0.86	0.0074
MT007207	TC85631	V.	Respiratory-chain NADH dehydrogenase	1.17	0.0477	0.24	0.3939	0.86	0.0026
MT000172	TC85552	V.	Hydroxymethylglutaryl-coenzyme A reductase	0.05	0.7565	2.55	0.0014	0.84	0.0469
MT015145	TC76767	VI.	Probable chalcone synthase 2.3.1.74	0.82	0.0292	0.59	0.0292	0.87	0.0064
MT015146	TC85138	VI.	Naringenin-chalcone synthase 2.3.1.74	0.81	0.0027	0.44	0.2847	0.86	0.0059
MT015072	TC85146	VI.	Naringenin-chalcone synthase 2.3.1.74	0.63	0.1032	1.64	0.0010	0.99	0.0013
MT015080	TC85174	VI.	Naringenin-chalcone synthase	0.71	0.0055	0.32	0.4244	0.79	0.0019
MT015149	TC76765	VI.	Chalcone synthase 2.3.1.74	0.27	0.4231	0.97	0.0051	1.07	0.0018
MT015188	TC85328	VI.	Gibberellin regulated protein	0.59	0.0584	0.94	0.0025	1.40	0.0001
MT000931	TC86588	VIII.	Myb DNA-binding domain	0.63	0.0232	0.29	0.3259	0.67	0.0223
MT000176	TC85529	VIII.	K+ channel tetramerisation	0.21	0.3971	0.99	0.0084	0.98	0.0034
MT014204	BQ143785	XII.A.	mRNA capping enzyme	1.04	0.0000	1.58	0.0003	1.46	0.0000
MT015106	TC76511	XII.A.	Bet v I allergen	0.73	0.0002	0.57	0.0620	0.60	0.0072
MT015465	TC77767	XII.A.	Heavy metal transport/detoxification protein	0.06	0.8064	1.36	0.0030	0.69	0.0028

1. Functional groups: I. Cell Wall; II. Cytoskeleton; III. Membrane transport; IV. Vesicular trafficking secretion and protein sorting; V. Primary metabolism; VI. Secondary metabolism and hormone metabolism; VII. Chromatin and DNA metabolism; VIII. Gene expression and RNA metabolism; IX. Protein synthesis and processing; X. Signal transduction/post-translational regulation; XI. Cell division cycle; XII. Miscellaneous; XII.A. Defense and cell rescue; XII.B. Abiotic stimuli and development; XII.C. Unknown function; XIII. No homology.
2. Annotation was derived from the latest MENS (*Medicago truncatula* EST navigation system) database or TIGR *Medicago* Gene Indices.
3. Calculated probability of Type I error.

Table 4.8 List of 37 Probes Detected to be Down-regulated by Inoculation/NH Treatment by *Mt16OLI1* Microarray

Oligo ID	TIGR ID	Functional Group[1]	Annotation[2]	6hrNH	P[3]	12hrNH	P	24hrNH	P
MT005958	TC84652	I.	Beta-1,3-glucanase-like protein	-0.62	0.0398	-0.18	0.6038	-0.89	0.0048
MT007972	TC77631	I.	Cellulose synthase	-0.44	0.0075	-0.64	0.0099	-0.65	0.0005
MT000669	TC77589	I.	Putative cell wall protein	-0.81	0.0255	-0.64	0.0464	-0.65	0.0171
MT007832	TC86537	I.	Putative arabinogalactan protein	-0.83	0.0020	-1.10	0.0104	-0.53	0.0135
MT014004	TC85550	I.	Probable O-Methyltransferase	-0.69	0.0127	-0.81	0.0113	-0.20	0.4132
MT007017	TC85263	III.	MIP family	-0.77	0.0003	-0.74	0.0002	-0.22	0.0178
MT007036	TC76601	III.	MIP family	-0.65	0.0002	-0.93	0.0010	-0.10	0.4718
MT015028	TC83942	III.	Putative sugar transporter	-0.80	0.0391	-0.81	0.0376	-0.52	0.0384
MT007028	TC76540	III.	MIP family; SecY protein	-0.84	0.0007	-0.76	0.0002	-0.15	0.0433
MT014261	TC85392	IX.	Heat shock protein Hsp70	-0.73	0.0002	-1.13	0.0004	-0.32	0.0307
MT014262	TC85390	IX.	Heat shock protein Hsp70	-1.69	0.0018	-0.62	0.0028	-0.22	0.0706
MT014263	TC85392	IX.	Heat shock protein Hsp70	-2.04	0.0090	-1.36	0.0483	-0.47	0.2210
MT007628	TC77515	IX.	Translation initiation factor SUI1	-1.87	0.0000	-0.84	0.0087	-0.48	0.1297
MT013273	TC91546	V.	Hydroxymethylglutaryl-coenzyme A reductase 1.1.1.34	-0.87	0.0034	-1.02	0.0135	-0.53	0.0073
MT008596	TC87421	V.	H(+)/hexose cotransporter	-0.16	0.0182	-0.82	0.0014	-0.69	0.2847
MT007167	TC76360	V.	ATP-sulfurylase 2.7.7.4	-0.48	0.0338	-0.85	0.0205	-0.61	0.0179
MT000106	TC76584	V.	Acid phosphatase \(Class B\) 3.1.3.2	-0.62	0.0231	-0.87	0.0292	-0.78	0.0089
MT008479	TC87442	V.	Putative glutenin	-0.82	0.0021	-1.66	0.0103	-0.60	0.0906
MT000126	TC85379	VI.	S-adenosylmethionine decarboxylase proenzyme	-1.29	0.0000	-1.52	0.0000	-0.20	0.0804
MT014219	TC85379	VI.	S-adenosylmethionine decarboxylase proenzyme	-1.38	0.0003	-1.51	0.0030	-0.30	0.1532
MT014220	TC85388	VI.	S-adenosylmethionine decarboxylase	-1.63	0.0000	-1.44	0.0049	-0.47	0.0242
MT014222	TC85380	VI.	S-adenosylmethionine decarboxylase	-1.51	0.0003	-1.58	0.0028	-0.29	0.0577
MT014223	TC85382	VI.	S-adenosylmethionine decarboxylase	-1.14	0.0041	-1.44	0.0025	-0.17	0.2634
MT007443	TC77258	VI.	Cytochrome P450 1.14.-.-	-0.59	0.0011	-0.60	0.0161	-0.67	0.0043
MT000035	TC76454	X.	Serine/Threonine protein kinase	-0.70	0.0144	-0.79	0.0206	-0.17	0.4125
MT002376	TC79821	X.	Protein phosphatase 2A, regulatory B subunit	-0.59	0.0020	-0.71	0.0002	-0.63	0.0037
MT011635	TC77188	X.	Probable SNF1-Related protein kinase	-0.83	0.0065	-0.90	0.0017	-0.20	0.2288
MT000511	TC77262	XII.	Legume lectin	-0.16	0.3625	-0.73	0.0054	-1.06	0.0000
MT007023	TC76558	XII.	Glycine-rich RNA-binding protein	-0.24	0.0545	-0.62	0.0084	-1.13	0.0001
MT015261	TC76796	XII.A.	Pathogenesis-related transcriptional factor and ERF	-0.68	0.0372	-0.86	0.0007	-0.18	0.1790
MT006837	TC91327	XII.A.	Heavy metal transport/detoxification protein	-0.61	0.0041	-0.66	0.0059	-0.71	0.0021
MT013646	TC80377	XII.A.	Haem peroxidase	-1.20	0.0118	-1.82	0.0025	-0.68	0.0181

Table 4.8 List of 37 Probes Detected to be Down-regulated by Inoculation/NH Treatment by *Mt16OLI1* Microarray (Continued)

Oligo ID	TIGR ID	Functional Group[1]	Annotation[2]	6hrNH	P[3]	12hrNH	P	24hrNH	P
MT015227	TC85451	XII.A.	2 4-D inducible glutathione S-transferase	-0.76	0.0000	-1.00	0.0005	-0.23	0.1853
MT014257	TC76699	XII.B.	Dehydrin	-1.07	0.0000	-0.70	0.0126	-0.69	0.0113
MT015128	TC76538	XII.B.	Dehydrin	-0.66	0.0265	-0.97	0.0397	-0.58	0.0161
MT007924	TC86281	XII.B.	Dehydrin	-0.90	0.0054	-1.25	0.0032	-0.38	0.0817
MT015165	TC85296	XII.B.	Putative Gigantea-like protein	-0.64	0.0051	-0.91	0.0009	-0.88	0.0001
MT000275	TC85758	XII.B.	AUX/IAA protein	-0.63	0.0033	-1.16	0.0007	-0.35	0.0112

1. Functional groups: I. Cell Wall; II. Cytoskeleton; III. Membrane transport; IV. Vesicular trafficking secretion and protein sorting; V. Primary metabolism; VI. Secondary metabolism and hormone metabolism; VII. Chromatin and DNA metabolism; VIII. Gene expression and RNA metabolism; IX. Protein synthesis and processing; X. Signal transduction/post-translational regulation; XI. Cell division cycle; XII. Miscellaneous; XII.A. Defense and cell rescue; XII.B. Abiotic stimuli and development; XII.C. Unknown function; XIII. No homology.
2. Annotation was derived from the latest MENS (*Medicago truncatula* EST navigation system) database or TIGR *Medicago* Gene Indices.
3. Calculated probability of Type I error.

and 4.8) were separately compared with 0h0N. Using this analysis strategy, 47 probes were identified to be up-regulated and 36 probes were down-regulated by inoculation-only treatment; 217 probes were up-regulated and 29 probes were down-regulated by inoculation/NO; 19 probes were up-regulated and 60 probes were down-regulated by inoculation/NH treatment. However, only probes with well defined function were included in Table 4.3-Table 4.8; all probes that had unknown functions or no homology in gene bank were placed in the Appendix B. A detailed discussion about some of these annoted probes' molecular function and their possible involvement in the three treatments are addressed in the Discussion section.

4.2.5 Selected Genes Presumably Related to Nodulation

The analysis conducted so far is based on the probes that exist across all the ten samples and 20 microarrays as stated before. Due to this stringent criterion, some probes that were significantly up-/down-regulated in some samples might not be included because their signals were lost in one or more samples or slides. As a complement to the above analysis, several key words were used to search against the name and annotation of all the probes on the microarray to select the probes that might be related to nodulation or nitrate/ ammonium treatment. The key words used for probes' selection were "auxin", "cytokinin", "ethylene", "gibberellin", "nitrate", "ammonium", and "nod". All the selected probes were then filtered through the SNR$\geq$2 criterion. For each probe, fold change and significance analysis were conducted only on the samples where the probe had signals on both replicate microarrays, and otherwise the data from that sample was excluded from the analysis. All the probes that showed 1.5 fold changes in relative to 0h0N at 0.05 significance level on at least one sample are summarized in Table 4.9.

Two probes representing auxin-induced proteins-encoding genes (TC88867 and TC82846) were down-regulated at one time point of inoculation-only treatments. These two probes were also down-regulated in inoculation/NO treatment (TC88867, 6 hpi) or inoculation/NH treatment (TC82846, 6 hpi). One probe representing auxin influx carrier protein-encoding gene (TC86757) was down-regulated by inoculation/NH treatment at 6h. The only up-regulated probe related auxin was one corresponding to the auxin response factors (TC79570).

A probe corresponding to Cytokinin receptor (TC92758) was identified to be up-regulated in 24hNH sample. Another probe (TC91741) annoted to gibberellin-20 oxidase was up-regulated in 12hNO sample. In addition, three ethylene-responsive element binding factors (ERFs) were detected to be specifically up-regulated by nitrate at 12 hpi.

A second probe (TC78158) corresponding to high affinity nitrate transporter protein-encoding gene was detected in this analysis to be up-regulated throughout the three time points by the inoculation/NO treatment. The other two nitrate transporters putatively belong to the low affinity transporter family (peptide transporter family). One of them (TC79437) was down-regulated in 24hNH sample and the second one (TC89683) was repressed by nitrate (at 6h).

Concerning the detected expression of the thirteen nodulin genes in inoculation-only treatment, three nodulins were detected to be up-regulated (TC90651, 79496, 77897) at 6 hpi, one nodulin precursor (BI309313, EST#) was repressed at 24 hpi, and the other seven nodulins were not detected to be significantly changed. In inoculation/NH treatment, two nodulins (TC85858 and TC77897) were up-regulated at one time point whereas five nodulins (TC77133, TC85603, TC85604, TC85605, and BI309313) were

Table 4.9 Summary of the Expression of the 27 Specially Selected Probes at All Time Points and Treatments

Oligo ID	TIGR ID	Tentative Annotation	6h0N	24h0N	6hNH	24hNH	6hNO	12hNO	24hNO
MT008110	TC86757	Auxin influx carrier protein			down				
MT009460	TC88867	Auxin-induced protein-like	down				down		
MT011223	TC82846	Auxin induced proline rich protein		down	down				
MT002071	TC79570	Auxin response factor 3							up
MT013731	TC92758	Cytokinin receptor CRE1b				up			
MT000060	TC76339	Ethylene-responsive element binding protein homolog	down						
MT009243	TC79268	Ethylene-responsive element binding protein 1		up				up	
MT015271	TC76842	Ethylene responsive element binding factor 5 (ATERF5)						up	
MT015272	TC76841	Ethylene responsive element binding factor 5						up	
MT002563	TC79954	Ethylene responsive element binding factor 3 (AtERF3)						up	
MT015960	TC91741	Putative gibberellin 20-oxidase						up	
MT002156	TC79437	Nitrate transporter (NTL1)				down			
MT002501	TC78158	Probable high affinity nitrate transporter protein					up	up	up
MT003394	TC89683	Nitrate transporter					down		
MT004315	TC90651	Nodulin-like protein	up				up		
MT007328	TC85858	*M. truncatula* enod40 mRNA for non-translatable RNA				up			
MT007364	TC77133	Early nodulin 12B precursor (N-12B),			down				
MT009148	TC79496	Nodulin 14 precursor (N-14)	up				up		
MT012442	TC90621	Nodulin-like protein					up		
MT001044	TC77897	Nodulin-like protein	up		up		up	up	up
MT014945	TC91854	Nodulin-like protein						up	
MT015153	TC85603	Nodulin precursor			down				
MT015154	BI309313	Nodulin precursor		down	down				
MT015155	TC85605	Nodulin precursor			down				
MT015156	TC85604	Nodulin precursor			down				
MT015194	TC76631	Putative nodule membrane protein					up	up	
MT001597	TC78291	Nodulin-like protein						down	down

down-regulated at one time point. In inoculation/NO treatment, there were 6 nodulins (TC90651, TC79496, TC90621, TC77897, TC91854 and TC76631) were detected to be up-regulated. Two of them (TC77897 and TC76631) were up-regulated at more than one time point by inoculation/NO. Only one nodulin-like protein-encoding gene (TC78291) was detected to be down-regulated.

4.2.6 Differential Effects of Inoculation/NO and Inoculation/NH Treatments on the Expression of Nodulation-related Genes

To screen nodulation-related genes that were differentially regulated by nitrate or ammonium, all the 59 probes that differentially expressed in the inoculation-only treatment were selected and tracked for their expression in the other two treatments (Table 4.10 and Table 4.11). Since the purpose of this comparison is to find out the differential effect of nitrate and ammonium on the nodulation-related genes, different from all the above comparisons which compare all the genes' expression levels in each of the 9 samples (3 treatments x 3 time points) to their expression levels in 0h0N (non-inoculated root), all the nodulation-related genes' expression levels at each time point in inoculation/NO and inoculation/NH treatments are compared to their expression levels at the same time point in the inoculation-only treatment (i.e., the nodulation-related genes' expression levels in 6hNH and 6hNO samples were compared to their expression levels in 6h0N sample respectively and the gene expression levels in 12hNH and 12hNO were compared to their expression levels in 12h0N sample). The results of the comparison are summarized in Table 4.10 and Table 4.11. The analysis of these two tables is put in the Discussion section.

Table 4.10 Effects of Inoculation/NO and Inoculation/NH Treatments on the 35 Probes Detected to be Up-regulated by Inoculation-only Treatment by *Mt16OLI1* Microarray

Oligo ID	TIGR ID	Annotation	6hNH	6hNO	12hNH	12hNO	24hNH	24hNO
MT000172	TC85552	Hydroxymethylglutaryl-coenzyme A reductase		up	up		down	
MT000176	TC85529	K^+ channel tetramerisation; BTB/POZ domain					down	
MT000326	TC85855	Heavy metal transport/detoxification protein						
MT000812	TC77754	Zn-finger, modified RING						
MT003548	TC80587	Probable *rip-1* peroxidase gene product (3'UTR) [nodulin]						
MT004212	TC81363	No apical meristem \(NAM\) protein	down					
MT006913	TC82952	Probable albumin/Leginsulin						
MT007207	TC85631	Respiratory-chain NADH dehydrogenase, subunit 1						up
MT007350	TC77094	Lipase, class 3 3.1.1.3						
MT007617	TC86303	Calcium-binding EF-hand					down	
MT007980	TC78144	Probable cold and water-stress induced portein-like protein						
MT009165	TC79619	Ras small GTPase, Rab type	down		up			
MT009590	TC88987	Putative phospholipase C		up		up		up
MT010049	TC85194	Lipoxygenase, LH2 domain 1.13.11.12			down			
MT010227	AL381280	Putative albumin/Leginsulin		up		up		up
MT013418	TC92778	UDP-glucose glucosyltransferase-like protein			up			
MT013424	TC92311	HMG1/2 \(high mobility group\) box	down		down	up	down	
MT014204	BQ143785	mRNA capping enzyme-like protein						
MT014651	TC78310	NADPH:quinone oxidoreductase						
MT014682	TC89001	RNA-binding region RNP-1						
MT015051	TC85153	Haem peroxidase 1.11.1.7			down			
MT015059	TC85161	Lipoxygenase, LH2 domain 1.13.11.12						
MT015105	TC76514	RNA-binding region RNP-1	down		down			up
MT015080	TC85174	Naringenin-chalcone synthase			down		down	
MT015144	TC76770	Naringenin-chalcone synthase						
MT015145	TC76767	Naringenin-chalcone synthase (EC 2.3.1.74)					down	
MT015146	TC85138	Naringenin-chalcone synthase 2.3.1.74					down	
MT015147	TC76769	Naringenin-chalcone synthase		up	down		down	
MT015149	TC76765	Chalcone synthase 2.3.1.74					down	
MT015188	TC85328	Gibberellin regulated protein						

Table 4.10 Effects of Inoculation/NO and Inoculation/NH Treatments on the 35 Probes Detected to be Up-regulated by Inoculation-only Treatment by *Mt16OLI1* Microarray (Continued)

Oligo ID	TIGR ID	Annotation	6hNH	6hNO	12hNH	12hNO	24hNH	24hNO
MT015213	TC76652	Granulin; Papain cysteine protease \(C1\)						
MT015276	TC85679	ATP citrate lyase						
MT015465	TC77767	Heavy metal transport/detoxification protein					down	
MT015537	TC78576	Heavy metal transport/detoxification protein						
MT015627	TC79321	Gibberellin regulated protein		up				

Table 4.11 Effects of Inoculation/NO and Inoculation/NH Treatments on the 24 Probes Detected to be Down-regulated by Inoculation-only Treatment by *Mt16OLI1* Microarray

Oligo ID	TIGR ID	Annotation	6hNH	6hNO	12hNH	12hNO	24hNH	24hNO
MT000126	TC85379	S-adenosylmethionine decarboxylase proenzyme						
MT000511	TC77262	Legume lectin						
MT003897	TC82820	60S ribosomal protein L32 RP49			up	up		down
MT005666	TC83381	Caffeic acid O-methyltransferase	up					
MT006734	TC90867	Probable natural resistance-associated macrophage protein						
MT007028	TC76540	Protein transport protein MIP family;						
MT007297	TC76955	Putative phosphatase						
MT007766	CA989617	Glyoxalase/Bleomycin resistance protein/dioxygenase domain						
MT008479	TC87442	Putative glutenin						
MT009448	TC88937	Glycoside hydrolase, family 32 3.2.1.26						
MT013646	TC80377	Haem peroxidase						
MT014114	TC85431	Plant lipid transfer/seed storage/trypsin-alpha amylase inhibitor		up				
MT014219	TC85379	S-adenosylmethionine decarboxylase proenzyme						
MT014220	TC85388	S-adenosylmethionine decarboxylase						
MT014222	TC85380	S-adenosylmethionine decarboxylase						
MT014223	TC85382	S-adenosylmethionine decarboxylase						
MT014263	TC85392	Heat shock protein Hsp70						
MT014697	TC79658	Serine/Threonine protein kinase;						
MT014721	TC80862	protein transport					up	
MT014813	TC82572	Leucine-rich repeat, plant specific				up		
MT015103	TC85301	Extensin-like protein; Proline-rich region						
MT015128	TC76538	Cold acclimation responsive protein BudCAR5						
MT015278	TC76902	Plant lipid transfer/seed storage/trypsin-alpha amylase inhibitor [NODULIN MtN5]						
MT015314	TC85491	Plastocyanin-like	up				up	

5.0 DISCUSSION

5.1 Plant Growth Responses

Although many legumes can live with fixed atmospheric N_2 as their sole nitrogen source, they are generally more productive when grown with the addition of mineral N (Harper, 1974; Yinbo et al., 1997). The inferior performance of legumes without external nitrogen can be due to the higher energy cost to develop, maintain and operate N_2-fixing nodules than to assimilate available N (Gan et al., 2004). The results of this study are in agreement with previous studies: the whole plant growth was stimulated by both ammonium and nitrate and higher nitrogen concentrations promoted more accumulation of dry weight. These observations are also consistent with previous experiments conducted on pea and white clover (Gulden and Vessey, 1997; Fei and Vessey, 2004). However, in contrast to the results of Bollman (2002) and Xu et al. (1992), which indicated that at low concentrations both mineral nitrogen forms had very similar effects on growth, the growth of nitrate-treated plants was much more vigorous than the ammonium-treated ones at all the concentration levels and in all three experiments conducted in this study (Fig 4.1). Jointly with the poorer performance of ammonium-treated plants, it was also observed that starting from 12-13 DAI these plants showed potassium-deficiency symptoms (deficiency symptoms appeared on the old leaves, leaf chlorosis starts from leaf tip and progress down the margin toward the leaf base, no interveinal chlorosis was observed, McCauley et al., 2003) in both Exp. 1a and Exp. 2,. The inhibition of potassium absorption by ammonium has been long observed (Mengel and Hehl, 1976), which was considered as a result of competition between the absorption

of these two cations. One possible reason for this competition is that these two ions might share a transport system (Forde and Clarkson, 1999). It was reported that biomass production of ammonium-grown plants increased with K^+ concentration in the nutrient medium between 0.1 to 3 mM (Marschner, 1995) and in our experiment, potassium concentration in the ammonium-containing nutrient solutions were 1 mM. Therefore, increasing the concentration of K^+ may be a possible way to overcome the observed poorer performance of plants treated with ammonium as sole nitrogen source.

5.2 Plant Nodulation Responses

As legume plants grown with additional nitrate or ammonium generally develop much larger root system than those that use N_2-fixation as a sole nitrogen source, regardless of whether the mineral N (especially at low concentration) has a stimulatory or inhibitory effect on the specific nodulation, the total number of nodules per plant can be stimulated (Gan et al., 2004; Bollman, 2002; Gulden and Vessey, 1997). This can be explained by the fact that the nitrogen-enhanced root growth supplies many more sites for the infection by rhizobia. In this study, the whole plant nodule number increased with the increasing concentration of either ammonium or nitrate (Fig. 4.3) which is in accordance to the results of most of other studies, although contrary to one previous study (Waterer and Vessey 1993b) which found nitrate concentration as low as 0.1 mM significantly inhibited whole plant nodule number in pea at 21 DAI.

A more informative parameter to evaluate the effect of mineral N on nodulation is specific nodulation (nodule number per g root DW). Ammonium, at concentration levels of 0.1-2.0, was observed to stimulate specific nodulation in pea (Waterer et al., 1992; Gulden and Vessey, 1997) and in white clover (Fei and Vessey, 2004). However, in this

study, ammonium did not display any stimulating effect on specific nodulation at the tested concentration range (0.1-1.0 mM), although it exerted less inhibitory effect on specific nodulation than the same levels of nitrate at all three concentrations tested (Fig. 4.4). The lack of stimulation of specific nodulation in *M. truncatula* by ammonium may be related to the poorer performance of the plants due to potassium deficiency. Moreover, the stimulating effect of low concentrations of ammonium on nodulation of temperate legumes was hypothesized to be the consequence of the suppression of the autoregulation system of legume plants (Waterer et al., 1992). The specific nodulation-stimulating concentration of ammonium in pea plants varied from 0.1 mM-2.0 mM with different culture systems (Waterer et al., 1992; Gulden and Vessey, 1997; Fei and Vessey, 2003) and recently, it was found that the stimulating effect was not evident until NH_4^+ concentration as low as 0.1 mM in white clover (Fei and Vessey, 2004). These observations underlie the possibility that the autoregulation system in *M. truncatula* could be more sensitive to ammonium concentration than other temperate-origin legumes, and hence it probably requires a lower concentration of ammonium to stimulate specific nodulation. Due to the small physical size of the *M. truncatula* plants, maintaining the nitrogen concentration lower than 0.1 mM (e.g. 0.05 mM) will be feasible by increasing the speed by which the nutrient solution is pumped into the root zone (e.g., using 2ml/min instead of 1 ml/min used in present exprements).

Nitrate, at the concentration levels of 0.1-0.5 mM, inhibits the specific nodulation in pea (Waterer and Vessey, 1993; Bollman, 2002). The results of current study also support these previous observations (Fig 4.4.B and Fig. 4.4.C). The inhibitory effects of

nitrate on the initiation of nodulation were suggested to be manifested through its interaction with plant hormones (Ferguson and Mathesius, 2003).

The most distinguishing effects on specific nodulation of ammonium and nitrate existed at the concentration of 0.1 mM. At this concentration, ammonium-treated plants had the same level of specific nodulation as the control plants (Fig. 4.4.A and Fig. 4.4.C), but nitrate significantly inhibited specific nodulation at 0.05 probability level in the growth pouch culture system (Fig. 4.4.C) and at 0.059 probability level in sand culture system (Fig. 4.4.B).

Why are legumes more sensitive to the negative effects of nitrate on nodulation than ammonium? Firstly, this could be a consequence of the long term adaptation of legumes to their living environment. As in most of the soil, the concentration of NO_3^- are often 10-1000 times higher than those of ammonium (Marschner, 1995) and hence nitrate is the predominant mineral nitrogen form that legume plants are able to make use of. Therefore, nitrate naturally becomes the most effective "triggering molecule" for the suppression of the establishment of the more-costly biological N_2-fixation. Secondly, ammonium is a major product during the N_2-fixation process, and it's estimated that the concentrations of ammonium in nodules cells are 12 mM in the bacteroids and 0.21 mM in the cytosol (Streeter, 1989). The existence of substantial concentration of ammonium in the nodules may be another reason why ammonium has less negative effect on nodulation than nitrate.

The addition of mineral N has been reported to cease the growth of the nodules of several legumes (*M. sativa*, *P. sativum* and *Glycine max* (L.) Merr.) (Patriarca et al., 2002; Fujikake, 2003). In this study, *M. truncatula* plants treated with either nitrate or

ammonium had smaller nodules than the control plants (Fig. 4.5.A and Fig. 4.5.B), which is also in agreement with Gulden and Vessey's (1997) observation in pea. Moreover, nodule growth was more sensitive to nitrate addition than to additions of ammonium (Imsande, 1986). Similarly, we observed in this study that at 0.5 mM concentration level, nitrate inhibits nodule growth whereas ammonium has no effect (Fig. 4.5.C).

The specific nodule DW is an indicator of both the specific nodulation and the development of the nodules (nodule mass). Gan's *et al.* (2004) reported that at the 1 mM level, both ammonium and nitrate inhibited the specific nodule DW. Similar results were observed in this study (Fig. 4.7.A and Fig. 4.7.B). Moreover, nitrate exerted a higher inhibitory effect than ammonium at both concentrations tested in growth pouch culture system (Fig. 4.7.C). Again, this supports the observation of generally more negative effects of nitrate on the nodulation process than ammonium.

5.3 Plant Nitrogen Accumulation and Nitrogen Fixation Responses

As expected, whole plant nitrogen content (Fig. 4.8) and concentration (Fig. 4.9) increased with the increased availability of mineral nitrogen (either NH_4^+ or NO_3^-). Bollman's observation (2002) and Gan's observation (2004) that there were no significant differences in total nitrogen content between ammonium-treated legume plants and nitrate-treated plants at 0.5 mM. In contrast, significantly higher content and concentrations of nitrogen in nitrate-treated plants than ammonium-treated one at 0.5 mM level was observed in present experiments. This may be another indication of better performance of nitrate-treated plants than ammonium-treated plants.

Nitrogenase activity has been long known to be inhibited by the addition of mineral N (Vessey and Waterer, 1992). In early studies, the reported low limits of the

concentration range which can cause an inhibitory effect of nitrogenase activity were 2.5 mM for NH_4^+ (Silsbury, 1986). Experiments by Gulden and Vessey (1997) using H_2 gas exchange measurements have indicated that the whole plant nitrogenase activity was inhibited by ammonium at concentration as low as 0.5 mM. Consistent with Gulden and Vessey's (1997) observation, in present experiment, the total NDFA was lower in all ammonium-treated plants than the control plants (Fig. 4.11.A and Fig. 4.11.C). Taking the fact that all ammonium treatments had equal or higher number of nodules (Fig. 4.3.A and Fig. 4.3.C), this observation indicates a generally inhibitory effect on nitrogenase activity by ammonium. In contrast to Streeter's (1988) conclusion that 3 mM is the nitrogenase inhibitory concentration for nitrate, it was found that NO_3^- at 0.5 mM and above exerted inhibitory effects on total NDFA (Fig. 4.10) in this study. The observation that 0.1 mM nitrate-treated plants fixed more nitrogen (Fig. 4.11.C) or equal nitrogen (Fig. 4.11.B) compared to control plants can be related to the fact that the nitrate-treated plants possess more nodules than (Fig. 4.3.C) or similar number of nodules to (Fig. 4.3.B) that in control plants. So the apparent higher NDFA in 0.1 mM NO_3^- does not indicate a higher or lower nitrogenase activity. Several hypotheses were proposed to explain the mechanisms by which mineral N inhibits nitrogenase activity (Streeter, 1988; Vessey and Waterer, 1992; Bacanamwo and Harper, 1997). Although it's not clear exactly how mineral N inhibits the nitrogenase activity, the reason for this response of the legume is easy to understand: the biological costs in terms of carbon requirement for nitrate uptake and assimilation are approximately one third lower than the costs of N_2-fixation, and cost for ammonium assimilation can be lower than the cost of nitrate assimilation (Pate and Layzell, 1990).

Although the total NDFA of nitrate treatments were higher than or equal to that of ammonium treatments at both 0.1 and 0.5 mM concentration levels (Fig. 4.11.C), the %NDFA of nitrate treatments were significantly lower than that of ammonium treatments at both levels (Fig. 4.10.C). This may also indicate that *M. truncatula* plants couldn't uptake/assimilate ammonium as efficiently as nitrate.

5.4 Analysis of Differential Gene Expression During the Initiation of Symbiosis With and Without the Presence of NH_4^+ and NO_3^- by Utilizing *Mt16kOLI1* Microarrays

5.4.1 Fidelity of the Microarray Results

The reliability of experimental data is indisputably the most crucial thing for any experiment. Especially when using an experimental technique involving complicated procedures such as microarrays, the control of the data quality becomes one of the essential parts of the experiment. DNA microarray being a relatively new technique, there are not many conventional ways to monitor the quality of the data; the data quality measuring methods used in this experiment were mainly based on the recommendations of the protocols of some commercial labelling kits (Amino-allyl cDNA labelling kit, Ambion) and the handbook of commercial data analysis software (Acuity 4.0). The quality of total RNA (Fig. 4.13), Cyanine-labelled cDNA (Fig. 4.14 and Fig. 4.15) and the quality of DNA microarray data (Fig. 4.16, 4.17, and 4.18) were examined in this experiment, and all the results of these examination suggested that the microarray data are reliable.

The general good agreement on the signal intensity and signal color (Fig. 4.16) between the two replicates spots on the microarray indicates the consistency of hybridization within each of the total 48 blocks of spots on the microarray. More green colored spots were observed than red colored ones because the green fluorescence dye (Cy3) was used to label the common reference which was a mixture of all the ten samples and therefore any gene that was turned on in any of the ten samples will at least emit a green fluorescence.

In the hierarchical clustering graph (Fig. 4.17), almost every pair of replicate microarrays were clustered together, which reflects the good reproducibility between the data from each pair of replicate microarray. The only exception was the three replicate microarrays for 12h0N sample. The distant relationship between the three replicates of 12h0N sample could be well explained by the way they were processed. The second replicate of the microarrays for the 12h0N treatment (12hr_0N_2, Fig. 4.17) was severely contaminated during washing steps, which could contribute to its dissimilarity to the first replicate microarray (12hr_0N_1, Fig. 4.17). The third replicate microarray (12hr_0N_3, Fig. 4.17) microarray was hybridized and processed at a different time as a complement to the contaminated second replicate, therefore the variations caused by the day to day operational differences (such as the different hybridization time etc.) or instrument performance variation (such as the fluctuation of the temperature in the hybridization oven etc.) were included in this replicate. In contrast, these day to day variations were not included in other replicates microarrays since each all other replicate microarrays was done in the same day and processed at the same time.

The general agreement between the regulation tendency (up- or down-regulation) of the three marker genes obtained from DNA microarray and real time qRT-PCR techniques again reflects the reliability of microarray data (Table 4.1). The discrepancy in the exact ratios between real time qRT-PCR and DNA microarray are observed quite often (Manthey, 2004; Hohnjec, 2005), which could be due to the facts that real-time qRT-PCR is a more sensitive technique than hybridization-based DNA microarray and cross-hybridization is not likely an issue in the PCR-base technique (Manthey, 2004).

The analysis of the detected ratios of the three probes representing both ends and the middle region of *GAPDH* mRNA (Fig. 4.18) proves that the majority of *GAPDH* mRNA was reversely-transcribed into full length cDNA and quite possibly the same for all the mRNA species in the samples. The 70-mer probes on the microarray were selected from any region within 1000 bp range of the 3' end of each gene[5], so to obtain full length cDNA is important for the reliable of the result. In 12hNH sample, the higher ratio of probe corresponding to 3' end of *GAPDH* mRNA and the lower ratio of the probe corresponding to 5' end of *GAPDH* mRNA indicate that only a portion of all the *GAPDH* mRNAs in the cell was reversely-transcribed into full length cDNA, and the other portion of the *GAPDH* mRNAs was only partially reversely-transcribed. Therefore any conclusion based on the data from this sample should be considered with caution. Moreover, the small variation of expression level (within 1.3 fold change in relative to 0h0N) among all the nine samples supported the house keeping gene feature of *GAPDH*, not to be significantly influenced by general treatments and this result also founded the use of this gene as endogenous control in real-time qRT-PCR.

5.4.2 Generalizations Based Upon the Microarray Results

That generally more up-regulated probes than down-regulated genes were detected for each of the samples (Table 4.2) can be explained by the fact that the majority of the down-regulated probes exhibited low expression level which generally display higher variation (Kouchi, 2004). The numbers of up-regulated probes in the inoculation/NO treatment are much higher than those in the other treatments across all three time points probably indicates that the root of *M. truncatula* underwent more dramatic changes in their cell metabolic functions after nitrate was added compared to the

[5] Array-Ready Oligo Set™ for the *Medicago* Genome Version 1.0, Introduction file

addition of the other two treatments. This could be explained by the fact that it takes two reducing steps to convert nitrate into ammonium in the plants (Crawford, 1995).

5.4.3 Analysis of Some of Differentially Expressed Genes

Generally, there are tens of genes up-/down-regulated by each of the three treatments: inoculation-only, inoculation/NO and inoculation/NH. However, only genes that were documented to be related to nodulation, nitrate or ammonium metabolisms are discussed in the following discussion part.

5.4.3.1 Genes Differentially Expressed in the Inoculation-only Treatment

5.4.3.1.1 Up-regulated Probes (Table 4.3)

In the Secondary Metabolism and Hormone Metabolism functional category (group VI), several tentative consensuses (TCs) representing chalcone synthase (CHS) (TC85138, TC76767, TC85174, TC76769, TC76770, TC76765) were up-regulated. The CHS enzyme is involved in the first step committed to flavonoid biosynthesis (McKhann, 1997). Specific flavonoids secreted by legume root are important signal molecules inducing the bacterial nodulation genes (*nod* genes) in the initiation of symbiosis between legume and rhizobia (Vance, 2002) and the synthesis of these *nod*-gene inducing flavonoids are further stimulated by inoculation (Recourt et al., 1992). However, the flavonoid biosynthesis pathway also leads to the synthesis of isoflavonoids, the precursors of phytoalexins. The phytoalexins are synthesized as part of the hypersensitive response to incompatible pathogens (Dixon, 1986), and in legume plants they are generally not significantly induced by compatible rhizobia (Mellor and Collinge, 1995). Estabrook and Sengupta-Gopalan (1991) found that symbiosis partner and pathogen induce the expression of different members of CHS gene family in soybean. It was also

reported that the expression level of two CHS gene family members, which were identified to express in nitrogen-fixing nodules, increased in alfalfa roots inoculated with wild-type rhizobia compared to those inoculated with incompatible strains or and exopolysaccharide mutant at 2 to 4 days post inoculation (McKhann, 1997). However, there is no reference about which ones of these TCs on the microarray represent the symbiosis-specific CHS. Furthermore, exactly what are the specific compounds derived from rhizobia to induce the production of *nod*-gene inducing flavonoids and inhibit the production of phytoalexins are not known (Mithofer, 2002).

Legume nodules generally contain higher levels of GAs than adjacent root tissue (Ferguson and Mathesius, 2003). It was also found that application of GA_3 or GA_4 induced the formation of nodule-like structure on the roots of *L. japonicus*, and this induction was completely suppressed by the addition of nitrate (Kawaguchi, 1996), which indicates that GA might play a role in the initiation of legume nodules. The up-regulation of two gibberellin-regulated proteins (TC79321 and TC85328) in our results also provides indirect proof of the involvement of gibberellin in the initiation of nodulation.

An important tentative consensus in group XII.A (Defense and Cell Rescue) is the TC representing 3'-untranslation region of *rip*-1 peroxidase gene (TC80587). *Rip1* was reported to be continuously induced by rhizobia and Nod factors during the first 3 to 96 h post inoculation in *M. truncatula* (Cook, 1995). Moreover, the induction of *rip-1*, just as the induction of some of other initial symbiosis events, requires the presence of a sulfate moiety in the Nod factor structure (Ramu et al., 2002). *Rip-1* is generally used as a transcriptional marker for early Nod factor responses (Kuppusamy et al., 2004). The *rip-1*

gene product was proposed to participate in the peroxidase-mediated cell wall modification during *S. meliloti* infection and nodule organogenesis (Ramu et al., 2002).

Another group of TC (TC77767, TC78576, TC85855) encoding the proteins that have the putative heavy metal transport/detoxification function. One of them (TC78576) was found to be induced in arbuscular mycorrhiza fungi-colonized *M. truncatula* roots (Hohnjec, 2005), and was related to the heavy metal detoxification feature of mycorrhizal roots. Arbuscular mycorrhizal fungi are able to colonize the root of almost 80% of all living land plants including legumes and their major function is to assist plant in acquiring phosphorus nutrient (Newman and Reddel, 1987). Some genes that were required for legume-rhizobia symbiosis were also found to be required for the symbiosis between legume and arbuscular mycorrhizal fungi and these group of genes were named as "common *SYM* genes" (Kistner and Parniske, 2002). As a result, although this gene's induction by rhizobia inoculation has not been reported previously, it may be another common *SYM* gene.

The albumin/leginsulin family genes are strongly expressed both in seeds and in nodules. These genes encode toxic peptides which could protect seeds and nodules (rich carbon and nitrogen source) from pathogen and pest attacks (Gressent et al., 2003). In this study, two members of this gene family (AL381280 and TC82952) were observed to be induced. Several members of this family were also detected to be up-regulated in nodules in relative to non-inoculated *M. truncatula* roots (El Yahyaoui, 2004), but there is no reference about those genes' up-regulation in the inoculated root at the initiation of nodulation. The accumulation of these toxic peptides in seedling roots at the initiation of

nodulation may also be an induced resistance response associated with the infection of the root by rhizobia.

A group of genes putatively related to signal transduction were also found to be up-regulated by inoculation of *S. meliloti*. In legume roots, a sharp oscillations of cytoplasmic calcium ion, termed calcium spiking, is triggered by Nod factors (Wais, 2000). Calcium oscillations play a role in signal transduction in several systems. The calcium-binding EF-hand (TC86303) is the calcium-binding domain of a series of calcium-binding protein. One group of these proteins, calmodulin is reported to play a role in the signal transduction process in the establishment of symbiosis (Mitra, 2004). Phospholipase C (TC88987) was implicated to be required in the Nod factor-induced calcium spiking (Engstrom, 2002).

5.4.3.1.2 Down-regulated Probes (Table 4.4)

It is generally accepted that, during nodulation process, the successful colonization of host plant root tissue by compatible rhizobia needs to suppress the plant defense reactions normally induced by pathogen (Mithofer, 2002). However, under certain stages of nodulation process, some plant defense reactions are triggered. For example, Vasse *et al.* (1993)'s study showed that elicitation of a hypersensitive reaction was part of the mechanism of the autoregulation in legume-rhizobia symbiosis. Furthermore, Gamas *et al.* (1998) found that two nodulin genes MtN1 and MtN13 putatively encode proteins whose structures are actually related to plant defense reactions-related proteins. One of their explanation about the induction of plant defense related protein by compatible rhizobia is to protect the nodules from other pathogens (Gamas et al., 1998). Therefore, it easy to understand that in the study of legume-rhizobia

symbiosis using DNA microarray techniques, the gene expression profiling always proves that some of the defense-related genes are down-regulated by inoculation and others are up-regulated (El Yahyaoui, 2004; Kouchi, 2004). The same situation was observed in this study. Several plant defense-related genes (TC85153, TC82952, AL38128, TC80587, and TC78144) were up-regulated and another group of plant defense-related genes were down-regulated (TC90867, TC85392, TC85431, TC76902, TC80377, and TC76538). A probe probably encodes protein (TC80377) belonging to the peroxidase family is intriguing. Whereas this peroxidase-representing TC was down-regulated, the other two peroxidase-representing TCs (TC80587 and TC85153) were detected to be up-regulated (Table 4.3) on the same microarray slides. These three peroxidase-representing TCs may represent different members of the peroxidase family and thus may reflect the fact that during the development of symbiosis, the symbiosis-specific genes take over the function of non-symbiotic members of the same family (Yahyaoui, 2004).

S-adenosylmethionine decarboxylase (TC85388, TC85379, TC85379, TC85382, and TC85380) is a key enzyme in the polyamine biosynthesis pathway, which catalyze the production of spermidine and spermine using S-adenosylmethionine and putrescine as precursors (Walters, 2000). Polyamines are aliphatic nitrogenous poly-cations that contain two or more amine groups. They are found in virtually all organisms including microorganisms, plants and animals (Evans and Malmberg 1989). Putrescine, spermidine and spermine are the most abundant and physiologically active polyamines in plants (Martin-Tanguy, 2001). Polyamines are implicated in a variety of growth, physiological and developmental process in higher plants and are considered to be plant growth

regulators (Evans and Malmberg, 1989). In legume-rhizobia symbiosis, putrescine was found to promote the dry weight accumulation of nodules and shoots of both chickpea and vetch inoculated with both commercial inoculants and indigenous strains of *R. leguminosarum* (Atici et al., 2005). In another study, all the three polyamines promoted the nodulation of Goat's rue (*Galega orientalis*) by *Rhizobium galegae*, with putrescine the most effective nodulation-promoting polyamine (Vassileva and Ignatov, 1999). There are no literatures about how the transcript abundance of S-adenosylmethionine decarboxylase changes during the initiation of symbiosis or the exact function of polyamines in the symbiosis. However, taken the promoting effect of putrescine on nodulation observed in other studies and the decreased S-adenosylmethionine decarboxylase observed in this study together, a brave assumption could be made: the plant putrescine may play important role in the initiation of nodulation and the hence the synthesis of spermidine and spermine is suppressed by decreasing the S-adenosylmethionine decarboxylase so as to facilitate the accumulation of putrescine. Certainly, the content of all three polyamines in inoculated roots need to be compared to that in non-inoculated roots to exam this assumption.

MtN5 (TC76902) belongs to the family of nonspecific lipid transfer proteins and was identified as a nodulin gene (Gamas et al., 1996). MtN5 was found to be up-regulated in the whole root system harvested 3 dpi in relative to no-inoculated root in *M. truncatula* (El Yahyaoui, 2004). In contrary, this gene was detected to be down-regulated in inoculated root in the first 12 hpi in this study. However, since nobody has reported about the expression of this nodulin genes in such a short time after inoculation as in our

study, there is the possibility that MtN5 is down-regulated in first 12 hpi and then up-regulated at 3dpi.

5.4.3.2 Genes Differentially Expressed in Inoculation/NO Treatment

5.4.3.2.1 Up-regulated Probes (Table 4.5).

Two genes possibly directly related to nitrate metabolism were detected, which are a high affinity nitrate transporter (TC78157) and a glutamate dehydrogenase (TC77578). The high affinity nitrate transporter is nitrate-inducible and it plays a major role in nitrate uptake when the available nitrate concentration is low (usually lower than 0.5 mM) (Williams and Miller, 2001). Glutamate dehydrogenase is a branch point enzyme with an important link to energy metabolism and it catalyzes the reaction of converting free ammonia and α-ketoglutarate to glutamate and the reverse reaction. The forward reaction incorporates the reducing product of nitrate—the ammonium, into the amino acid, and the latter is also a principle donor to other amino acids in subsequent transamination reactions. The reverse reaction is a key process linking amino acid metabolism with TCA cycle via converting glutamate to ammonium and oxidizable TCA cycle intermediates (Andersson and Roger, 2003). Its up-regulation in the inoculation/NO treatment relative to 0h0N treatment quite possibly indicates that the increased capacity of plant root cells to incorporate ammonium into amino acid as a consequence of the increased nitrate absorption and metabolism.

Interestingly, there are quite a number of plant resistance/stress-related genes were detected to be up-regulated by inoculation/NO (TC87724, 79735, 81627, 78144). These genes were not identified in inoculation-only treatments, so they are more likely related to the rapid addition of nitrate from none. In a microarray research focusing on

nitrate-induced genes (Wang, 2001), some abiotic and biotic stress responsive genes were also detected and they suggested the possible reason could be that rapid nitrate supply causes a transiently increased production of nitrite, which can be toxic to plants and hence triggered plant defense system. Another possible explanation for the up-regulation of plant resistace/stress-related genes by inoculation/NO could be the production of nitric oxide (NO) in plant cells associated with the transiently increased production of nitrite. Nitric oxide is considered as a signal in plant defense responses and can be synthesized from nitrite reductase in plants (Wendehenne et al., 2001).

5.4.3.2.2 Down-regulated Probes (Table 4.6)

A probe encoding the probable nitrate transporter (TC89683) was down-regulated by inoculation/ NO_3^- treatment. This nitrate transporter is homology to the low affinity transporter family (peptide transporter family). Although at the 0.1 mM NO_3^- level (Williams, 2001), the high affinity nitrate transporter would be expected to function (this is supported by the up-regulation of one high affinity nitrate transporter (TC78157)), the down-regulation of low affinity nitrate transporter by low NO_3^- level has not been reported before (Glass, 2002; Forde, 2000; Orsel, 2002; Williams, 2001).

5.4.3.3 Genes Differentially Expressed in Inoculation/NH Treatment

No genes in Table 4.7 and Table 4.8 were affected specifically by the ammonium treatment. As stated in physiological part of this experiment, *M. truncatula* plants treated with ammonium did not grow as well or absorb as much mineral N as nitrate-fed plants, possibly due to the inhibitory effect on K^+ uptake. Due to the lower growth rate and lower N uptake, it is possible that genes specially associated with ammonium metabolism (such as glutamine synthase) were not significantly affected. Because DNA microarrays

are not very sensitive in detecting the low level differential gene expression, the relatively small increase in these ammonium metabolism-genes may not have been detectable on the slides. In contrast, the effect of this inoculation/NH treatment on the up-regulation of *MtGsb* was by detected by the more sensitive real time qRT-PCR method (Fig 4.20).

5.4.3.4 Analysis of the Specially Selected Genes Presumably Related to Nodulation

Cautions should be taken in these specially selected genes since in contrast to the genes included in table 4.2 to 4.8, these genes' up-/down-regulation were usually transient and hence will be more difficult to validate in the further work. Generally, there were no genes showed distinct differential expression between three treatments (i.e., up-regulated in some treatments and down-regulated in other treatments). However, several genes that were up-/down-regulated only in certain treatments (samples) are worthy of mention.

The down-regulation of the two probes representing auxin-induced proteins-encoding genes (TC88867 and TC82846) at one time point (6h and 24h, respectively) by inoculation-only treatment (Table 4.9) could be an indicative of lower auxin concentration in the inoculated roots as reported by Mathesius et al. (1998). Auxin response factors (ARF) (TC79570) are transcriptional factors that bind specifically to the DNA sequence 5'-TGTCTC-3' found in the auxin-responsive promoter elements (AuxREs). They could act as transcriptional activator or repressor. Although auxin response factor 3 was up-regulated at 24hNO data point, there was no report about the auxin-dependent changes of the expression of the ARF genes (Liscum, 2002).

The up-regulation of one probe (TC92758) corresponding to the cytokinin receptor gene could reflect the increased cytokinin concentration in the ammonium-

treated plant roots at 24 hpi, which is in agreement with Fei and Vessey's report (2003) that low concentration of NH_4^+ promoted the endogenous *t*-Zeatin level in pea. Gibberellin 20 oxidase (TC91741) is a key enzyme involved in the biosynthetic pathway of active GAs (Lange, 1994); its up-regulation in 12hNO sample could indicate the increased gibberellin concentration in the nitrate-treated plants roots. Ethylene responsive factors (ERFs) (TC78158) are involved in mediating plants' response to ethylene as well as some biotic and abiotic stress (Onate-Sanchez, 2002). Ethylene was observed to inhibit nodulation in a number of legumes (Mulder, 2005). The up-regulation of ERFs in 12hNO sample could be an indicative of increased ethylene concentration in nitrate-treated plants, and if this is the case, the increased endogenous ethylene could be involved in the inhibitory effect of nitrate on nodulation as we observed in physiological experiment.

Concerning the genes related to nitrate metabolism, another high affinity nitrate transporter (TC78158) was found to be up-regulated by inoculation/NO treatment at all three time points. This gene was not included in Table 4.4 because its data was missing in 24h0N microarrays probably due to this gene's signal was too low. The down-regulation of low affinity nitrate transporter (TC79437) by ammonium (24 hpi) was observed which is in agreement with Touraine's (1997) report. Surprisingly, the second example of down-regulation of the low affinity nitrate transporter (TC89683) by nitrate (at 6h) was observed in this analysis.

More nodulins were up-regulated in inoculation/NO treatment, but not in the inoculation-only treatment, supports the fact that some of the nodulin genes are not specifically related to nodulation, instead, they are also involved in other plant cell metabolism process (Vance, 2000).

The oligo DNA (TC77448) representing the nodulation receptor kinase, which is distantly related to *GmNARK* (a gene that is involved in autoregulation) at protein sequence level (Searle et al., 2003), was also monitored for its expression among the treatment, however, it was not detected to be differentially regulated by any of the treatments, probably due to the low sensitivity of DNA microarray technique or the possible large false negative rate due to the small replicates used in this experiment.

5.4.3.5 Analysis of the Differential Effects of Inoculation/NO and Inoculation/NH Treatments on the Expression of Nodulation-related Genes

It is rational to assume that the differential effect of NH_4^+ and NO_3^- at 0.1 mM level on specific nodulation may reflect on their differential effects on the nodulation-related genes which ultimately determine the number of nodules on the root system. For example, some nodulation-related genes may be involved in the mechanism of autoregulation by which the legume controls how many nodules are to be established (Rolfe and Gresshoff, 1988). As shown in Table 4.10 and Table 4.11, the expression levels of quite a few of nodulation-related genes were influenced by the addition of ammonium or nitrate.

Among the genes that were up-regulated by the inoculation-only treatment relative to 0h0N, the expression levels of several TCs representing chalcone synthase (CHS) (TC85174, TC76767, TC85138, TC76769 and TC76765) were depressed by ammonium. As discussed above, CHS is a key enzyme in the biosynthesis of flavonoid (Mckhann, 1997) and the increase of the expression level of CHS gene may indicate the increased synthesis of *nod*-gene inducing flavonoids to facilitate the initiation of the legume-rhizobia symbiosis. From this point of view, the depressed expression of CHS by

ammonium seems to be contradictory to the observation that nitrate inhibited the specific nodulation more than ammonium. However, since the increase of CHS gene expression may also indicate the increased production of phytoalexins (Dixon, 1986), the up-regulation of CHS may be actually due to the initiation of plant defense reaction by rhizobia, and if this is the case, ammonium may manifest their less inhibitory effect on nodulation by repressing the plant defense reactions.

Among the 24 probes that were down-regulated by the inoculation-only treatment in relative to 0h0N, the expression of a plant lipid transferase which is related to pathogenesis (Yahyaoui et al., 2004) was promoted by nitrate at 6 hpi. This may indicate the inhibitory effect of nitrate on nodulation is related to the triggering of the plant defense reaction to against the invasion of rhizobia. However, no reference was found to relate the inhibitory effect of nitrate on nodulation to the induction of plant defense reaction, although Vasse *et al.* (1993) observed that the abortion of infection during the *Rhizobium meliloti*-alfalfa symbiotic interaction is accompanied by a hypersensitive reaction.

The majority of those nodulation-related genes that were significantly influenced by nitrate or ammonium are hard to interpret as the understanding of the mechanisms of autoregulation, via which the effect of ammonium and nitrate on nodulation may manifest themselves (Waterer et al., 1992), are still at the preliminary stage (Searle et al., 2003).

5.5 The Validation of Three Marker Genes Using Fluorescence Real Time qRT-PCR

As expected, the expression level of the high affinity nitrate transporter (*Nrt2*) was up-regulated by nitrate (Fig. 4.19) and the expression level of the cytosolic glutamine synthetase (*MtGsb*) was up-regulated by both nitrate and ammonium (Fig. 4.20). Furthermore, the cytosolic glutamine synthetase was only up-regulated 0.4-0.6 fold in the nitrogen treatments comparing to the N-free treatment, which proved that the real time RT-PCR was a very sensitive method in determining the gene expression level.

The regulation of the putative cytokinin receptor was not as we hypothesized (Fig. 4.21). The most possible reason is that the TC we chose did not actually represent the cytokinin receptor in *M. truncatula*. Actually, the TC sequence we used in this experiment was one of the four TC sequences in TIGR databases that have the tentative annotation to *Cre1b* (TIGR database) and another one TC sequence that was annoted to *Cre1b* (TC92758) was actually detected to be up-regulated specifically by 0.1 mM NH_4^+ at 24 hpi (Table 4.9), which could be a sequence that truly represents cytokinin receptor in *M. truncatula* and is worthy of further analysis.

5.6 General Discussion

Although it is generally recognized that the existence of mineral N will negatively influence the legume-rhizobia symbiosis (Streeter, 1988), the differential effects of ammonium and nitrate on the symbiosis in terms of the nodulation (Waterer et al., 1992; Waterer et al., 1993b) and the growth of nodules (Imsande, 1986) have been documented. Moreover, in pea and white clover, it was found that low, static concentrations of NH_4^+ (0.1-2.0 mM) actually result in a stimulation of specific nodulation (Gulden and Vessy,

1997; Fei and Vessey, 2004) whereas similar low concentrations of NO_3^- (0.1-0.5 mM) inhibit specific nodulation (Waterer et al., 1993b; Bollman, 2002).

This study is the first one focusing on the differential effect of low concentration of NH_4^+ and NO_3^- on the *M. truncatula-S. meliloti* symbiosis. In this study, ammonium and nitrate at the same concentrations in the range 0.1-1.0 mM exerted differential effects on the specific nodulation, nodule growth and the growth of whole plant of *M. truncatula*. Although the promoting effect of ammonium on specific nodulation was not observed in the concentration ranges used in this experiment, the concentration at which the differential effects of nitrate and ammonium on nodulation were most distinguishing was determined to be 0.1 mM.

By utilizing *Mt16KOLI1* microarray, tens of genes were detected to be differentially expressed in *M. truncatula* roots treated with *S. meliloti* inoculation-only, inoculation plus 0.1 mM NH_4^+ and inoculation plus 0.1 mM NO_3^- in relative to non-inoculated root (0h0N) (Table 4.3-Table 4.8).

Several intriguing genes were found to be up-regulated by inoculation, including genes encoding a key enzyme in flavonoid synthesis--chalcone synthase (Mckhann, 1997), an early Nod factor responsive gene—*rip-1* (Cook, 1995), two Gibberellin-regulated proteins (Kawaguchi, 1996), albumin/Leginsulin gene encodes toxic peptide against pathogen (Gressent et al., 2003) and several plant defense-related genes. Interesting genes that were down-regulated by inoculation-only treatment including the key enzyme in the polyamine biosynthesis pathway—S-adenosylmethionine decarboxylase and several plant defense-related genes. Genes directly related to the metabolism of nitrate including two high affinity nitrate transporter and a glutamate

dehydrogenase (Andersson and Roger, 2003). No gene differentially expressed in inoculation/NH treatment is directly related to the metabolism of ammonium.

A group of nodulation-related genes were found to be significantly influenced by the addition of nitrate or ammonium (Table 4.10 and Table 4.11). These genes may mediate the differential effects of ammonium and nitrate on the nodulation. However, exactly how they may be involved in is open to future examination as to this point, the mechanism by which the legume controlling the number of nodules (autoregulation) is just starting to be understood (Searle et al., 2003) and also because most of the genes have multiple functions and/or are involved in multiple metabolism pathways.

6.0 CONCLUSIONS

Medicago truncatula plants treated with ammonium and nitrate fertilizer performed better than those depended solely on the N_2-fixation to attain their nitrogen nutrient. These better performances of nitrogen-treated plants included higher DW accumulation, higher tissue nitrogen content, and higher tissue nitrogen concentration. The performance of the plants was positively related to the concentration of mineral nitrogen they were exposed to. Plants grown on nitrate-fertilizer performed better than those grown on ammonium-fertilizer.

The influences of the two mineral nitrogen forms on nodulation of *M. truncatula* plants were distinctive. While NO_3^- was inhibiting at 0.1 mM, NH_4^+ had similar nodulation level as the control plants. Moreover, the growth of nodules was inhibited by NO_3^- more than NH_4^+ at concentration 0.5 mM or above.

The fidelity of the DNA microarray experiment in this study was evaluated and confirmed in terms of both the quality of the Cy3/Cy5-labeled target cDNA and the quality of the microarray data produced for this study.

By utilizing *Mt16kOLI* DNA microarray, a group of genes (e.g. chalcone synthase, *rip-1* etc.) known to be involved in the initiation of nodulation events were identified to be up-regulated in the roots of the seedlings inoculated with *S. miloliti* comparing to the roots that did not see any inoculant. Also a group of genes known to be involved in the plant defense resistance were found to be down-regulated in the roots inoculated with *S. miloliti*. The similar groups of genes that were up-regulated or down-regulated in inoculation-only treatment were also identified to be up-regulated or down-

regulated in a similar way by inoculation plus NH_4^+ treatment and inoculation plus NO_3^- treatments. Also some genes related to nitrate metabolism were identified to be up-regulated in this study. In addition, for each of the three comparisons, a large group of probes whose functions are not known or who have no homology in Gene bank were found to be differentially expressed too. Moreover, some of the nodulation-related genes were found to be significantly influenced by nitrate and ammonium which potentially are involved in the differential effects of ammonium and nitrate on nodulation of *M. truncatula*.

Real-time qRT-PCR was shown to be an effective, sensitive and rapid method to detect the transcripts abundance changes of individual gene expression. Two genes, a putative high affinity nitrate transporter and a cytosolic glutamine synthetase, were confirmed to be up-regulated by ammonium and nitrate by real time qRT-PCR.

Based on the results of this study, several investigations could be conducted to further elucidate the mechanisms involved in the differential effects of ammonium and nitrate on nodulation of *M. truncatula*. These includes: (1) To get a much better confidence on the generality of the genes' responses to our treatments, a post-microarray validation experiment could be conducted by using real time qRT-PCR method or Northern blotting in one or more biological replicates on some interesting genes such as cytokinin receptor (TC92758) (Table 4.9) and the down-regulated auxin-induced proteins (TC88867 and TC82846) (Table 4.9) etc; (2) Determine whether *M. truncatula* will grow better on ammonium as sole nitrogen source with a higher K^+ concentration such as 5 mM. (3) Investigate the effect of NH_4^+ and NO_3^- at concentrations lower than 0.1 mM on the nodulation of *M. truncatula*. (4) For the genes that are validated, the reverse-genetics

(gene over-expression or gene silencing) could be employed to investigate the effects of some of the genes (e.g. chalcone synthase) on nodulation.

7.0 REFERENCES

Abd-Alla MH. 2001. Regulation of nodule formation in soybean-Bradyrhizobium symbiosis is controlled by shoot or/and root signals. Plant Growth Regulation 34: 241-250

Amarasinghe BHRR, de Bruxelles GL, Braddon M, Onyeocha I, Forde BG and Udvardi MK. 1998. Regulation of *GmNRT2* expression and nitrate transport activity in roots of soybean (*Glycine max*). Planta 206, 44-52.

Andersson JO and Roger AJ. 2003. Evolution of glutamate dehydrogenase genes: evidence for lateral gene transfer within and between prokaryotes and eukaryotes. BMC Evolutional Biology 3: 14-23

Atici O, Ogutcu H and Algur OF. 2005. Effect of putrescine on inducing symbiosis in chickpea and vetch inoculated with commercial or indigenous strains of *Rhizobium*. Symbiosis 38: 163-174

Ardourel M, Demont N, Debelle FD, Maillet F, Debilly F, Prome JC, Denarie J and Truchet G. 1994. Rhizobium-meliloti lipooligosaccharide nodulation factors - different structural requirements for bacterial entry into target root hair-cells and induction of plant symbiotic developmental responses. Plant Cell 6: 1357-1374

Arrese-Igor C, Gordon AJ, Minchin FR and Denison RF. 1998. Nitrate entry and nitrite formation in the infected region of soybean nodules. Journal of Experimental Botany 49: 41-48

Arrese-Igor C, Minchin FR, Gordon AJ and Nath AK. 1997. Possible causes of the physiological decline in soybean nitrogen fixation in the presence of nitrate. Journal of Experimental Botany 48: 905-913

Bacanamwo M and Harper JE. 1997. The feedback mechanism of nitrate inhibition of nitrogenase activity in soybean may involve asparagine and/or products of its metabolism. Physiologia Plantarum 100: 371-377

Barker DG, Bianchi S, Blondon F, Dattée Y, Duc G, Essad S, Flament P, Gallusci P, Génier G, Guy P, Muel X, Tourneur J, Denarie J and Huguet T. 1990. *Medicago truncatula*, a model plant for studying the molecular genetics of the rhizobium-legume symbiosis. Plant Molecular Biological Report 8: 40-49

Bauer P, Ratet P, Crespi MD, Schultze M and Kondorosi A. 1996. Nod factors and cytokinins induce similar cortical cell division, amyloplast deposition and MsEnod12A expression patterns in alfalfa roots. Plant Journal 10: 91-105

Bergersen FJ. 1997. Regulation of nitrogen fixation in infected cells of leguminous root nodules in relation to O_2 supply. Plant and Soil 191: 189-203

Bollman MI. 2002. Comparison of the effect of nitrate and ammonium on nodulation, growth and root morphology in *Pisum Sativum* L. PhD thesis. University of Manitoba

Bustin SA. 2000. Absolute quantification of mRNA using real-time reverse transcription polymerase chain reaction assays. Journal of Molecular Endocrinology 25: 169-193

Caba JM, Poveda JL, Gresshoff PM and Ligero F. 1999. Differential sensitivity of nodulation to ethylene in soybean cv. Bragg and a supernodulating mutant. New Phytologist 142: 233-242

Caba JM, Recalde L and Ligero F. 1998. Nitrate-induced ethylene biosynthesis and the control of nodulation in alfalfa. Plant Cell and Environment 21: 87-93

Caetano-Anollès G and Gresshoff PM. 1991. Plant genetic control of nodulation. Annual Review of Microbiology 45: 345-382

Carroll BJ and Mathews A. 1990. Nitrate inhibition of nodulation in legumes. *In* Gresshoff PM. Molecular Biology of Symbiotic Nitrogen Fixation. CRC Press, Boca Raton, Fla. pp. 159–180.

Charon C, Johansson C, Kondorosi E, Kondorosi A and Crespi M. 1997. Enod40 induces dedifferentiation and division of root cortical cells in legumes. Proceedings of the National Academy of Sciences of the United States of America 94: 8901-8906

Cho MJ and Harper JE. 1991a. Effect of inoculation and nitrogen on isoflavonoid concentration in wild-type and nodulation-mutant soybean roots. Plant Physiology 95: 435-442

Cho MJ and Harper JE. 1991b. Effect of localized nitrate application on isoflavonoid concentration and nodulation in split-root systems of wild-type and nodulation-mutant soybean plants. Plant Physiology 95: 1106-1112

Chuaqui RF, Bonner RF, Best CJM, Gillespie JW, Flaig MJ, Hewitt SM, Phillips JL, Krizman DB, Tangrea MA, Ahram M, Linehan WM, Knezevic V and Emmert-Buck MR. 2002. Post-analysis follow-up and validation of microarray experiments. Nature Genetics 32: 509-514

Cook D, Dreyer D, Bonnet D, Howell M, Nony E and Vandenbosch K. 1995. Transient induction of a peroxidase gene in *Medicago truncatula* precedes infection by rhizobium-meliloti. Plant Cell 7: 43-55

Coronado C, Zuanazzi JAS, Sallaud C, Quirion JC, Esnault R, Husson HP, Kondorosi A and Ratet P. 1995. Alfalfa root flavonoid production is nitrogen regulated. Plant Physiology 108: 533-542

Crawford NM. 1995. Nitrate: nutrient and signal for plant growth. Plant Cell 7: 859-868

Crespi M and Galvez S. 2000. Molecular mechanisms in root nodule development. Journal of Plant Growth Regulation 19: 155-166.

D'Apuzzo E, Rogato A, Simon-Rosin U, El Alaoui H, Barbulova A, Betti M, Dimou M, Katinakis P, Marquez A, Marini AM, Udvardi MK and Chiurazzi M. 2004. Characterization of three functional high-affinity ammonium transporters in *Lotus japonicus* with differential transcriptional regulation spatial expression. Plant Physiology 134: 1763-1774

Dazzo FB and Hubbell HD. 1975. Cross-reactive antigens and lectins as determinants of symbiotic specificity in the rhizobium-clover association. Applied Microbiology 30: 1017-1033

Diaz CL, Melchers LS, Hooykaas PJJ, Lugtenberg BJJ and Kijne JW. 1989. Root lectin as a determinant of host-plant specificity in the rhizobium-legume symbiosis. Nature 338: 579-581

Dixon, R. A. 1986. The phytoalexin response: Elicitation, signaling, and control of host gene expression. Biological Review 61:239-291.

Dusha I, Bakos A, Kondorosi A, de Bruijn FJ and Schell J. 1989. The *rhizobium meliloti* early nodulation genes (nod ABC) are nitrogen regulated: isolation of a mutant strain with efficient nodulation capacity on alfalfa in the presence of ammonium. Molecular and General Genetics 219: 89–97

Eisen MB and Brown PO. 1999. DNA arrays for analysis of gene expression. cDNA Preparation and Characterization 303: 179-205

El Yahyaoui F, Kuster H, Ben Amor B, Hohnjec N, Puhler A, Becker A, Gouzy J, Vernie T, Gough C, Niebel A, Godiard L and Gamas P. 2004. Expression profiling in *Medicago truncatula* identifies more than 750 genes differentially expressed during nodulation, including many potential regulators of the symbiotic program. Plant Physiology 136: 3159-3176

Engstrom EM, Ehrhardt DW, Mitra RM and Long SR. 2002. Pharmacological analysis of Nod factor-induced calcium spiking in *Medicago truncatula*. Evidence for the requirement of type IIA calcium pumps and phosphoinositide signaling. Plant Physiology 128: 1390-1401

Estabrook EM and Sengupta-Gopalan C. 1991. Differential expression of phenylalanine ammonia-lyase and chalcone synthase during soybean nodule development. Plant Cell 3: 299-308

Evans PT and Malmberg RL. 1989. Do polyamines have roles in plant development? Annual Review of Plant Physiology and Plant Molecular Biology 40: 235–269

Fedorova M, van de Mortel J, Matsumoto PA, Cho J, Town CD, VandenBosch KA, Gantt JS and Vance CP. 2002. Genome-wide identification of nodule-specific transcripts in the model legume *Medicago truncatula*. Plant Physiology 130: 519-37

Fei HM and Vessey JK. 2003. Involvement of cytokinin in the stimulation of nodulation by low concentrations of ammonium in *Pisum sativum*. Physiologia Plantarum 118: 447-455

Fei HM and Vessey JK. 2004. Further investigation of the roles of auxin and cytokinin in the NH_4^+-induced stimulation of nodulation using white clover transformed with the auxin-sensitive reporter *GH3 : gusA*. Physiologia Plantarum 121: 674-81

Fisher K and Newton WE. 2002. Nitrogen fixation- a general overview. Pp 1-34. *In* Leigh GJ. 2002. Nitrogen Fixation at the Millennium. Elsevier Science B. V. Amsterdam, the Netherlands.

Ferguson BJ and Mathesius U. 2003. Signaling interactions during nodule development. Journal of Plant Growth Regulation 22: 47-72

Forde BG and Clarkson DT. 1999. Nitrate and ammonium nutrition of plants: physiological and molecular perspectives. Advances in Botanical Research Incorporating Advances in Plant Pathology 30: 1-90

Forde BG. 2000. Nitrate transporters in plants: structure, function and regulation. Biochimica et Biophysica Acta-Biomembranes 1465: 219-35

Frugoli J and Harris J. 2001. *Medicago truncatula* on the move! Plant Cell 13: 458-63

Fujikake H, Yamazaki A, Ohtake N, Sueyoshi K, Matsuhashi S, Ito T, Mizuniwa C, Kume T, Hashimoto S, Ishioka NS, Watanabe S, Osa A, Sekine T, Uchida H, Tsuji A and Ohyama T. 2003. Quick and reversible inhibition of soybean root nodule growth by nitrate involves a decrease in sucrose supply to nodules. Journal of Experimental Botany 54: 1379-88

Fujikake H, Yashima H, Sato T, Ohtake N, Sueyoshi K and Ohyama T. 2002. Rapid and reversible nitrate inhibition of nodule growth and N_2 fixation activity in soybean (*Glycine max* (L.) Merr.). Soil Science and Plant Nutrition 48: 211-7

Gadkari D. 2002. A novel nitrogenase superoxidase-dependent nitrogen fixation. Pp 263-299. *In* Leigh GJ. 2002. Nitrogen Fixation at the Millennium. Elsevier ScienceB. V. Amsterdam, the Netherlands.

Gamas P, Niebel Fde C, Lescure N and Cullimore J. 1996. Use of a subtractive hybridization approach to identify new *Medicago truncatula* genes induced during root nodule development. Molecular Plant-Microbe Interaction 9: 233-242

Gamas P, de Billy F, Truchet G. 1998. Symbiosis-specific expression of two *Medicago truncatula* nodulin genes, MtN1 and MtN13, encoding products homologous to plant defense proteins. Molecular Plant-Microbe Interactions 11: 393-403

Gan YB, Stulen I, van Keulen H and Kuiper PJC. 2004. Low concentrations of nitrate and ammonium stimulate nodulation and N_2 fixation while inhibiting specific nodulation (nodule DW g^{-1} root dry weight) and specific N_2 fixation (N_2 fixed g^{-1} root dry weight) in soybean. Plant and Soil 258: 281-292

Garcia-Plazaola JI, Hernandez A, Becerril JM and Arrese-Igor C. 2000. Long term effects on lucerne (*Medicago sativa* L.) nitrogen fixation is not influenced by the denitrification status on microsymbiont. Plant and Soil 216: 139-145.

Glass ADM, Britto DT, Kaiser BN, Kinghorn JR, Kronzucker HJ, Kumar A, Okamoto M, Rawat S, Siddiqi MY, Unkles SE and Vidmar JJ. 2002. The regulation of nitrate and ammonium transport systems in plants. Journal of Experimental Botany 53: 855-864

Gressent F, Rahioui I and Rahbe Y. 2003. Characterization of a high affinity binging site for the pea albumin 1b (PA1b) entomotoxin in the weevil Sitophilus. Europe Journal of Biochemistry 270: 2429-2435

Gulden RH and Vessey JK. 1997. The stimulating effect of ammonium on nodulation in *Pisum sativum* L. is not long lived once ammonium supply is discontinued. Plant and Soil 195: 195-205

Gulden RH and Vessey JK. 1998. Low concentrations of ammonium inhibit specific nodulation (nodule number g^{-1} root DW) in soybean (*Glycine max* [L] Merr). Plant and Soil 198: 127-136

Handberg K and Stougaard J. 1992. *Lotus japonicus*, an autogamous, diploid legume species for classical and molecular genetics. Plant Journal 2: 487-496.

Hansen AP. 1994. Symbiotic N_2 Fixation of Crop Legumes. Margraf Verlag, Weikersheim, Germany. 248pp

Harper JE. 1974. Soil and symbiotic nitrogen requirements for optimum soybean production. Crop Science14: 255-260.

Heidstra R, Geurts R, Franssen H, Spaink HP, vanKammen A and Bisseling T. 1994. Root hair deformation activity of nodulation factors and their fate on *Vicia sativa*. Plant Physiology 105: 787-797

Heidstra R, Yang WC, Yalcin Y, Peck S, Emons AM, vanKammen A and Bisseling T. 1997. Ethylene provides positional information on cortical cell division but is not involved in Nod factor-induced root hair tip growth in rhizobium-legume interaction. Development 124: 1781-1787

Hohnjec N, Vieweg ME, Puhler A, Becker A and Kuster H. 2005. Overlaps in the transcriptional profiles of *Medicago truncatula* roots inoculated with two different Glomus fungi provide insights into the genetic program activated during arbuscular mycorrhiza. Plant Physiology 137: 1283-1301

Imsande J. 1986. Inhibition of nodule development in soybean by nitrate or reduced nitrogen. Journal of Experimental Botany 37: 348–355.

James EK. 2000. Nitrogen fixation in endophytic and associative symbiosis. Field Crops Research 65: 197-209

Jordan B. 2001. DNA Microarrays: Gene Expression Applications. Springer-Verlag Berlin Heidelberg, New York, USA. 140pp

Kaiser BN, Finnegan PM, Tyerman SD, Whitehead LF, Bergersen FJ, Day DA and Udvardi MK. 1998. Characterization of an ammonium transport protein from the peribacteroid membrane of soybean nodules. Science 281: 1202-6

Kawaguchi M, ImaizumiAnraku H, Fukai S and Syono K. 1996. Unusual branching in the seedlings of *Lotus japonicus* - gibberellins reveal the nitrogen-sensitive cell divisions within the pericycle on roots. Plant and Cell Physiology 37: 461-470

Kistner C and Parniske M. 2002. Evolution of signal transduction in intracellular symbiosis. Trends in Plant Science 7: 511–518

Kohane IS, Kho AT and Butte AJ. 2003. Microarrays for An Integrative Genomics. The MIT press, Cambridge, Massachusetts, London, England. 306pp

Kouchi H, Shimomura K, Hata S, Hirota A, Wu GJ, Kumagai H, Tajima S, Suganuma N, Suzuki A, Aoki T, Hayashi M, Yokoyama T, Ohyama T, Asamizu E, Kuwata C, Shibata D and Tabata S. 2004. Large-scale analysis of gene expression profiles during early stages of root nodule formation in a model legume, *Lotus japonicus*. DNA Research 11: 263-274

Kuppusamy KT, Endre G, Prabhu R, Penmetsa RV, Veereshlingam H, Cook DR, Dickstein R, VandenBosch KA. 2004. LIN, a *Medicago truncatula* gene required for nodule differentiation and persistence of rhizobial infections. Plant Physiology 13: 3682-3691

Kuster H, Hohnjec N, Krajinski F, El Yahyaoui F, Manthey K, Gouzy J, Dondrup M, Meyer F, Kalinowski J, Brechenmacher L, van Tuinen D, Gianinazzi-Pearson V, Puhler A, Gamas P and Becker A. 2004. Construction and validation of cDNA-based Mt6k-RIT macro- and microarrays to explore root endosymbioses in the model legume *Medicago truncatula*. Journal of Biotechnology 108: 95-113

Lange T. 1994. Purification and partial amino-acid-sequence of gibberellin 20-oxidase from *Cucurbita maxima* endosperm. Planta 195: 108-115

Lee KH and Larue TA. 1992. Ethylene as a possible mediator of light-induced and nitrate-induced inhibition of nodulation of *Pisum sativum* l Cv Sparkle. Plant Physiology 100: 1334-8

Ligero F, Caba JM, Lluch C and Olivares J. 1991. Nitrate inhibition of nodulation can be overcome by the ethylene inhibitor aminoethoxyvinylglycine. Plant Physiology 97: 1221-1225

Limpens E, Franken C, Smit P, Willemse J, Bisseling T and Geurts R. 2003. LysM domain receptor kinases regulating rhizobial Nod factor-induced infection. Science 302: 630-3

Liscum E and Reed JW. 2002. Genetics of Aux/IAA and ARF action in plant growth and development. Plant Molecular Biology 49: 387-400

Liu KH, Huang CY and Tsay YF. 1999. CHL1 is a dual-affinity nitrate transporter of arabidopsis involved in multiple phases of nitrate uptake. Plant Cell 11: 865-874

Livak KJ and Schmittgen TD. 2001. Analysis of relative gene expression data using real-time quantitative PCR and the $2^{-\Delta\Delta C}{}_T$ method. Methods 25: 402-408

Lohar DP, Schaff JE, Laskey JG, Kieber JJ, Bilyeu KD and Bird DM. 2004. Cytokinins play opposite roles in lateral root formation, and nematode and rhizobial symbioses. Plant Journal 38: 203-14

Lopez-Garcia SL, Vazquez TEE, Favelukes G and Lodeiro AR. 2001. Improved soybean root association of N-starved *Bradyrhizobium japonicum*. Journal of Bacteriology 183: 7241-7252

Loque D and von Wiren N. 2004. Regulatory levels for the transport of ammonium in plant roots. Journal of Experimental Botany 55: 1293-1305

Lorkowski S and Cullen P. 2003. Analysing Gene Expression-A Handbook of Methods, Possibilities and Pitfalls. WILEY-VCH Verlag GmbH&Co. KGaA, Weinheim, Germany. 950pp.

Madsen EB, Madsen LH, Radutoiu S, Olbryt M, Rakwalska M, Szczyglowski K, Sato S, Kaneko T, Tabata S, Sandal N and Stougaard J. 2003. A receptor kinase gene of the LysM type is involved in legume perception of rhizobial signals. Nature 425: 637-640

Manthey K, Krajinski F, Hohnjec N, Firnhaber C, Puhler A, Perlick AM and Kuster H. 2004. Transcriptome profiling in root nodules and arbuscular mycorrhiza identifies a collection of novel genes induced during *Medicago truncatula* root endosymbioses. Molecular Plant Microbe Interactions 17: 1063-1077

Marschner H. 1995. Mineral Nutrition of Higher Plants. 2nd ed. Academic, London, 889 pp.

Martin-Tanguy J. 2001. Metabolism and function of polyamines in plants: recent development (new approaches). Plant Growth Regulation. 34: 135–148

Mathesius U, Charon C, Rolfe BG, Kondorosi A and Crespi M. 2000. Temporal and spatial order of events during the induction of cortical cell divisions in white clover by *Rhizobium leguminosarum* bv. trifolii inoculation or localized cytokinin addition. Molecular Plant-Microbe Interactions 13: 617-628

Mathesius U, Schlaman HRM, Spaink HP, Sautter C, Rolfe BG and Djordjevic MA. 1998. Auxin transport inhibition precedes root nodule formation in white clover roots and is regulated by flavonoids and derivatives of chitin oligosaccharides. Plant Journal 14: 23-34

McCauley A, Jones C and Jacobsen J. 2003. Plant nutrient functions and deficiency and toxicity symptoms. Nutrient management Module No. 9. Montana State University. http: //landresources.montana.edu/NutrientManagement/Modules/Module9.pdf

McKhann HI, Paiva NL, Dixon RA and Hirsch AM. 1997. Chalcone synthase transcripts are detected in alfalfa root hairs following inoculation with wild-type *rhizobium meliloti*. Molecular Plant-Microbe Interaction 10: 50-58

Mellor RB and Collinge DB. 1995. A simple model based on known plant defence reactions is sufficient to explain most aspects of nodulation. Journal of Experimental Botany 48: 1-18

Mengel K, Viro M. and Hehl G. 1976. Effect of potassium on the uptake and incorporation of ammonium-nitrogen of rice plant. Plant and soil 44: 547-558

Mirabella R, Franssen H and Bisseling T. 2002. LCO signaling in the interaction between rhizobia and legumes. Pp 250-271. *In* Scheel D and Wasternack C. 2002. Plant Signal Transduction. Oxford University Press. Oxford. 346pp.

Mithofer A. 2002. Suppression of plant defence in rhizobia-legume symbiosis. Trends in Plant Science 7: 440-444

Mitra RM, Gleason CA, Edwards A, Hadfield J, Downie JA, Oldroyd GED and Long SR. 2004. A Ca^{2+}/calmodulin-dependent protein kinase required for symbiotic nodule development: Gene identification by transcript-based cloning. Proceedings of the National Academy of Sciences of the United States of America 101: 4701-4705

Mulder L, Hogg B, Bersoult A and Cullimore JV. 2005. Integration of signalling pathways in the establishment of the legume-rhizobia symbiosis. Physiologia Plantarum 123: 207-218

Neo HH and Layzell DB. 1997. Phloem glutamine and the regulation of O_2 diffusion in legume nodules. Plant Physiology 113: 259-267

Newman EI and Reddell P. 1987. The distribution of mycorrhizas among families of vascular plants. New Phytologist 106: 745-751

Onate-Sanchez L and Singh KB. 2002. Identification of arabidopsis ethylene-responsive element binding factors with distinct induction kinetics after pathogen infection. Plant Physiology 128: 1313-1322

Orsel M, Filleur S, Fraisier V and Daniel-Vedele F. 2002. Nitrate transport in plants: which gene and which control? Journal of Experimental Botany 53: 825-833

Pan B and Smith DL. 2000. Preincubation of *B. japonicum* cells with genistein reduces the inhibitory effects of mineral nitrogen on soybean nodulation and nitrogen fixation under field conditions. Plant and Soil 223: 235-42

Pate JS and Layzell DB. 1990 Energetics and biological costs of nitrogen assimilation. *In* Miflin BJ and Lea PJ. The Biochemistry of Plants, 16: Intermediary Nitrogen Metabolism. Academic Press, San Diego, USA, 1990. pp. 1–42

Patriarca EJ, Tate R and Iaccarino M. 2002. Key role of bacterial NH_4^+ metabolism in rhizobium-plant symbiosis. Microbiology and Molecular Biology Reviews 66: 203-222

Patriarca EJ, Tate R, Ferraioli S and Iaccarino M. 2004. Organogenesis of legume root nodules. International Review of Cytology - A Survey of Cell Biology 234: 201-262

Peirson SN, Butler JN and Foster RG. 2003. Experimental validation of novel and conventional approaches to quantitative real-time PCR data analysis. Nucleic Acids Research 31: 1-7

People MB, Giller KE, Herridge DF and Vessey JK. 2001. Limitations to biological nitrogen fixation as a renewable source of nitrogen for agriculture. Pp 356-360. *In* Finan TM, O'Brian MR, Layzell DB, Vessy JK, and Newton W. Nitrogen Fixation: Global Perspective. CABI Publishing, Wallingford, Oxon, UK, 2002. 555 pp.

Piper MD, Daran-Lapujade P, Bro C, Regenberg B, Knudsen S, Nielsen J and Pronk JT. 2002. Reproducibility of oligonucleotide microarray transcriptome analyses. An interlaboratory comparison using chemostat cultures of *Saccaromyces cerevisiae*. Journal of Biological Chemistry. 277: 37001-37008.

Postgate JR. 1998. Nitrogen Fixation. 3rd ed. Cambridge University Press. NY. 112pp.

Radutoiu S, Madsen LH, Madsen EB, Felle HH, Umehara Y, Gronlund M, Sato S, Nakamura Y, Tabata S, Sandal N and Stougaard J. 2003. Plant recognition of symbiotic bacteria requires two LysM receptor-like kinases. Nature 425: 585-92

Ramu SK, Peng HM and Cook DR. 2002. Nod factor induction of reactive oxygen species production is correlated with expression of the early nodulin gene *rip1* in *Medicago truncatula*. Molecular Plant-Microbe Interaction 15: 522-528

Recourt K, van Tunen AJ, Mur LA, van Brussel AAN, Lugtenberg BJJ, and Kijne JW. 1992. Activation of flavonoid biosynthesis in roots of Vicia sativa subsp. nigra plants by inoculation with *Rhizobium leguminosarum* biovar *viciae*. Plant Molecular Biology 19: 411-420.

Riely BK, Ane JM, Penmetsa RV and Cook DR. 2004. Genetic and genomic analysis in model legumes bring Nod-factor signaling to center stage. Current Opinion in Plant Biology 7: 408-13

Ririe KM, Rasmussen RP and Wittwer CT. 1997. Product differentiation by analysis of DNA melting curves during the polymerase chain reaction. Analytical Biochemistry 245: 154-60

Schena M, Shalon D, Davis RW and Brown PO. 1995. Quantitative monitoring of gene-expression patterns with a complementary-DNA microarray. Science 270: 467-70

Silsbury JH, Catchpole DW, and Wallace W. 1986. Effects of nitrate and ammonium on nitrogenase (C_2H_2 reduction) activity of swards of subterranean clover, Tri*folium subterraneum* L. Australian Journal of Plant Physiology 13: 257-273

Smit G, Swart S, Lugtenberg BJJ and Kijne JW. 1992. Molecular mechanisms of attachment of rhizobium bacteria to plant-roots. Molecular Microbiology 6: 2897-903

Spaink HP. 2000. Root nodulation and infection factors produced by rhizobial bacteria. Annual Review of Microbiology 54: 257-88

Speed T. 2003. Statistical Analysis of Gene Expression Microarray Data. CRC press, Florida, USA. 222pp

Stanford AC, Larsen K, Barker DG and Cullimore JV. 1993. Differential expression within the glutamine-synthetase gene family of the model legume Medicago truncatula. Plant Physiology 103: 73-81

Streeter J. 1988. Inhibition of legume nodule formation and N_2 fixation by nitrate. CRC Critical Reviews in Plant Science 7: 1-23

Streeter J. 1989. Estimation of ammonium concentration in the cytosol of soybean nodules. Plant Physiology 90: 779-782

Stumpe M, Carsjens JG, Stenzel I, Gobel C, Lang I, Pawlowski K, Hause B and Feussner I. 2005. Lipid metabolism in arbuscular mycorrhizal roots of *Medicago truncatula*. Phytochemistry 66: 781-91

Tobin AK and Yamaya T. 2001. Cellular compartmentation of ammonium assimilation in rice and barley. Journal of Experimental Botany 52: 591-604

Touraine B and Glass ADM. 1997. NO_3^- and ClO_3- fluxes in the chl1-5 mutant of *Arabidopsis thaliana* - Does the CHL1-5 gene encode a low-affinity NO_3^- transporter? Plant Physiology 114: 137-144

van Rhijn P, Fujishige NA, Lim PO and Hirsch AM. 2001. Sugar-binding activity of pea lectin enhances heterologous infection of transgenic alfalfa plants by *Rhizobium leguminosarum* biovar viciae. Plant Physiology 126: 133-144

van Rhijn P, Goldberg RB and Hirsch AM. 1998. *Lotus corniculatus* nodulation specificity is changed by the presence of a soybean lectin gene. Plant Cell 10: 1233-1249

Vance CP. 2002. Root-bacteria interactions: symbiotic N_2 fixation. Pp 839-868. *In* Waisel Y, Eshel A, and Kafkafi U. 2002. Plant Roots-The Hidden Half. Marcel Dekker, Inc. New York.

Vasse J, Debilly F and Truchet G. 1993. Abortion of infection during the Rhizobium meliloti-alfalfa symbiotic interaction is accompanied by a hypersensitive reaction. Plant Journal 4: 555-566

Vassileva V and Ignatov G. 1999. Polyamine-induced changes in symbiotic parameters of the *Galega orientalis-Rhizobium galegae* nitrogen-fixing system. Plant and Soil 210: 83-91

Vessey JK and Waterer J. 1992. In search of the mechanism of nitrate inhibition of nitrogenase activity in legume nodules - recent developments. Physiologia Plantarum 84: 171-6

Vessey JK, Pawlowski K and Bergman B. 2004. Root-based N_2-fixing symbioses: Legumes, actinorhizal plants, Parasponia sp and cycads. Plant and Soil 266: 205-30

Vessey JK, York EK, Henry LT and Raper CD, Jr. 1988. Uniformity of environmental conditions and plant growth in a hydroponic culture system for use in a growth room with aerial CO_2 control. Biotronics. 17: 79-94

Wais RJ, Galera C, Oldroyd G, Catoira R, Penmetsa RV, Cook D, Gough C, Denarie J and Long SR. 2000. Genetic analysis of calcium spiking responses in nodulation mutants of *Medicago truncatula*. Proceedings of the National Academy of Sciences of the United States of America 97: 13407-12

Walsh KB and Carroll BJ. 1992. A reappraisal of nitrate inhibition of nitrogenase in A317, a nitrate reductase-deficient mutant of pea (*Pisum sativum*). Physiologia Plantarum 84: 283-91

Walters DR. 2000. Polyamines in plant-microbe interactions. Physiological and Molecular Plant Pathology 57: 137-46

Wang SP and Stacey G. 1990. Ammonia regulation of nod genes in Bradyrhizobium japonicum. Molecular and General Genetics 223: 329-331

Wang YH, Garvin DF and Kochian LV. 2001. Nitrate-induced genes in tomato roots. Array analysis reveals novel genes that may play a role in nitrogen nutrition. Plant Physiology 127: 345-59

Waterer JG and Vessey JK, Raper CD. 1992. Stimulation of nodulation in field peas (*Pisum-sativum*) by low concentrations of ammonium in hydroponic culture. Physiologia Plantarum 86: 215-20

Waterer JG and Vessey JK. 1993a. Nodulation response of autoregulated or NH_4^+-inhibited pea (*Pisum sativum*) after transfer to stimulatory (low) concentrations of NH_4^+. Physiologia Plantarum 88: 460-6

Waterer JG and Vessey JK. 1993b. Effect of low static nitrate concentrations on mineral nitrogen uptake, nodulation, and nitrogen-fixation in field pea. Journal of Plant Nutrition 16: 1775-89

Wendehenne D, Pugina A, Klessigb DF and Durnerc J. 2001. Nitric oxide: comparative synthesis and signaling in animal and plant cells. Trends in Plant Science 6: 177-183

Williams LE and Miller AJ. 2001. Transporters responsible for the uptake and partitioning of nitrogenous solutes. Annual Review of Plant Physiology and Plant Molecular Biology 52: 659-688

Wojtaszek P and Peretiatkowicz M. 1992. A simple method for visualization of phenolics exudation by roots of intact lupin plants - the effect of nitrate and PH. Acta Biochimica Polonica 39: 307-16

Xu QF, Tsai CL and Tsai CY. 1992. Interaction of potassium with the form and amount of nitrogen nutrition on growth and nitrogen uptake of maize. Journal of Plant Nutrition 15: 23-33

Yinbo G, Peoples MB and Rerkasem B. 1997. The effect of N fertilizer strategy on N_2 fixation, growth and yield of vegetable soybeans. Field Crops Research 51: 221-229

Yost CK, Rochepeau P and Hynes MF. 1998. *Rhizobium leguminosarum* contains a group of genes that appear to code for methyl-accepting chemotaxis proteins. Microbiology-Sgm 144: 1945-56

8.0 APPENDICES

Appendix A: Calculation Formulas of Cyanine-dye Labeled cDNA

Extinction coefficients
150,000 $M^{-1}cm^{-1}$ at 550 nm for Cy3
250,000 $M^{-1}cm^{-1}$ at 650 nm for Cy5

Calculation equations

cDNA amount (μg/ml)= A260×37×dilution factor×(z μl) ×(w cm)

pmol Cy3 in purified sample= (A_{550}/150,000) ×dilution factor×(z μl) ×(w cm) ×1012
pmol Cy5 in purified sample= (A_{550}/250,000) ×dilution factor×(z μl) ×(w cm) ×1012

A_{260}, A_{550}, A_{650} = absorbance at 260 (cDNA), 550 (Cy3), 650 (Cy5)
z μl = the volume of sample after purification
w cm =optical path in cuvette

1μg cDNA = ~3030 pmol of nucleotides

Labeling density= (pmol CyDye in labeled sample) / (pmol nucleotides in labeled sample)

The calculation formulas were cited from "Microarray Handbook", Amersham Biosciences Inc., on line technical resources, http://www5.amershambiosciences.com/aptrix/upp00919.nsf/Content/WD:Microarray+Hand(219987857-B500)

There are also two websites where the calculation could also be done automatically after inputting the absorbance data:

http://www.pangloss.com/seidel/Protocols/percent_inc.html

http://www.ambion.com/techlib/misc/aama_dye_calc.html

APPENDIX B: Identified Probes with Unknown Function or No Homology

Table 8.1 List of 24 Probes Regulated by Inoculation-only Treatment with Unknown function

Oligo ID	TIGR ID	Functional group	6hr0N	P	12hr0N	P	24hr0N	P
Up-regulated								
MT015488	TC86842	XII.C. Unknown function	0.49	0.0322	1.07	0.0010	1.29	0.0001
MT003224	TC80899	XII.C. Unknown function	0.66	0.0054	0.39	0.0376	0.18	0.2379
MT015855	BF64004	XII.C. Unknown function	0.55	0.0701	0.85	0.0120	1.45	0.0002
MT015466	TC77769	XII.C. Unknown function	0.41	0.1475	0.88	0.0046	1.47	0.0005
MT015163	BQ14418	XII.C. Unknown function	2.22	0.0000	0.86	0.0009	0.00	0.9923
MT015162	TC85295	XII.C. Unknown function	2.23	0.0000	0.83	0.0030	0.06	0.7321
MT015161	BQ14418	XII.C. Unknown function	2.39	0.0000	0.87	0.0001	0.08	0.4232
MT007830	TC77790	XII.C. Unknown function	0.09	0.8307	1.17	0.0004	1.18	0.0008
MT005586	TC92140	XII.C. Unknown function	2.53	0.0001	1.36	0.0111	0.24	0.4108
MT009672	TC88561	XII.C. Unknown function	0.99	0.0029	0.65	0.0296	1.67	0.0005
MT009059	TC79439	XII.C. Unknown function	2.29	0.0000	1.09	0.0338	0.68	0.0309
MT014141	TC76474	XII.C. Unknown function	0.20	0.3383	0.81	0.0000	2.13	0.0000
Down-regulated								
MT000303	TC77028	XII.C. Unknown function	-1.19	0.0082	-1.22	0.0184	-0.74	0.0637
MT007504	TC77354	XII.C. Unknown function	-0.74	0.0037	-0.53	0.0294	-0.62	0.0007
MT015235	TC85246	XII.C. Unknown function	-0.68	0.0005	-0.28	0.0795	-0.71	0.0010
MT015110	TC85261	XII.C. Unknown function	-0.90	0.0004	-0.97	0.0006	-0.62	0.0122
MT012911	TC84918	XII.C. Unknown function	-1.39	0.0016	-1.21	0.0077	-0.56	0.0775
MT010534	TC81648	XII.C. Unknown function	-0.80	0.0047	-0.23	0.1419	-0.76	0.0141
MT014672	TC80018	XII.C. Unknown function	-0.79	0.0035	-0.92	0.0036	-0.75	0.0072
MT007738	TC76889	XII.C. Unknown function	-0.94	0.0002	-0.65	0.0433	-0.37	0.0142
MT005182	TC84763	XII.C. Unknown function	-0.23	0.3726	-0.87	0.0023	-0.61	0.0045
MT010587	TC81185	XIII. No homology	-0.93	0.0371	-0.90	0.0256	-0.52	0.1342
MT011321	TC90663	XIII. No homology	-1.63	0.0002	-0.97	0.0223	-0.49	0.0016
MT014812	TC91446	XIII. No homology	-0.66	0.0030	-0.52	0.0088	-1.00	0.0001

Table 8.2 List of 102 Probes Regulated by Inoculation/NO Treatment with Unknown function

Oligo ID	TIGR ID	Functional group	6hrNO	P	12hrNO	P	24hrNO	P
Up-regulated								
MT003894	TC87248	XII.C. Unknown function	0.11	0.6322	0.87	0.0038	0.72	0.0052
MT015706	TC87248	XII.C. Unknown function	0.70	0.0010	1.04	0.0000	0.07	0.7874
MT010270	TC81640	XII.C. Unknown function	0.85	0.0045	0.88	0.0013	0.25	0.1421
MT001316	TC78240	XII.C. Unknown function	0.65	0.0043	0.91	0.0002	0.52	0.0258
MT009418	TC87006	XII.C. Unknown function	0.88	0.0035	0.87	0.0004	0.66	0.0015
MT012946	TC92805	XII.C. Unknown function	0.93	0.0050	0.92	0.0033	0.13	0.4230
MT004791	TC80335	XII.C. Unknown function	0.96	0.0026	0.67	0.0169	0.47	0.0546
MT002172	TC79036	XII.C. Unknown function	1.17	0.0012	0.80	0.0046	0.27	0.0459
MT008406	TC87575	XII.C. Unknown function	1.00	0.0024	0.58	0.0054	0.60	0.0001
MT004873	TC91414;	XII.C. Unknown function	0.90	0.0000	0.68	0.0321	0.38	0.0190
MT011769	TC82733	XII.C. Unknown function	0.82	0.0013	1.10	0.0013	0.63	0.0197
MT002390	TC78881	XII.C. Unknown function	0.99	0.0003	0.63	0.0491	0.35	0.0332
MT014962	TC84879	XII.C. Unknown function	0.99	0.0014	0.60	0.0164	0.65	0.0042
MT005064	TC91968	XII.C. Unknown function	0.96	0.0043	0.86	0.0129	0.41	0.0597
MT000285	TC85719	XII.C. Unknown function	0.87	0.0156	0.92	0.0056	0.82	0.0078
MT007360	TC85829	XII.C. Unknown function	0.72	0.0184	1.02	0.0049	0.54	0.0617
MT000519	TC89036	XII.C. Unknown function	1.43	0.0000	0.81	0.0000	0.30	0.0089
MT012400	TC83546;	XII.C. Unknown function	1.12	0.0204	1.51	0.0001	1.08	0.0001
MT012247	TC83660	XII.C. Unknown function	0.88	0.0210	0.65	0.0144	0.70	0.0039
MT002563	TC79954	XII.C. Unknown function	0.35	0.0299	0.66	0.0022	0.63	0.0327
MT012575	TC92230;	XII.C. Unknown function	1.49	0.0019	1.04	0.0002	0.64	0.0142
MT003976	TC81940	XII.C. Unknown function	1.38	0.0094	0.89	0.0341	0.47	0.2601
MT008443	TC77839	XII.C. Unknown function	0.81	0.0032	0.63	0.0061	0.09	0.6171
MT000646	TC77460	XII.C. Unknown function	0.78	0.0447	0.77	0.0054	0.27	0.2684
MT014141	TC76474	XII.C. Unknown function	1.44	0.0000	0.71	0.0010	0.71	0.0058
MT000610	TC86215	XII.C. Unknown function	0.67	0.0059	0.68	0.0028	0.37	0.0380
MT015536	TC78577	XII.C. Unknown function	0.78	0.0295	0.73	0.0257	0.12	0.6764
MT007836	TC86633	XII.C. Unknown function	0.33	0.1899	0.91	0.0051	0.87	0.0108

Table 8.2 List of 102 Probes Regulated by Inoculation/NO Treatment with Unknown function (Continued)

Oligo ID	TIGR ID	Functional group	6hrNO	P	12hrNO	P	24hrNO	P
Up-regulated								
MT001414	TC78744	XII.C. Unknown function	0.84	0.0138	0.92	0.0096	0.73	0.0137
MT009059	TC79439	XII.C. Unknown function	2.26	0.0000	2.27	0.0000	1.84	0.0000
MT002170	TC79470	XII.C. Unknown function	0.88	0.0144	0.74	0.0499	0.39	0.1992
MT003674	TC89422	XII.C. Unknown function	0.87	0.0445	1.02	0.0083	0.51	0.0978
MT006299	TC92844	XII.C. Unknown function	0.78	0.0198	1.01	0.0002	0.47	0.0303
MT008797	TC87171	XII.C. Unknown function	0.64	0.0360	1.07	0.0003	0.64	0.0200
MT009672	TC88561	XII.C. Unknown function	1.60	0.0006	0.93	0.0074	0.71	0.0726
MT013448	TC92337	XII.C. Unknown function	0.91	0.0006	0.97	0.0000	0.27	0.0693
MT014919	TC83212;	XII.C. Unknown function	1.20	0.0002	0.96	0.0018	0.41	0.0919
MT001007	TC86860	XII.C. Unknown function	0.79	0.0001	0.64	0.0262	0.37	0.0041
MT015465	TC77767	XII.C. Unknown function	1.07	0.0043	0.81	0.0062	0.67	0.0600
MT006416	TC92673	XII.C. Unknown function	1.84	0.0005	2.08	0.0002	1.29	0.0017
MT008180	TC77638	XII.C. Unknown function	0.67	0.0295	0.81	0.0114	0.85	0.0102
MT015194	TC76631	XII.C. Unknown function	0.64	0.0015	0.77	0.0006	0.36	0.0130
MT000939	TC77947	XII.C. Unknown function	1.12	0.0019	1.11	0.0025	0.74	0.0122
MT005098	TC91868	XII.C. Unknown function	0.62	0.0037	0.77	0.0001	0.17	0.0978
MT005586	TC92140	XII.C. Unknown function	2.70	0.0001	2.31	0.0002	2.10	0.0001
MT005414	TC92202	XII.C. Unknown function	1.39	0.0018	1.96	0.0001	1.68	0.0002
MT005932	TC84963	XII.C. Unknown function	0.82	0.0071	0.68	0.0300	0.25	0.3436
MT005872	TC91340;	XII.C. Unknown function	1.78	0.0016	1.76	0.0018	1.35	0.0010
MT006773	TC84005	XII.C. Unknown function	1.24	0.0000	1.32	0.0001	1.26	0.0000
MT006785	TC83486	XII.C. Unknown function	1.43	0.0006	1.66	0.0000	1.52	0.0001
MT006786	TC82264	XII.C. Unknown function	0.32	0.3757	0.73	0.0256	0.67	0.0389
MT006812	TC88943	XII.C. Unknown function	1.04	0.0030	0.99	0.0004	0.89	0.0044
MT006629	TC84505	XII.C. Unknown function	1.25	0.0043	1.26	0.0013	0.72	0.0077
MT000051	TC76478	XII.C. Unknown function	1.02	0.0000	0.95	0.0001	0.21	0.2717
MT007830	TC77790	XII.C. Unknown function	1.44	0.0001	0.85	0.0016	0.94	0.0076
MT008590	TC87584	XII.C. Unknown function	1.01	0.0031	0.78	0.0018	0.53	0.0073

Table 8.2 List of 102 Probes Regulated by Inoculation/NO Treatment with Unknown function (Continued)

Oligo ID	TIGR ID	Functional group	6hrNO	P	12hrNO	P	24hrNO	P
Up-regulated								
MT009036	TC88350	XII.C. Unknown function	1.66	0.0003	1.70	0.0000	1.06	0.0001
MT010401	TC81083	XII.C. Unknown function	0.81	0.0000	0.63	0.0003	0.41	0.0036
MT010592	TC89392	XII.C. Unknown function	0.75	0.0049	0.79	0.0066	0.27	0.1676
MT010698	TC89526	XII.C. Unknown function	0.87	0.0143	0.78	0.0016	0.27	0.6675
MT011304	TC79311;	XII.C. Unknown function	0.72	0.0003	0.79	0.0001	0.37	0.0366
MT012084	TC83741	XII.C. Unknown function	0.47	0.0833	1.06	0.0032	0.77	0.0059
MT012108	TC91880	XII.C. Unknown function	1.46	0.0001	1.83	0.0000	1.68	0.0000
MT012132	TC84750	XII.C. Unknown function	0.98	0.0017	0.87	0.0007	0.57	0.0348
MT012259	TC83040	XII.C. Unknown function	1.24	0.0007	0.89	0.0009	0.53	0.0067
MT012840	TC82245	XII.C. Unknown function	0.91	0.0062	1.18	0.0000	0.06	0.6511
MT013138	TC92750	XII.C. Unknown function	0.87	0.0018	0.61	0.0298	0.42	0.0056
MT014448	TC86342	XII.C. Unknown function	1.29	0.0001	1.36	0.0001	0.81	0.0009
MT014670	TC78649	XII.C. Unknown function	1.17	0.0791	1.08	0.0048	0.80	0.0283
MT014945	TC91854	XII.C. Unknown function	1.32	0.0035	1.35	0.0006	0.36	0.4027
MT015488	TC86842;	XII.C. Unknown function	0.39	0.0826	0.80	0.0004	1.13	0.0002
MT015541	TC87356	XII.C. Unknown function	0.66	0.0461	0.88	0.0066	0.47	0.0706
MT015466	TC77769	XII.C. Unknown function	1.19	0.0024	1.07	0.0020	0.79	0.0883
MT015685	TC79746	XII.C. Unknown function	1.11	0.0071	0.98	0.0020	0.35	0.1381
MT002590	TC88978	XII.C. Unknown function	2.93	0.0000	2.51	0.0000	1.78	0.0004
MT002927	TC89369	XII.C. Unknown function	1.30	0.0035	0.78	0.0405	0.53	0.1802
MT003278	TC90373	XII.C. Unknown function	3.13	0.0007	3.09	0.0006	2.41	0.0037
MT003224	TC80899	XII.C. Unknown function	0.74	0.0025	0.62	0.0053	0.36	0.1083
MT005693	TC91989	XII.C. Unknown function	0.93	0.0125	0.81	0.0107	0.27	0.2405
MT005960	TC81246	XII.C. Unknown function	2.26	0.0000	2.66	0.0000	2.02	0.0000
MT007920	TC77703	XII.C. Unknown function	2.21	0.0001	2.38	0.0001	1.79	0.0002
MT008489	TC78933	XII.C. Unknown function	0.77	0.0003	0.65	0.0026	0.20	0.0346
MT001044	TC77897	XII.C. Unknown function	1.59	0.0060	1.94	0.0008	1.48	0.0045
MT005040	TC83253	XIII. No homology	1.83	0.0000	1.89	0.0000	1.71	0.0000

Table 8.2 List of 102 Probes Regulated by Inoculation/NO Treatment with Unknown function (Continued)

Oligo ID	TIGR ID	Functional group	6hrNO	P	12hrNO	P	24hrNO	P
Up-regulated								
MT006797	TC92094	XIII. No homology	1.29	0.0001	1.33	0.0009	1.60	0.0000
MT011135	TC90779	XIII. No homology	1.41	0.0001	0.69	0.0149	0.84	0.0097
MT011637	TC91491	XIII. No homology	0.68	0.1482	1.26	0.0042	0.79	0.0360
MT013751	TC82223	XIII. No homology	0.58	0.1120	0.76	0.0202	1.25	0.0073
MT014309	TC85761	XIII. No homology	0.91	0.0320	0.98	0.0023	0.16	0.4096
MT014881	TC9236	XIII. No homology	0.65	0.0417	1.52	0.0005	0.21	0.4695
MT006040	TC93655	XIII. No homology	1.08	0.0003	0.79	0.0206	0.28	0.1106
Down-regulated								
MT015110	TC85261	XII.C. Unknown function	-0.70	0.0061	-0.33	0.0742	-0.82	0.0010
MT001597	TC78291	XII.C. Unknown function	-0.55	0.0117	-2.24	0.0002	-1.85	0.0001
MT009491	TC88947	XII.C. Unknown function	-0.67	0.2015	-0.51	0.0491	-0.64	0.0054
MT001217	TC87099	XII.C. Unknown function	-0.10	0.6402	-0.64	0.0044	-0.70	0.0278
MT001656	TC87681	XII.C. Unknown function	-0.65	0.0274	-0.11	0.7052	-0.68	0.0043
MT004930	TC92615	XII.C. Unknown function	-1.00	0.0988	-0.67	0.0155	-0.80	0.0218
MT012911	TC84918	XII.C. Unknown function	-1.06	0.0197	-1.14	0.0034	-1.71	0.0012
MT001164	TC78067	XII.C. Unknown function	-0.13	0.5862	-0.85	0.0020	-0.76	0.0070
MT009126	TC79826	XII.C. Unknown function	-0.87	0.0170	-0.59	0.0322	-0.89	0.0003
MT010860	TC81629	XII.C. Unknown function	-0.02	0.9169	-0.68	0.0331	-0.72	0.0186
MT010587	TC81185	XIII. No homology	-2.01	0.0607	-1.20	0.0472	-1.04	0.0248
MT011321	TC90663	XIII. No homology	-1.10	0.0002	-1.09	0.0000	-1.46	0.0001

Table 8.3 List of 28 Probes Regulated by Inoculation/NH Treatment with Unknown function

Oligo ID	TIGR ID	Functional group	6hrNO	P-value	12hrNO	P-value	24hrNO	P-value
Up-regulated								
MT015465	TC77767	XII.C. Unknown function	0.06	0.8064	1.36	0.0030	0.69	0.0028
MT006913	TC82952	XII.C. Unknown function	0.46	0.0239	1.24	0.0063	0.63	0.0193
MT015161	BQ144186	XII.C. Unknown function	1.85	0.0000	1.22	0.0003	0.39	0.0062
MT015162	TC85295	XII.C. Unknown function	1.95	0.0000	0.88	0.0080	0.13	0.5084
MT015163	BQ144186	XII.C. Unknown function	1.98	0.0000	1.21	0.0045	0.09	0.5444
MT015510	TC78133	XII.C. Unknown function	0.70	0.0249	0.80	0.0285	0.61	0.0035
Down-regulated								
MT013455	TC84186	XII.C. Unknown function	-0.69	0.0424	-1.27	0.0182	-0.67	0.2044
MT015261	TC76796	XII.C. Unknown function	-0.68	0.0372	-0.86	0.0007	-0.18	0.1790
MT015110	TC85261	XII.C. Unknown function	-0.73	0.0025	-0.88	0.0277	-0.78	0.0021
MT005182	TC84763	XII.C. Unknown function	-0.62	0.0194	-0.66	0.0120	-0.75	0.0003
MT002743	TC88788	XII.C. Unknown function	-0.64	0.0008	-1.09	0.0000	-0.38	0.0072
MT004605	TC81497	XII.C. Unknown function	-0.56	0.0042	-0.84	0.0032	-0.65	0.0485
MT015178	TC76528	XII.C. Unknown function	-0.65	0.0003	-0.94	0.0006	-0.68	0.0004
MT001217	TC87099	XII.C. Unknown function	-0.53	0.0090	-1.27	0.0032	-0.72	0.0039
MT003412	TC80942	XII.C. Unknown function	-0.73	0.0046	-0.78	0.0401	-0.28	0.0480
MT009083	TC79207	XII.C. Unknown function	-0.83	0.0057	-0.60	0.0410	-0.34	0.1017
MT014672	TC80018	XII.C. Unknown function	-0.64	0.1257	-1.10	0.0090	-0.39	0.0324
MT009126	TC79826	XII.C. Unknown function	-0.61	0.0020	-1.13	0.0020	-0.51	0.0018
MT003273	TC89815;	XII.C. Unknown function	-0.72	0.0019	-0.29	0.0068	-0.61	0.0002
MT007094	TC85358	XII.C. Unknown function	-0.25	0.4012	-1.19	0.0319	-0.67	0.0358
MT007297	TC76955	XII.C. Unknown function	-0.77	0.0001	-0.80	0.0021	-0.14	0.2203
MT008133	TC77255	XII.C. Unknown function	-0.72	0.0027	-0.73	0.0001	-0.62	0.0585
MT015384	TC85993	XII.C. Unknown function	-0.82	0.0006	-0.83	0.0063	-0.16	0.3660
MT001910	TC88034	XII.C. Unknown function	-0.60	0.0120	-0.52	0.0980	-0.64	0.0142
MT002590	TC88978	XII.C. Unknown function	-0.40	0.1126	-1.51	0.0342	-1.41	0.0093
MT006797	TC92094	XIII. No homology	-0.89	0.0454	-0.96	0.0098	-0.55	0.0407
MT007598	TC86287	XIII. No homology	-0.61	0.0042	-1.23	0.0799	-0.59	0.0380

Table 8.3 List of 28 Probes Regulated by Inoculation/NH Treatment with Unknown function (Continued)

Oligo ID	TIGR ID	Functional group	6hrNO	P-value	12hrNO	P-value	24hrNO	P-value
Down-regulated								
MT008714	TC79091	XIII. No homology	-0.41	0.1631	-0.67	0.0187	-0.66	0.0239
MT011201	TC89470	XIII. No homology	-0.63	0.0011	-0.14	0.6229	-0.67	0.0085

APPENDIX C: Complete Protocol of DNA Microarray Experiment

Note: This complete protocol was mainly derived from the *Mt16kOLI1* Microarray Manual V 1.01(Helge Küster and Anke Becker, Department of Genetics, Institute of Genome Research, Bielefeld University) and the Manual of Amino Allyl cDNA Labeling Kit (Ambion, Inc., Austin, TX, USA).

RNA denature gel detection

1.2% denature gel
Agarose 0.6g
1xMOPS 50ml
Dissolve in microwave then cool to 60C
Add 2.5ml 37% formaldehyde under chemical hood
Add 2 ul 10mg.ml ethidium bromide
Pour gel and dry under chemical hood.
RNA denaturation solution
Total RNA 2ug/2ul
10X MOPS 1ul
Formaldehyde 2ul
Formamide 5ul
Heat to 65C for 15 min, immediately chilled on ice for 10 min, add 2ul RNA loading buffer. At the same time: run blank gel for 5 min
Run gel at 4-5V/cm (~80V with small electrophoresis device) for about 30 mins and then observe under UV.

Remove Contaminated DNA from total RNA by RNase-free DNase

Protocol
1. Add 34 nuclease-free water into the 10 µg/10 ul total RNA (in a 200 µl tube) to bring the volume to 44 µl
2. Add 5 µl 10XDNase I Buffer and 1 µl rDNase I to the 10 µg (µl) total RNA and mix gently by vortex. Spin briefly.
3. Incubate at 37 °C for 30 min.
4. Add 2.6ul 100 mM EDTA to achieve 5 (4.94) mM EDTA final conc. Mix and brief spin.
5. Incubate at 75 °C for 10 min.
6. Cool down on ice and proceed to Microcon 30 purification step (most EDTA will be rinsed away in this step).

Purify and concentrate total RNA by using Microcon YM-30

1. Wear gloves, place Microcon-30 filters (Millipore, one per RNA preparation) in collection tubes (red ring up) and prepare appropriate empty nuclease-free collection tubes in a row per Microcon-30 filter. Label Microcon-30 columns at their sides. Label the 2nd set of tubes on the lid.
2. Fill up the DNase I-treated 50µg total RNA from each of two replication of a sample as well as each of two replication of common reference (in a 1.5 nuclease-free tube) with

DEPC water to 500 µl and apply the mix to on Microcon-30 filter without touching the membrane with the pipette tip. Cap column.
3. Place assembly in centrifuge by aligning the cap strap toward the center of the rotor and counterbalance with a similar device. Spin at 13.000g for 10 min at 20°C, leave ~50 ul on membrane.
4. Pipette out the flow-through, put filter back into the first tube, and add 500 µl of DEPC water.
5. Spin at 13.000 g for 10 min at 20°C and discard flow-through.
6. Pipette out the flow-through, put filter back into the first tube, and add 500 µl of DEPC water.
7. Spin at 13.000 g for 9 min at 20°C and discard flow-through
8. Check with 100 ul pipettor, if there are more than 15 ul solution left on the top of the membrane, spin another 30 sec – 1 min at 12, 000 g 20 °C and discard flow-through
9. Place Microcon-30 filter upside-down in a new collection tube and spin for 1000 g for 3 min
10. Now, at least 20 µl should be in the collection tube. If not, invert the Microcon-30 filter and add the collected solution back to the membrane, add several DEPC treated H_2O to reach 20 ul totally. Leave for 1 min at RT to completely eluting RNA from the filter.
11. Place the filter upside-down in the same collection tube and spin for 1000 g for 3 min
12. Use 0.5 ul for denatured agarose gel and 0.5 ul for spec.

Amino Allyl cDNA Labeling Kit[6]

Thaw dT, Nuclease free water, RT buffer, RNase inhibitor, dNTP mix, dTTP +AAdUTP Mix, RTase, NaOH, HEPES, Sodium Acetate on ice.
Reverse Transcribe the RNA Sample
1. Mix RNA and RT primer, and denature at 75°C for 10 min
a. In a 200 ul RNase-free microfuge tube at room temperature, mix the following:

Amount	Component
11ul	20 ug total RNA
2 µl	Oligo(dT) Primers

After heating, briefly centrifuge the tube to collect the contents at the bottom, and keep the tube(s) at room temperature
2. Add the remaining reaction components and mix well

Amount	Component
2 µl	10X RT Buffer
1 µl	RNase Inhibitor
1 µl	dNTP Mix (no dTTP)
1 µl	dTTP + AA dUTP Mix
2 µl	M-MLV Reverse Transcriptase

Mix thoroughly by gentle vortexing, then centrifuge briefly to collect the reaction at the bottom of the tube.

[6] Total RNA used below was treated with DNase I and purified by passing through Microcon-30 and then quantify under spectrophotometer and denatured gel to make sure equal amount of RNA was put in.

3. Incubate reaction at 42°C for 2 hr
4. Add 4 µl 1 M NaOH, mix thoroughly firstly by pippetor tip and then by gentle vortexing, briefly spin to collect liquid and incubate at 65°C for 15 min
5. Add 10 µl (for 20ul reaction)/ 20 ul (for 40 ul reaction) 1 M HEPES and mix thoroughly, then transfer all solution into a 1.5 ml amber tube.
6. Recover the cDNA by ethanol precipitation
a. Add the following to the cDNA:

Amount	Component
3.4 µl	3M Sodium Acetate
100 µl	100% ethanol

b. Mix well; incubate 1.5 hr at -20 C.
c. Microcentrifuge for 15 minutes at maximum speed (12,000 x g or higher) at 4°C, then carefully aspirate the supernatant into a transparent new nuclease free tube to avoid loss of samples.
d. Wash the cDNA pellet by adding ~0.5 ml of 75% ethanol and vortex briefly (a small piece of pellet is visible and floating when vortexing, and store cDNA pellet in the 75% ethanol at –20C overnight if necessary.
Dye-coupling:
1. Warm DMSO and two packs of Cy3 to room temperature, and thaw the coupling buffer, Nuclease-free water, 4M Hydroxylamide on ice.
2. Resuspend *two* vials Cy3 with 3 ul DMSO respectively and keep in the dark at RT for up to 1 hr until ready to use it.
3. Microcentrifuge the tube for ~5 minutes at 4°C, and carefully aspirate the supernatant to a transparent nuclease free tube to avoid loss of samples.
4. To remove the last traces of ethanol, re-centrifuge the tube containing the cDNA pellet briefly to collect all residual fluid at the bottom of the tube. Then use a fine-bore pipette tip to gently aspirate away the residual fluid. Watch the solution in pipette tip in case of absorb pellet by mistake. Dry cDNA pellet under fume hood for 5 min in the dark.
5. Resuspend precipitated cDNA in 4.5 µl Coupling Buffer and mix thoroughly by gentle vortexing. Centrifuge the tube briefly.
6. Add 2.5 µl Nuclease-free Water. Mix gently but thoroughly and centrifuge the tube briefly.
7. Add 3 µl of Cy5/Cy3 into appropriate 20 ul reaction product.
Mix thoroughly by brief gentle vortexing and centrifuge the tube briefly to collect the liquid. Incubate 1 hour at room temperature in the dark (i.e. wrap the tube in foil and put it in a drawer).
(*at the same time*: Add 650 µl of Nuclease-free Water (from the 25 ml bottle) to the NucAway Spin Column, cap the column, vortex vigorously for ~10 seconds, tap out air bubbles, and store upright at room temperature for 1 hr (at least)–2 hours. Change rotor of centrifuge, warm centrifuge to room temperature)
8. Add 6 µl 4 M Hydroxylamine, , mix thoroughly by brief gentle vortexing and centrifuge the tube briefly to collect the liquid, and incubate 15 min in the dark at room temp.
(at the same time: Remove the bottom cap from the rehydrated NucAway Spin Column. Centrifuge rehydrated NucAway Spin Column at 750 x g for 2 min at room temperature.

Mark!! the orientation of the NucAway Spin Column in the rotor by marking the column on the opposite position of the rotor.)

9. Bring the cDNA preparation(s) to 85 µl by adding 69 ul Nuclease-free Water.

10. Discard the 2 ml wash tube from the previous step, put the NucAway Spin Column into a 1.5 ml collection tube (supplied), remove the upper cap from the column, and carefully apply the labeled cDNA directly to the center of the gel bed at the top of the column without disturbing the gel surface or touching the sides of the column with the pipette or reaction mixture. Notice: Add 85 ul solution drop by drop, stop for several seconds between drops to avoid over-saturate the top layer of the gel bed.

11. Place the tube plus spin column in the rotor, maintaining the orientation (!!!) used in the first centrifugation. Centrifuge at 750 x g for 2 minutes.

12. The dye labeled cDNA will run through to the 1.5 ml tube. Free dye is retained in the column matrix. Discard the spin column and continue with the procedure. After spin column purification, the labeled cDNA should only be slightly colored, if at all. If it has a strong red (Cy3) or blue (Cy5) color to it, then the dye removal procedure most likely failed. Most of the color should remain in the column matrix.

13. Concentrate the labeled cDNA by ethanol precipitation

Add the following to the labeled cDNA, and mix thoroughly:

Amount	Component
0.1 volume	3 M Sodium Acetate (~9 µl)
2.5 volumes	100% ethanol (~250 µl)

Incubate 1 hr at –20°C (frost free) or colder

(*At the same time*: Preheat a 50°C water bath (new), a 50°C dry bath (besides shaker) and a 80°C water bath (old)); Prepare 2 sets of tubes parallel with slides processing solutions in,(see next page for solution names))

14. Microcentrifuge for 15 minutes at 12,000 x g at 4°C, then carefully aspirates and discards the supernatant.

15. Wash the cDNA pellet by adding ~0.5 ml 75% EtOH; store cDNA pellete in 75% EtOH overnight at -20C

16. Microcentrifuge the tube for ~5 minutes at room temperature or 4°C, and carefully aspirate and discard the supernatant.

17. To remove the last traces of ethanol, re-centrifuge the tube containing the cDNA pellet briefly to collect all residual fluid at the bottom of the tube. Then use a fine-bore pipet tip to gently aspirate away the residual fluid.

18. The cDNA should form a small pellet, ~1–2 mm in diameter, which is visibly red (for Cy5) or blue (for Cy3).

19. Dissolve labeled cDNA in 10 ul nuclease free water, Pipette out 1 ul for EB free agarose gel detecting. Notice: Using freshly made, EB-free 0.5 x TBE as electrophoresis buffer.

20. The rest labeled cDNA is resuspended in 300 µl Nuclease-free Water for spectrophotometer detection.

21. After spectrophotometer detection, recover the 300 ul diluted cDNA, aliquot cDNA as 50 pmol (for Cy3) or 25 pmol dye each aliquot in amber tubes (~150 ul) and dry with speed vac for ~ 1.5 hr. Store the dried labeled cDNA at –20C freezer, label each tube and wrap with foil.

(at the same time: do the slide processing)

Processing of QMT epoxy microarrays prior to hybridization

Pre-warm dry bath to 50 C and water bath to 50C and 80C, place a steilized glass Petri-dish on the top of dry bath, place V bracket on the top of shaker; pre set centrifuge, temp, rotor, time.
Two tube 50ml MilliQ H2O+ 25 ul Triton X100, 80C 5 min
Two tube 50ml MilliQ H2O + 5 µl 37 % HCl
Two tube 50 ml 0.1 M KCl
22.5ml MilliQ H2O + 6 µl 37 % HCl in a 100ml glass bottle,using sterile disposable pipette under chemical fume hood.
Pre-warm the MilliQ/HCL mix to 50°C at water bath.
1. take out a sealed package with Mt16kOLI QMT glass slides and warm to RT for 5 min
2. wearing gloves, take out the desired Mt16kOLI QMT glass slides (only touch it at the corner where the scratch is or at the code no. at the bottom, the DNA side faces up when you can read the number or the scratch is at the bottom right corner)
3. seal the remaining slides of the box together with a new desiccation pack and return the sealed package to 18-20°C, place the old desiccation pack in the recycling box
QMT slide processing
- place the one slide in a 50ml eppendorf tube (so prepare 2 sets of tubes parallel for two slides) and carry out the processing by transferring the slides from one tube to the other, lay tube on the top of a shaker (500 rpm) during washing
- wash slides for 5 min **Timing** at room temperature in 50 ml of rinsing solution 1
- wash slides for 2 min **Timing** at room temperature in 50 ml of rinsing solution 2, repeat this step
- wash slides for 10 min at room temperature in 50 ml of rinsing solution 310 ml 4×QMT
At the same time: add 7.5 ml 4×QMT Blocking solution (stored at RT) into H2O/HCl mixture 5 min before use under luminar hood, shake well and pre-warm the complete Blocking solution to 50°C for at least 5 min **Timing**. Please note that the Blocking solution is instable and MUST NOT be stored longer!
- wash slides for 1 min **Timing** at room temperature in 50 ml of MilliQ H2O
At the same time: pour the QMT blocking solution into the plate and cover the plate
- Transfer two slides into the glass plate which is on the top of dry bath, put dry bath onto the shaker, incubate 2 slides for 15 min at 50 °C, and shake constantly (300rpm).
- Transfer two slides into two tubes with 50 ml of MilliQ H2O each; move dry bath down and put the tube on the shaker, shake for 1 min at 500 rpm at room temperature.
- Take sides out of tube and put on the steel rack, place rack on an 12x8 cm plastic micro plate cover containing 2 Kim wipes and immediately spin in the micro plate centrifuge at 1.200 rpm for 5 min.
Put the processed slides into microarray slides container.
Set the dry bath to 42C, the old water bath to 65 C and the new water bath to 42C. Add and take out some water from the water bath to decrease the temperature faster.)

Hybridization of 70mer oligonucleotide microarrays using a cover slip and a slide
50 pmol of Cy3 and 50 pmol of Cy5 dye labeled cDNA will be combined together for hybridization.

1st day

1. Right after slide processing preheat a 42°C water bath (new), a 42°C dry bath and a 65°C water bath (old)

2. During slide processing, pre warm the hybridization chamber on the top of the 42°C dry bath.

It is VERY IMPORTANT that this chamber is AT 42°C THROUGHOUT THE WHOLE PROCESS UNTIL THE COVER SLIP IS PLACED to avoid the local precipitation of targets or gradients

3. Dissolve the completely dried target which will be hybridized onto same slide in 70 µl filtered DIG Easy Hyb one by one (4 tubes totally) by pipetting up and down in the amber eppendorf tube. Combine 50 pmol Cy3 labeled common reference and 50 pmol Cy5 labeled treatment by dissolving them together into the 70 ul DIG hyb.

4. Add 0.5 µl of sonicated salmon sperm DNA (10µg/µl) into each Cy3/Cy3 dye mixture, mix by finger flicking and brief spin.

5. The total amount of hybridization solution containing mixed Cy3/Cy5-labeled targets is now 70.5 µl, incubate at RT in the dark until use. Take out one tube and do step 6-12 for one slide and then take out the second tube to do step 8-15 for the second slide.

6. Incubate one of the hybridization solutions containing the mixed Cy3/Cy5-labeled targets in a 65°C water bath for 5min -10 min

7. Place 14 µl of DIG in each hole at the side of the bottom of the slide chamber. The slide chamber is on top of the dry bath

8. Place the dried slide with the DNA side facing up into the slide chamber

9. Quickly spin down the denatured target and apply 68 µl as a drop to the center of the slide without touching the surface Notice: leave 1-2 ul in the tip to avoid producing bubble.

10. As quick as possible (!!): take a (clean!) cover slip (22x60mm) and place it on the left side of the slide (4 mm from the top of the slide), the scratch or the slide number is on the right side of the slide. At the right side, hold the cover slip with a fine forcep and quickly but carefully lower the cover slip. As soon as it touches the drop, take care that it does not reach over the corners of the slide and lower the cover slip. Avoid swimming of the cover slip from its destined position. A correction of the position of a wrongly placed cover slip is NOT possible since this causes severe problems later. All manipulations are carried out on the lid of the 42°C water bath

11. Place lid of the slide chamber on the chamber and tighten the four screws carefully but quickly in a diagonal manner

12. Put a level on the top of the hybridization cassette to judge the balance during transferring, place chamber on the bottom of the 42°C water bath.

13. Hybridize not less than 14 and not more than18 hours (16 hours) at 42°C

Preparation for tomorrow:

Set water bath in cool room to 18C before leaving

Fill 6 foil wrapped 250ml containers with appropriate washing solutions and one foil wrapped 50 ml container with 2XSDS) mark on the outside of foil, mark 1 and 2 in the order of using for those solution that are used twice, the lid of the tubes should be wrapped into foil too.

Two 2×SSC, 0.2 %(w/v) SDS washing buffer floating in the water bath used for hybridization; one 0.1×SSC floating in 18C; others go to room 347A;
Book Room 347A, book luminar hood, prepare timer

2nd day, washing steps should be done in Rome 342A where the temp is always below 24C

Need to prepare before everything happen:
Put the 18C water bath into 247A;
Set centrifuge speed, 1200 rpm, 3 min, 20C, and change the adaptor if necessary.
A fine tip steel forceps, a plastic forceps, paper towels, use curtain to block the light of the room.

14. Without glove, put a level on the top of chamber, hold the chamber horizontally, dry it from the outside and open the screws at diagonal ends, loose the middle 2 screws first, and the loose the other four one by one, little by little, until the bottom of chamber touched the bench. Turn off light, open the chamber.

15. Wear non latex gloves, remove the slide with the cover slip and quickly dump it while holding it with a plastic forceps into the first 50 ml 2×SSC, 0.2 %(w/v) SDS washing buffer (42°C) thereby washing off the cover slip

16. Place the slide in the and place it in the second foil-wrapped container with 250 ml 2×SSC, 0.2 %(w/v) SDS washing buffer pre-warmed to 42°C. Lay the tube on the top of shaker and shake for 5 min (500rpm).

17. Transfer to 0.2×SSC, 0.1 %(w/v) SDS (RT, at most 24°C) in a foil-wrapped 250 ml container, shake for 1 min in the dark

18. Transfer to 0.2×SSC, 0.1 %(w/v) SDS (RT, at most 24°C) in a foil-wrapped 250 ml container, shake for 1 min in the dark

19. Transfer to 0.2×SSC (RT, at most 24°C) in a foil-wrapped 50 ml tube, shake for 1 min in the dark

20. Transfer to 0.2×SSC (RT, at most 24°C) in a foil-wrapped 50 ml tube, shake for 1 min in the dark

21. Transfer to 0.1×SSC (Important: set to 18 °C and remove from the cooler immediately before use) in a foil-wrapped 50 ml tube, shake for 1 min in the dark

22. Place rack on an 12x8 cm plastic microplate cover (Genomics Solutions) containing 2 Kim-wipes and immediately centrifuge in the microplate centrifuge at 1.200 rpm for 5min. Use a stack of 3 used glass slides at every side of the plastic dish to lift up the rack with the slides, this avoids precipitation artetacts at the side of the slide. Be sure to counter-balance using an appropriate balance. If necessary, dry corners of the slide afterwards with a Kim-wipe. At the same time, take out the slide box.

23. Place dried slide in a box in the dark until scanner is ready. It might be recommendable to dry the slides in the container for at least 20 further min before scanning. This might avoid gradient bleaching effects in the Cy5 channel. Work quickly at all times; avoid direct light and exposure to high ozone concentrations, since this strongly enhances Cy5 bleaching.